FEDERAL UNIVERSITY OF RIO DE JANEIRO

ANGELA CAMILA PINTO DUNCKE

LIQUID CRYSTALS IN CRUDE OIL AND WATER EMULSIONS

RIO DE JANEIRO – RJ
2019

Angela Camila Pinto Duncke

LIQUID CRYSTALS IN CRUDE OIL AND WATER EMULSIONS

Thesis presented to the Post Graduate Program in Chemical and Biochemical Processes Engineering, School of Chemistry, Federal University of Rio de Janeiro, as a partial requirement to obtain the Ph.D. degree.

Advisor: Márcio Nele de Souza

RIO DE JANEIRO
2019

D911 Duncke, Angela Camila Pinto
Liquid Crystals in Crude Oil and Water Emulsions/ Angela Camila Pinto Duncke. – Rio de Janeiro, 2019

130 f.

Tese (doutorado) Universidade Federal do Rio de Janeiro, Escola de Química, Programa de Pós Graduação em Engenharia de Processos Químicos e Bioquímicos, 2019.

Orientador: Márcio Nele de Souza

1. liquid crystals. 2. crude oil. 3. emulsions, 4. interfacial rheology, 5. optical microscopy – I. Souza, Márcio Nele de, (Orient.). II. Título.

CDD: 660

Angela Camila Pinto Duncke

LIQUID CRYSTALS IN CRUDE OIL AND WATER EMULSIONS

Thesis presented to the Post Graduate Program in Chemical and Biochemical Processes Engineering, School of Chemistry, Federal University of Rio de Janeiro, as a partial requirement to obtain the Ph.D. degree.

Approved in:

_____

Márcio Nele de Souza, D.Sc., TPQB/UFRJ.

_____

Verônica de Araújo Calado, D.Sc., TPQB/UFRJ

_____

Erika Christina Nunes Chrisman, D.Sc., EQ/UFRJ

_____

Márcia Cristina Khalil de Oliveira, D.Sc., CENPES/Petrobras

_____

Flávio Albuquerque, D.Sc., CENPES/Petrobras

_____

Ana Maria Percebom, D.Sc., PUC-RJ

Para Clair, Ari e Cesar.
Para Pedro.

AGRADECIMENTOS

Agradecer. Mostrar ou manifestar gratidão, render graças. Reconhecer. Com estas definições inicio meus agradecimentos a todos que estiveram presentes neste ônibus que é/foi meu doutorado. Assim como quando se decide pegar um ônibus, você decide entrar no doutorado. Você escolhe qual ônibus tomar de acordo com o seu desejo de destino final. Agradeço à UFRJ e à Escola de Química pela seriedade e comprometimento com que conduz seus passageiros. Ao entrar você precisa pagar a passagem. Agradeço ao CNPq pela bolsa de fomento à pesquisa. Agradeço também a Petrobras pelo financiamento de projetos.

Então olha para o motorista, que vai te guiar durante sua viagem. Fale ao motorista somente o necessário, pois ele precisa manter a atenção na estrada e cuidar para que tudo corra bem para você e para os demais passageiros. Obrigada Márcio Nele por ter sido um motorista prudente, que com sua experiência orienta cada aluno em seu caminho nessa longa estrada.

Próximo passo, passar pela roleta. Ao passar pela roleta você dá uma olhada geral no interior do ônibus. Já tem algumas pessoas ali, ocupando alguns lugares. Você observa onde estão os assentos vagos. Cada assento representa uma linha de pesquisa. Você analisa e decide em qual assento vai passar os próximos quatro anos da sua viagem. Assento escolhido. Você agora deve andar até ele. E nesse trajeto entre a roleta e o assento você vai refletindo sobre sua escolha, estudando as possibilidades, vendo se vai bater sol ou não, se tem pessoas sentadas próximas... enfim você vai amadurecendo a ideia de sentar nesse lugar.

Devidamente sentado, você observa com mais atenção as pessoas próximas. Puxa um papo, vai trocando experiências, vai fazendo amizades, afinal todos estão no mesmo ônibus, seguindo na mesma direção. Agradeço infinitamente aos meus companheiros de trajeto, especialmente a Gizele Batalha, Thiago Marinho e Ali Hesamedini, por também comprar uma passagem para este ônibus.

Nesta viagem alguns passageiros que já estavam no ônibus chegam ao seu destino, puxam a cordinha e descem do ônibus. Outros estão sentados um pouco afastados e seu contato fica dificultado. Agradeço a Carla Barbato, Viviane Prates, Monique Lombardo, Troner de Souza, André Clemente, Lidiane Elias, Isabela Soares,

Alessandro Barros, Rodrigo Cunha, por dividirem este ônibus comigo, mesmo que por curtos períodos ou sentando um pouco distante.

Lá pela metade do trajeto, o ônibus é parado para fiscalização. A qualificação. Neste momento os fiscais se aproximam de você e verificam seus documentos e se sua passagem é válida. Você fica um pouco nervoso. Os fiscais te alertam sobre o restante da viagem e sobre normas de segurança para que nada de errado aconteça. Agradeço aos professores que estiveram em minha banca de qualificação. Felizmente tudo certo, podemos continuar a viagem. Mas, em seguida algo inesperado acontece.

Trânsito. Seu ônibus fica impedido de andar. Você começa a ficar preocupado. Tem pressa de chegar ao seu destino. Você cogita descer do ônibus ali mesmo e buscar outro caminho, mas não pode, pois está numa rodovia no meio do nada. O momento da crise. Não pode descer pois já investiu seu dinheiro e seu tempo naquela viagem. Seria terrível abandonar a jornada neste momento. Fora do ônibus a perspectiva é quase zero. Os outros passageiros também estão angustiados. Alguns conseguem disfarçar melhor que outros, mas todos estão ali numa batalha interna, buscando chegar ao destino.

O trânsito começa a fluir. É possível ouvir a música que vem de alguns carros próximos. Agradeço aos amigos do grupo de carona, Giselle Tavora, Rodrigo Vojta, Luca Massaglia, Thiago Balbino pelos momentos de descontração nestes quatro anos.

Porém, quando se dá conta seu ônibus está em um túnel. Muito escuro. Você não vê mais os seus amigos. Está sozinho, você e sua pesquisa. Você precisa aprender a lidar com o medo e com a responsabilidade da viagem. Você tenta se aproximar do motorista para saber sobre o caminho, mas nesse trajeto, tropeça. Alguns passageiros te ajudam. Agradeço a Angel Bassini, aos demais alunos de iniciação científica e aos laboratórios parceiros: Lapin (IMA), Labter (EQ), Dopolab (EQ), CENPES (Petrobras), LabPetro (UFES), LNLS, EngePol (EQ), LMSCP (EQ), pelo suporte. O motorista diz que vai dar tudo certo, que já estamos quase chegando. E nesse momento você começa a ver a luz no fim do túnel. Sua viagem está se aproximando do fim.

Você começa a retornar ao seu assento e a ver as pessoas no ônibus. Alguns rostos novos. Thamyres Leocadio, Nathalia Ferreira, aproveitem a viagem que está apenas começando. Outros não são mais só passageiros, são amigos. Outros você não teve a chance de se aproximar.

A viagem de quatro anos, tão longa, quando chega ao fim ainda deixa um sentimento de que não tivemos tempo suficiente. Tempo suficiente para fazer mais amigos, ou para explorar mais e mais o local onde escolheu se sentar. Voltando ao seu assento, no final da viagem, começa a relembrar de todo o trajeto, avaliando cada momento, e escrevendo sobre isso. Afinal de contas, seu relatório de viagem ainda será avaliado.

De repente você é surpreendido pela entrada de um vendedor de balas, e “sem atrapalhar o sossego da sua viagem”, você compra alguns doces. Agradeço a Anna Paola Carvalho, Sylvio Medeiros, Ronaldo Borges da Fonseca, Felipe Carvalho e Maíra Coelho por proporcionarem momentos alegres, de união e paz, inspirar coragem e determinação, pelo incentivo e apoio durante este período. Com vocês a viagem pôde ser mais doce e divertida.

Neste momento, você olha pela janela e vê uma paisagem com ruas, prédios, praias e montanhas. Rio de Janeiro, obrigada por cada banho de mar, de cachoeira, de chuva, de sol, de cultura e de perseverança.

A viagem está chegando ao fim. Você deve se levantar e puxar a cordinha. Solicitar a parada. Depois que descer, vai perceber que o destino não era o ponto final. Vai ter que escolher o próximo, e decidir mais uma vez, e outra, e mais outra, para sempre. Assim como já decidiu infinitas vezes antes de pegar o ônibus do doutorado. Agradeço, portanto aos amigos que fiz em viagens anteriores, pelos ônibus de rua, ônibus escolares, ônibus de universidade, etc.

Dentre estes infinitos ônibus, preciso agradecer ao ônibus do trabalho voluntário do Projeto Rondon. Nele conheci alguém que me ensinou sobre paciência, respeito, dedicação e amor. Pedro Carvalho, muito obrigada pelo suporte, pela compreensão e pelo carinho durante estes anos. Espero viajar contigo por muitas outras estradas.

Todas essas viagens não seriam possíveis sem o apoio das três pessoas mais extraordinárias e importantes da face da Terra. Clair Duncke, Ari Duncke e Cesar Duncke, a quem além de agradecer até a última batida do meu coração, dedico esta viagem com todo amor que cabe em mim. Vocês são seres iluminados que sempre estão ao meu lado não importando a distância. Vocês estão no meu coração desde o surgimento da minha alma.

Agradeço também a força maior que rege as nossas vidas, o universo e tudo que existe.

Por fim, o encerramento desta viagem me fez lembrar de um poema de Nicanor Parra, “Missão cumprida”. Adapto suas palavras ao meu “Balanço dos 30 anos”.

Árvores plantadas	58
Filhos	0
Obras publicadas	3
Total	61
Doenças crônicas	1
Ossos quebrados	0
Sessões de terapia	28
Total	29
Países	7
Estados brasileiros	11
Vacinas	27
Total	74
Amizades desfeitas	4
Rir até chorar	7 452
Beijos comuns	1 947
Amizades refeitas	4
Corações partidos	3
Total	86 439
Caronas	456
Bicicletas	4
Cavalos	3
Total	1 125
Novelos de linha	17
Panelas	3
Ventiladores	2
Total	9

“Há uma alma em mim,
Há uma calma que não condiz...
Com a nossa pressa!
Com o resto que nos resta!
Lamentavelmente eu sou assim...
Um tanto disperso,
As vezes desapareço,
Pois depois recomeço,
Mas antes me esqueço.

Nossa sina é se ensinar
A sina nossa é.”

Sina Nossa, Teatro Mágico

RESUMO

DUNCKE, Angela Camila Pinto. Cristais Líquidos em Emulsões de Petróleo e Água. Rio de Janeiro, 2019. Tese (Doutorado em Engenharia de Processos Químicos e Bioquímicos) - Escola de Química, Universidade Federal do Rio de Janeiro, Rio de Janeiro, 2019.

Durante a produção de petróleo, emulsões podem ser formadas devido às diferenças de densidade entre as fases, à presença de surfactantes naturais e ao regime de fluxo turbulento. A estabilidade de uma emulsão pode estar relacionada a diversos fatores, dentre eles a presença de cristais líquidos (CL). Do ponto de vista da indústria do petróleo, CL é uma classe de materiais pouco conhecida, mas possivelmente presentes nos processos de produção e transporte. Portanto, os principais objetivos deste estudo foram avaliar a influência de alguns fatores na formação da fase liquido cristalina, extrair e caracterizar o material com atividade interfacial capaz de formar CL. Verificou-se que a presença de CL não está condicionada à presença de parafinas do petróleo, nem mesmo à concentração de sais na fase aquosa. O teor, tipo de cátions dissolvidos e pH da fase aquosa, os valores de índice de acidez total e a viscosidade do petróleo, por sua vez estão relacionados à formação de CL. A avaliação desses fatores foi realizada por meio de microscopia óptica, tensão interfacial e reologia interfacial. Há fortes indícios de que os ácidos naftênicos são responsáveis pela formação dos CL em sistemas de petróleo, além de evidências acerca da alta estabilidade dos CL em amostras de água de produção.

Palavras-chave: cristal líquido, petróleo, emulsões, reologia interfacial, microscopia óptica.

ABSTRACT

DUNCKE, Angela Camila Pinto. Liquid Crystals in Crude Oil and Water Emulsions, Rio de Janeiro, 2019. Thesis (Ph.D. in Chemical and Biochemical Processes Engineering) - School of Chemistry, Federal University of Rio de Janeiro, Rio de Janeiro, 2019

During crude oil production, emulsions can be formed because of density differences between the phases, the presence of natural surfactants, and the turbulent regime flow. The stability of an emulsion could be related to several factors, among them the presence of liquid crystals (LC). From the petroleum industry's point of view, LC is a class of little-known materials, but possibly present in the production and transportation processes. Therefore, the main goals of this study were to evaluate the influence of some factors on the LC formation and to extract and characterize the material with interfacial activity capable of forming LC. It was verified that the presence of LC is not linked to the paraffinic composition of the crude oil nor to the salt concentration in the aqueous phase. The content, type of cations dissolved and pH of the aqueous phase, the total acid number and the viscosity of petroleum, are related to the LC formation. The evaluation of these factors was performed by optical microscopy, interfacial tension, and interfacial rheology. There are strong indications that naphthenic acids are responsible for the LC formation in crude oil systems, as well as evidence about the high stability of LC in production water samples.

Keywords: liquid crystal, emulsions, crude oil, interfacial rheology, optical microscopy.

Index of Figures

Index of Tables

INDEX

1. INTRODUCTION

Despite research efforts involving new sources of energy, especially renewable energies, with increasing population and market demands, petroleum is still considered the main component of the world energy matrix today. Understand this complex matrix, as well as its behavior in the various scenarios (production, transportation, refining, etc.) is essential for greater productivity.

Large amounts of water are involved during crude oil production. This water can be originally from the reservoir or from injection water. Because of the high polarity and small density differences between the aqueous and oily fractions, the presence of natural surfactants, and the turbulent regime flow, water and oil are mixed forming emulsions. Such emulsions may exhibit variable stability. In some cases, they are unstable and can be easily separated. In others, the emulsions formed are stable, which can cause difficulties in the separation processes, and consequently increase production costs. Thus, in crude oil production, the more stable the emulsion the less desirable it is.

The stability of an emulsion is related to several factors, such as temperature, shear rate, water content, phase's density and viscosity, surfactant type, presence of ions, oil phase composition, and droplet size, among others. In cosmetic emulsions, one of the main stabilizing factors is the presence of liquid crystals (LC) (KLEIN, 2008). These liquid crystals are located at the interface of the droplets, forming a barrier that hinders coalescence. From the petroleum industry's point of view, LC is a class of little-known materials, but possibly present in the production and transportation processes (URDAHL and SJÖBLOM, 1995). The liquid crystalline structures can modify the equilibrium and transport properties of the produced oil; therefore, it is extremely relevant to understand their influence on these systems.

Studies based on the crude oil emulsions stabilization by means of liquid crystalline films, as well as molecules characterizations and the formation mechanisms of these structures, are rare. Possible problems associated with LCs in crude oil emulsions are unknown. Therefore, one of the main reasons for the elaboration of this thesis is help to elucidate the existing doubts about LC, to evaluate the liquid crystalline structures in crude oil and water systems, and expand the knowledge, adding experimental evidence of this mesophase.

Liquid crystalline structures acting at the crude oil-water interface are scarcely reported in the literature. The investigation of these structures is relatively recent, having its first reports in the early 2000s, where special conditions for LCs formation were required, such as previous extraction processes or controlled atmospheres. Some authors suggest that LCs in crude oil systems are lamellar lyotropic structures, formed mainly by naphthenic acids and/or their salts (naphthenates). However, there are still unanswered questions, such as "What are LCs actually formed of? Are the naphthenic acids? The naphthenates? How is this structure organized? What factors can affect the formation of liquid crystals? Do they increase the stability of the emulsion?", etc. These questions were the basis for specific objectives of this work: to evaluate the influence of some factors on the LC formation and to extract and characterize the material with interfacial activity capable to form LC.

This thesis is organized into seven chapters. The first is the introduction of the thesis. The second chapter “Liquid Crystals” is the literature review, involving: what LC are; their classifications; explanations of lamellar phases; the relationship to emulsion stability; formation and factors that affect the crude oil emulsion stability; reports of LC in crude oil systems and the first LC observation in Brazilian emulsion. The third chapter “Originality of Thesis” presents the reasons why this thesis can be considered original. The fourth chapter “Liquid Crystal Formation” describe the methodologies, results and discussion about the factors that can possibly influence on the LC formation, such as the presence of waxes; salinity; aqueous phase content; pH; volume and valence of the cations on aqueous phase; and different crude oil types. To investigate these factors, which can affect the interfacial activity of LC, microscopy, interfacial rheology, and others were used. Based on the characterization of the crude oil samples and the evaluation of the factors, is possible to define systems in which LCs are more easily obtained.

Many compounds can act at the crude oil-water emulsions interface. Because of the intrinsic complexity and the heterogeneity of crudes around the world, it is difficult to reach a consensus on the mechanisms of emulsion stabilization in general. However, even with the difficulties of identifying the material at the oil-water interface, its study is very important, as well as determining its role in emulsion stabilization. The fifth chapter “Extraction and Characterization of the Interfacial Material” shows the methodologies, results and discussion about extraction and characterization of the material with interfacial activity, which can be responsible for LC formation. The sixth

chapter presents “Other Considerations” about LC as a suggestion of a mechanism of formation, and some examples of the stability of the liquid crystalline structures in produced water. The fourth, fifth and sixth chapters also present partial conclusions. The seventh chapter presents the general conclusion of the study.

2. LIQUID CRYSTALS

In the liquid state of matter, the molecules of a substance are disordered and able to move freely. In the solid state, the molecules are arranged in a rigid structure. However, between these two states, some substances have an intermediate phase (mesophase) that has liquid characteristics such as fluidity, and solid characteristics such as molecular organization. This intermediate phase is called liquid crystal (MARSH, 1973; GENNES and PROST, 1993; KUMAR, 2001).

Because of its structure, not all substances are able to form LC. LCs are usually formed by molecules that have one of their dimensions larger than the others, such as elongated molecules (calamitic), in the form of discs (discotic), cone-shaped (pyramidal), etc. (GENNES and PROST, 1993; HAMLEY, 2007). These structural features give to the molecules a degree of ordering parallel to each other, providing both solid and liquid characteristics.

LCs can be divided into two major groups: thermotropic and lyotropic. Thermotropics are composed of pure substances (mono-component systems), whose orientation of the molecules are highly influenced by the temperature variation (NETO and SALINAS, 2005; HAMLEY, 2007). Most everyday applications of thermotropic LCs are in the manufacture of monitors, televisions, and displays, owing to the color changes caused by the temperature variation (BECHTOLD, 2005; NETO and SALINAS, 2005).

Lyotropic liquid crystals are present in cell membranes (phospholipid bilayers) and are widely applied in cosmetics because of the formation of highly stable structures (KLEIN, 2008), as well as can be used in the pharmaceutical industry for controlled drug release (MAKAI *et al*., 2003; MÜLLER-GOYMANN, 2004; FORMARIZ, *et al*. 2005; SAULNIER *et al*., 2008; MANOVA *et al*., 2016). Lyotropic are named for the greek *Lio*, which means solvent, as the substance (surfactant molecules) requires the presence of a solvent (bi-component system), usually water, to generate a liquid crystalline structure. In addition, lyotropic LCs are dependent on the surfactant concentration in the solvent (DANIELSSON, 1976; HIEMENZ and RAJAGOPALAN, 1997).

2.1. LYOTROPIC LIQUID CRYSTALS

The formation of lyotropic LCs is linked to the presence of a solvent and some amphiphilic material (surfactant), which has part of its structure with an affinity for polar compounds (hydrophilic head) and part with an affinity for non-polar compounds (hydrophobic tail). These molecules can modify the properties of the interfaces between media with different polarities. According to Rosevear (1968), a water-diluted surfactant phase has a more elastic (rigid) characteristic than its pure phase (surfactant only), even having a substantially higher water content.

Unlike thermotropics that do not vary in structure due to the concentration of surfactant, the lyotropic present different characteristics as this parameter changes (RODRIGUEZ-ABREU *et al*., 2005; ZHENG *et al*., 2011). In this type of structure, the concentration constitutes an additional degree of freedom (BAGHERI *et al.,* 2012).

It is known that surfactant molecules tend to be oriented to promote contact between parts with similar polarities, forming micelles (NETO and SALINAS, 2005). For example, in a bi-component system, a surfactant added in a polar solvent will be arranged that its hydrophilic portion is in contact with the solvent, and its non-polar portion will tend to minimize the contact with this solvent, forming micelles (HIEMENZ and RAJAGOPALAN, 1997). In systems whose solvent is non-polar, occurs the formation of reverse micelles. **Figure 1** shows an illustrative schematic representation of the micelle and reverse micelle.

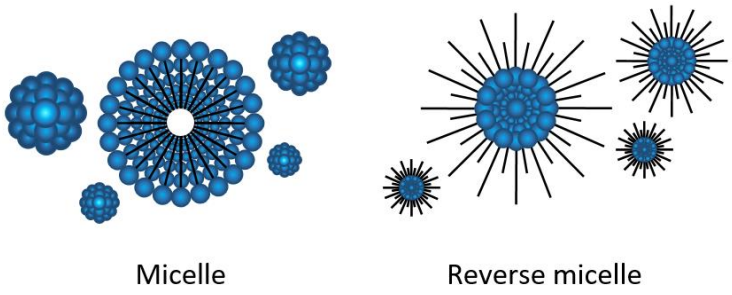

Figure 1: Schematic representation of micelle and reverse micelle.

The formation of micelles in a bi-component solvent-surfactant system, however, only occurs from a given concentration of surfactant. The lowest concentration in which micelles are formed is called the critical micellar concentration (CMC). The increase in surfactant concentration after this point alters some of the

physical properties of the system. **Figure 2** shows a graph containing typical behaviors of physical properties for a system close to the CMC value. CMC is defined as a sharp change in some thermodynamic quantities close to this value (HAMLEY, 2007).

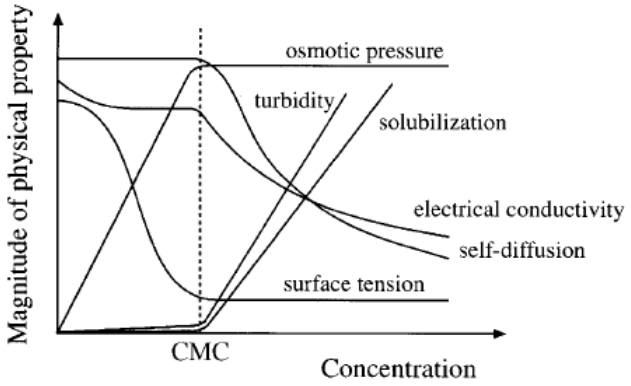

Figure 2: Some physical properties exhibiting discontinuity near CMC. (HAMLEY, 2007)

At concentrations slightly above the CMC, the micelles are generally spherical structures, with approximately two molecules in diameter. However, the typical concentration for the formation of liquid crystal structures is more than 100 times the CMC value (NETO and SALINAS, 2005). In this concentration, the micelles tend to be organized in cubic arrangements. As the concentration increases, the spheres become cylindrical of indeterminate length, organizing themselves into hexagonal structures. Further increasing the concentration, the surfactant cylinders are arranged in flat bilayers, the lamellar phases (ROSEVEAR, 1968; HIEMENZ and RAJAGOPALAN, 1997; HAMLEY, 2007). **Figure 3** represents these three arrangements. It is important to remember that not all surfactants are able to form liquid crystalline mesophases because of their molecular structure.

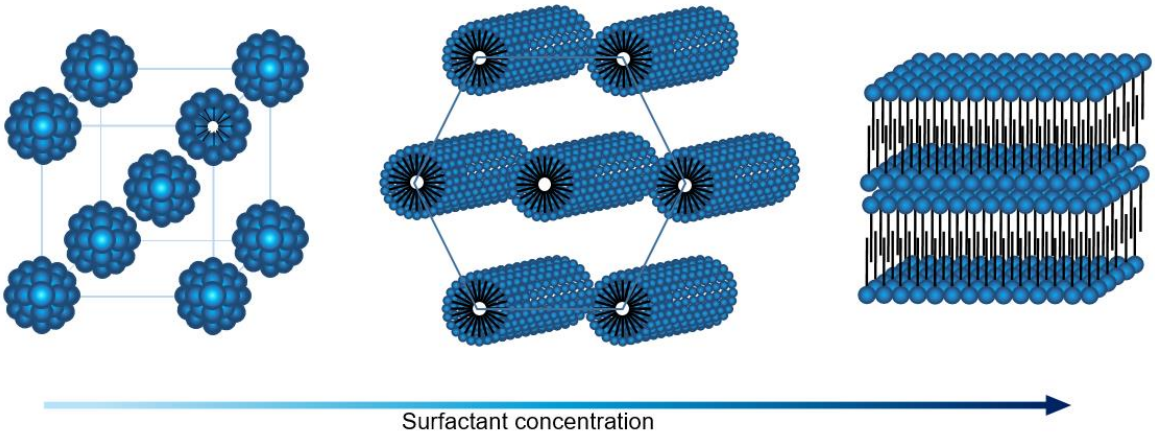

Figure 3: Schematic representation of the LC phase evolution with the increase of amphiphilic material concentration on spherical micelle in any cubic arrangement; cylindrical structures in a hexagonal arrangement; and flat bilayer or lamellar structure.

According to Myers (1999), the theory of liquid crystals suggests more than 18 different structures (including thermotropic). However, for lyotropic systems, the main ones are those described previously: cubic, hexagonal and lamellar. By adding a third phase with different polarity to the surfactant-solvent system, the micellar structures that will be formed are similar to those already described. That is because, as stated, the surfactant has an amphiphilic structure.

Water and oil systems without the presence of surfactants are unstable (MILLER *et al*., 2001). For example, a tri-component oil-surfactant-water system, the water being the solvent (polar) in greater quantity, will generate micelles whose interior will be filled by the oil phase (non-polar). If the compound in greater quantity were the oil phase, there would be the formation of reverse micelles whose interior would be formed by water. By increasing the surfactant concentration in these tri-component systems, it is also possible to observe the formation of liquid crystalline mesophases (MYERS, 1999; HAMLEY, 2007). In these cases, the polar and non-polar phases will be "isolated" by the surfactant molecules. The lamellar liquid crystalline structure with its surfactant bilayers will involve the non-polar phase as shown in **Figure 4.** The interior of the structure, in this case, is composed of an isotropic liquid, while the interfacial layer (liquid crystal) has a concentric radial arrangement with multilayers of surfactant (BAGHERI *et al.,* 2012).

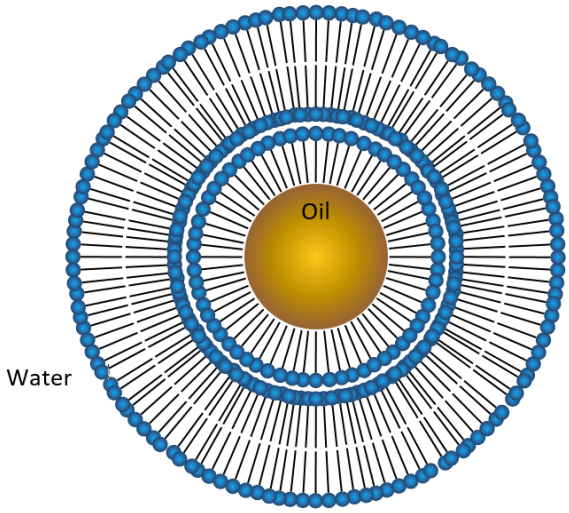

Figure 4: Lamellar LC structure representation with surfactant multilayer (liquid crystal).

It is possible to find emulsion systems containing these lamellar liquid crystalline structures formed around the dispersed phase. It is not a regular emulsion or a monophase of liquid crystal (OKA *et al*., 2008) but a system with "drops" that are coated by lamellar LCs. These structures are common in cosmetic emulsions (KLEIN, 2008). **Figure 5** shows an emulsion scheme containing these lamellar liquid crystals (the focus of this thesis).

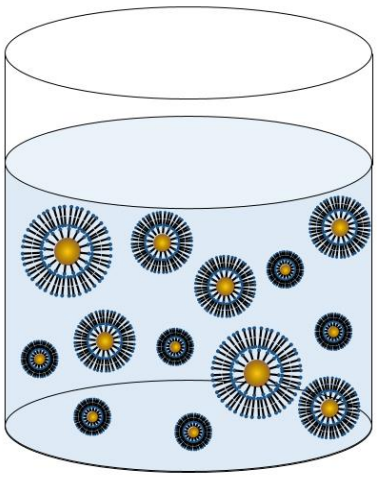

Figure 5: Representation of an emulsion containing lamellar liquid crystals.

2.1.1. Lamellar Liquid Crystals and Emulsion Stability

The emulsion stability depends on the interactions between the droplets, which may be related to Brownian motion and to hydrodynamic forces, as hydrogen bonds,

attractive London forces, electrostatic repulsive forces and steric barriers (MELE *et al*., 2003).

Interfaces with surfactant organized in a multilayer structure (lamellar LC) provide steric stabilization between water and oil, and between droplets (SJÖBLOM *et al*., 2003). Overlaying the layers increase the strength of the physical barrier and consequently further complicates the coalescence of the droplets (URDAHL and SJÖBLOM, 1995; MYERS, 1999; HORVÁTH-SZABÓ *et al.,* 2001a; FRANK *et al.,* 2005; GAO *et al*., 2010). Thus, the more layers of surfactant there are, the more difficult is the coalescence (OKA *et al*., 2008). **Figure 6** presents a scheme of the difference between a droplet coated by one surfactant layer and a droplet coated by lamellar liquid crystal.

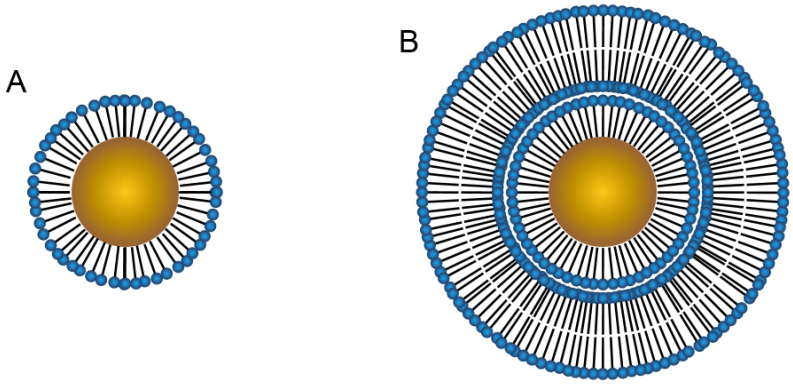

Figure 6: Difference of interfacial layer "thickness" of droplet coated by (A) one surfactant layer and (B) by lamellar liquid crystal.

Coalescence involves the elimination of interfacial films that separate the dispersed droplets in a continuous phase. It means the union of small droplets aiming at the formation of a larger droplet, and consequently leading to a phase separation (URDAHL and SJÖBLOM, 1995).

Figure 7 shows results obtained by Friberg and Solans (1986) in which the potential required to flocculate and coalesce drops of two model emulsions, one containing and one not containing LC at the droplet interface, was evaluated. Flocculation is the process where the distance between droplets is reduced; however, they retain their individual identities (URDAHL and SJÖBLOM, 1995). It is possible to verify a great reduction in the distance between the drops of the emulsion without LC, as the potential (dashed line) is increased. On the other hand, the emulsion containing lamellar LC (solid line) was more resistant to flocculation and coalescence. Thus, it is

reasonable to assume that the presence of lamellar LC acts against coalescence.

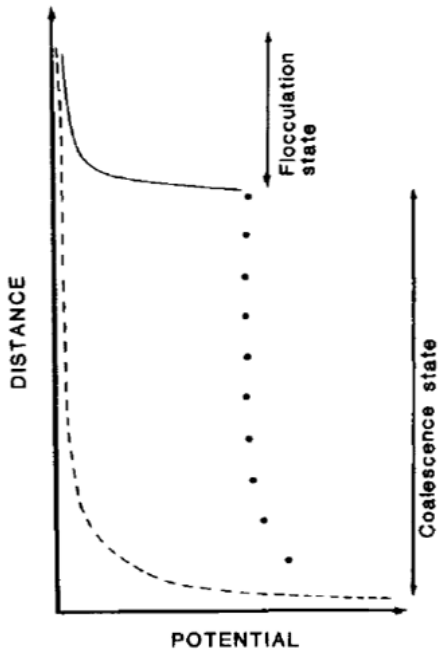

Figure 7: Distance between the droplets as a function of the potential for emulsions containing LC at the interface (solid line) and without LC at the drop interface (dashed line).
(FRIBERG and SOLANS, 1986).

According to Klein (2008), the presence of liquid crystals in cosmetic emulsions favors the increase of viscosity and stability. In these systems, the LCs contain large portions of concentrated water between the surfactant multilayers. Due to this imprisonment of water, its evaporation is smaller than in the case of emulsions composed by normal micelles. With this, the moisture content is maintained for a long period, so that transepidermal water loss is replaced by long-lasting hydration (MAKAI *et al.*, 2003).

2.2. LIQUID CRYSTAL IDENTIFICATION BY MICROSCOPY

Tong *et al.* (2008) in their studies on the structure and composition of chicken egg yolk verified the presence of lamellar liquid crystals. **Figure 8** shows a Transmission Electron Microscopy (TEM) of the cross-section of one of these frozen structures. The visible multilayers are composed of lipids and calcium carbonate. Unfortunately, it is not possible to state that the structure of **Figure 8** is identical to the lamellar LC structure present in crude oil emulsion, which will be discussed later in this

thesis, but it is an excellent representation of a lamellar LC.

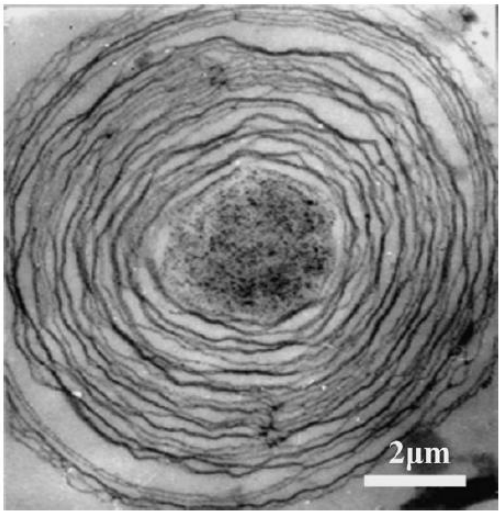

Figure 8: Cross-section TEM image of a frozen liquid crystal found in an egg yolk showing multilayers around a core.
(TONG *et al*., 2008).

Some LCs are in the class of anisotropic structures whose properties vary with the direction. Possibly the most striking proof of this anisotropy is the optical one, that is, double refraction, also called birefringence, whereby the sample appears bright when viewed between two crossed polarizers (DANIELSSON, 1976; LÉTOFFE *et al.* 1995).

For polarized light microscopy, it is necessary to use two polarizing filters in the path of light. These filters have grooves that allow the passage of light in only one direction. After to pass through the first filter, the light that initially vibrates in all directions will be oriented to vibrate in a single direction known as the plane of polarized light. Thus, by positioning the second filter perpendicularly to the first, the light is extinguished (CRABTREE and MINGOS, 2007). By inserting an anisotropic sample between the polarizers, all the light that would be blocked by the second polarizer, will deflect its course by the crystalline structures and will become visible after the second polarizer. **Figure 9** illustrates the principle of light polarization and how a birefringent sample reacts to this type of illumination.

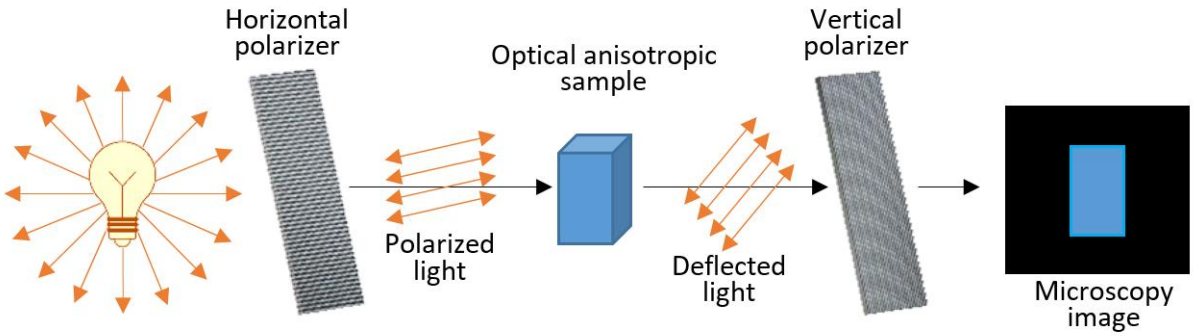

Figure 9: Principle of light polarization applied to a birefringent sample.

Through polarized light, lyotropic liquid crystals in lamellar and hexagonal phases (as shown in **Figure 3**) are readily identified. **Figure 10** shows polarized light microscopy images for lamellar LC (**Figure 10A** – composed of 9.0 wt. % oleic acid, 1.0 wt. % n-methylpyrrolidone, 50.0 wt. % water and 40.0 wt. % CETETH-20 (commercially known as Brij 58); and hexagonal LC (**Figure 10B** – composed of 20.0 wt. % n-methylpyrrolidone, 40.0 wt. % water and 40.0 wt. % CETETH-20) (OYAFUSO *et al*. 2017). Note that the system of **Figure 10A** used a high concentration of surfactant (40.0 wt. %), so the exposed structure represents a flat multilayer LC, rather than around a drop.

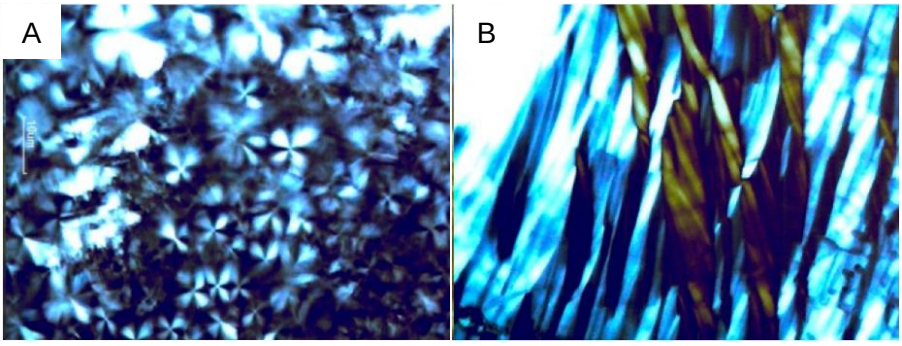

Figure 10: Polarized light microscopy of lyotropic liquid crystals lamellar (A) and hexagonal (B). (OYAFUSO *et al.* 2017)

When the orientation of the molecules of the crystalline material being analyzed by polarization is parallel to the polarizer filters, no deviation of the plane of light occurs, so the extinction of the light will be maintained. Thus, dark regions observed in cross-polarized samples refer to extinction points, due to the parallelism between sample and polarizers (CRABTREE and MINGOS, 2007). In addition, the dark regions may also refer to parts without crystalline structure.

Lyotropic liquid crystals are known to exist in at least three basic configurations

(cubic, hexagonal and lamellar). The lamellar phase can show the layers ordered in plan sheets (**Figure 10A**), or with the layers ordered in closed concentric “shells” (-EZRAHI *et al*., 1999). For the polarized light micrograph of this closed concentric “shells”, i.e. an isotropic spherical droplet covered by the lamellar liquid crystal (the focus of this thesis), it is possible to observe a characteristic pattern, called the Maltese cross (ONDRIS-CRAWFORD *et al*., 1991). This pattern is observed on **Figure 11.**

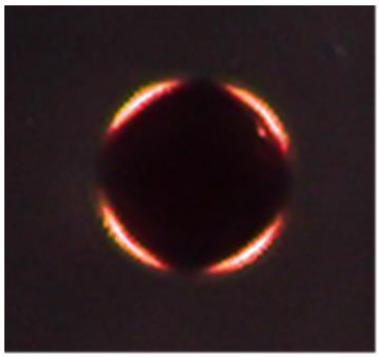

Figure 11: Maltese cross pattern observed by polarized light microscopy for a drop covered by lamellar LC.

The dark region dividing the circle into four quadrants (cross) corresponds to the points where the orientation of the anisotropic material is the same as that of the crossed polarizers (CARLTON, 2011). These dark axes do not change direction when the sample is rotated, in other words, the liquid crystalline structure is radially symmetrical (BAGHERI *et al.,* 2012). **Figure 12** shows an illustrative two-dimensional scheme for this situation, where the black cross represents the anisotropic material parallel to the polarizing filters.

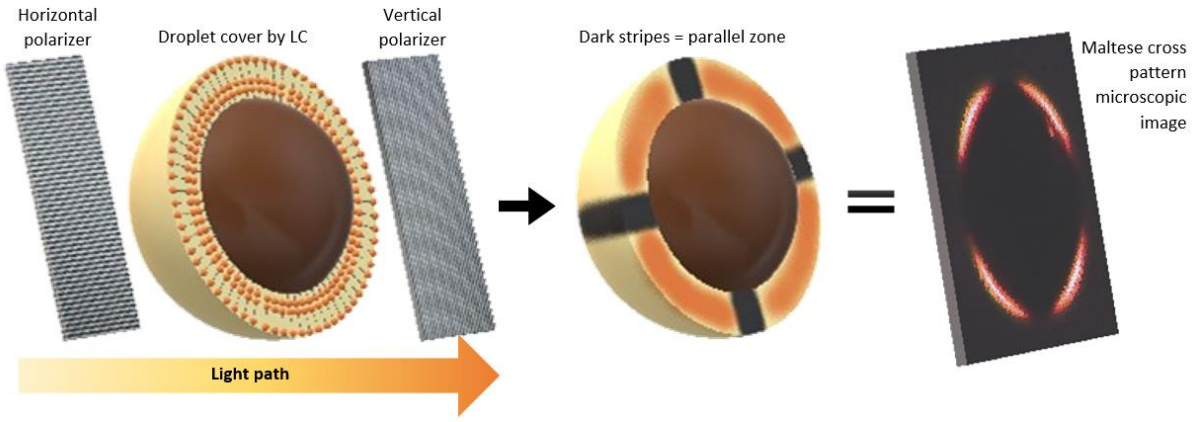

Figure 12: Illustrative two-dimensional diagram of the droplet covered by anisotropic material (LC), whose dark stripes represent the points at which the material is parallel to the polarizers.

Emulsions containing dispersed droplets with lamellar LCs (as represented previously in **Figure 5**), under polarized light will present their droplets with this Maltese cross pattern. **Figure 13** shows a polarized light micrograph of an emulsion containing dispersed lamellar liquid crystalline structures.

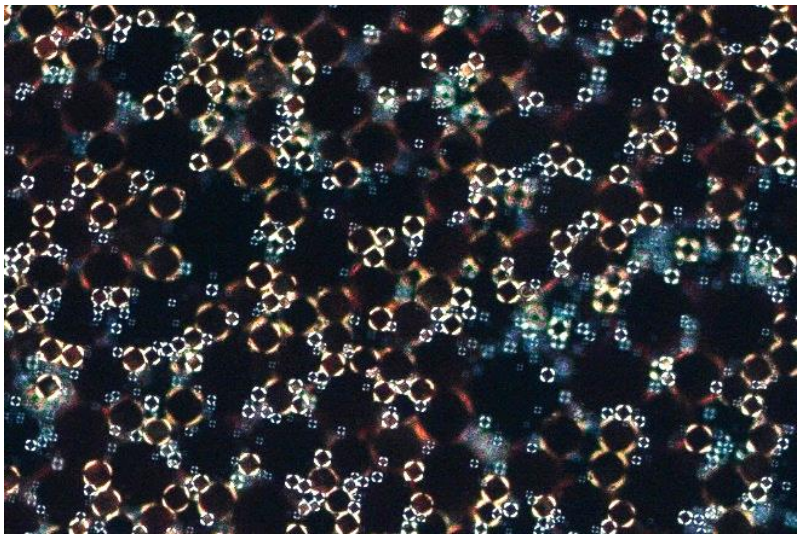

Figure 13: Polarized light micrograph of an oil/water emulsion containing lamellar liquid crystalline structures.

The geometry of the microscope and the properties of the coverslip to be used play a key role in the observations of these liquid crystal structures. There are two types of microscopes: regular, where the objective lenses are positioned above the sample; and inverted, where the lenses are at the bottom of the sample. **Figure 14** illustrates these two microscope models. There are also two types of possible light microscopy: transmitted and reflected light. In the transmitted mode, the light passes through the sample and is captured by the sensor; in the reflected mode, light does not pass through the sample, so the light captured by the sensor is the light that was reflected by the sample. Liquid crystals in petroleum are observed in the reflected light. The transmitted light is note used because of the light absorption by the oil

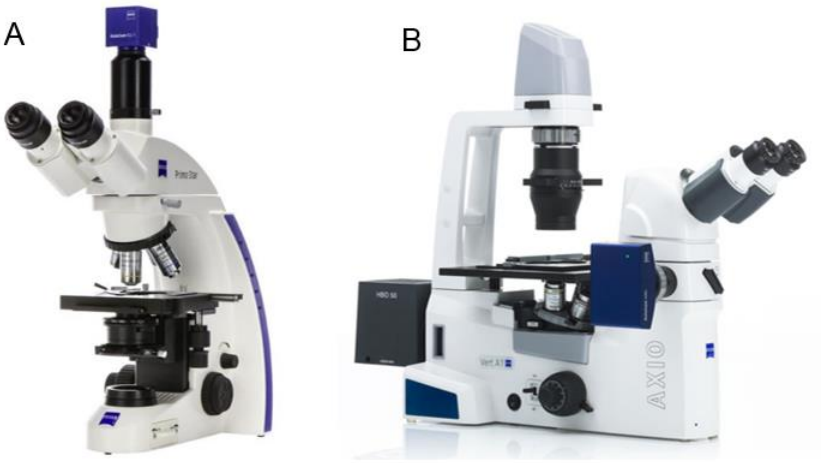

Figure 14: Microscopes (A) regular and (B) inverted.
(www.zeiss.com)

The type of coverslip to be used is also of fundamental importance (**Figure 15**). If the coverslip is transparent, the samples should be observed from the sample-cover slip interface. If the coverslip is opaque or reflective, LCs should be observed from the air-sample interface. LCs are not observed at the sample-air interface if a transparent coverslip is used, even if they are present in the sample (BAGHERI *et al*., 2012).

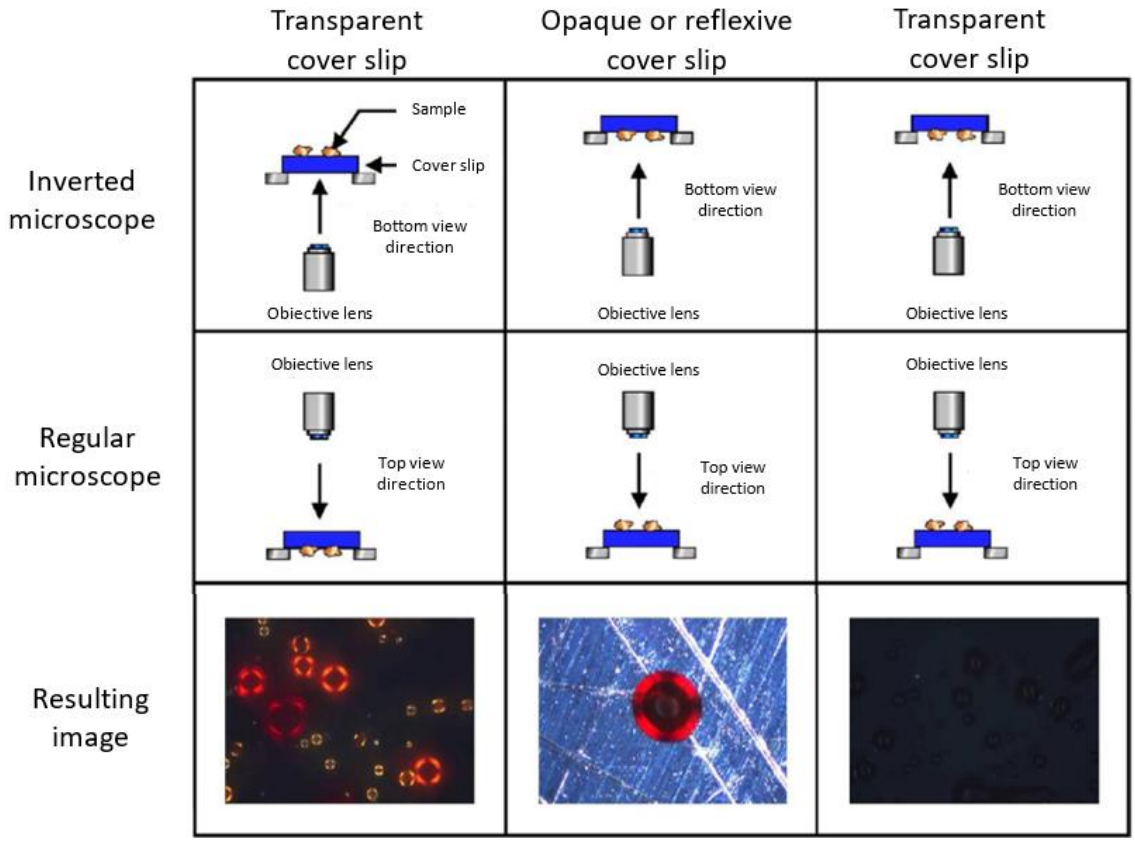

Figure 15: Polarized light microscope arrangements and the LC observation relation.
(BAGHERI *et al.,* 2012).

2.3. CRUDE OIL EMULSIONS

Until today, studies based on the crude oil emulsion stabilization by LC structures are scarce, as well as characterizations of the molecules and the mechanisms of formation. Because of this, potential problems associated with them are unknown. LCs in crude oil emulsions may play a role similar to that of cosmetic emulsions, with possible stability implications. Urdahl and Sjöblom (1995) suggested the presence of LCs located at the interface of emulsion droplets, being able to reduce their mobility and prevent coalescence. However, the first reports of liquid crystalline structures in crude oil emulsions are from the early 2000s (HORVÁTH-SZABO *et al.*, 2001a).

The production, recovery, and refining of crude oil are processes based on the use of large amounts of water (HIROMI *et al*., 2007). This water can be original from the reservoir or injection water. Because of the density differences between the aqueous and oily fractions, the presence of surfactants, and the turbulent flow regime, water and oil are mixed, forming emulsions, which are dispersions of one immiscible liquid in another (THOMPSON *et al*., 1985; URDAHL and SJÖBLOM, 1995; CLINGENPEEL *et al.* 2017, XU *et al*., 2016).

Emulsions can be formed from the reservoir, where oil and water flow through narrow pores and form droplets, until of the end of processing, where the oil undergoes a reduction of pressure in the choke valves causing the intense mixing of oil and water (SJÖBLOM *et al*., 2003). They can be unstable and easily separated, or stable. In any case, they must be broken to separate oil and water in order to increase the yield of the process (SIMMONS *et al*., 2002; CLINGENPEEL *et al.* 2017), satisfy the export and transportation specifications and comply with environmental legislation. The co-produced water in the form of an emulsion is highly undesirable, from the point of view of the process and from the quality of the product (SJÖBLOM *et al*., 2003; SZTUKOWSKI and YARRANTON, 2005a).

2.3.1. Compounds with Interfacial Activity

Emulsion stability may be related to physical factors (temperature, shear rate, water content, phase density, viscosity, etc.) as well as related to the compositional chemical aspects of the oil.

It is known that petroleum is a multi-component matrix. Different compounds present in the crude itself, such as asphaltenes, resins, waxes and fine solids act in the processes of emulsion stabilization (HODGE and ROUSSEAU, 2003; SJÖBLOM *et al*., 2003; KOKAL, 2005; SZTUKOWSKI and YARRANTON, 2005a; VISITIN *et al*., 2005; KASUMU *et al*., 2013; MARTINS *et al*., 2016; PRADILLA *et al*., 2016).

The waxes, due to their non-polar hydrocarbon structure, do not have interfacial activity; however, they can act in the emulsion stabilization forming a physical network that imprisons the water droplets forming a gel, as represented in **Figure 16** (VISITIN *et al*., 2008; BINKS and HOROZOV, 2008).

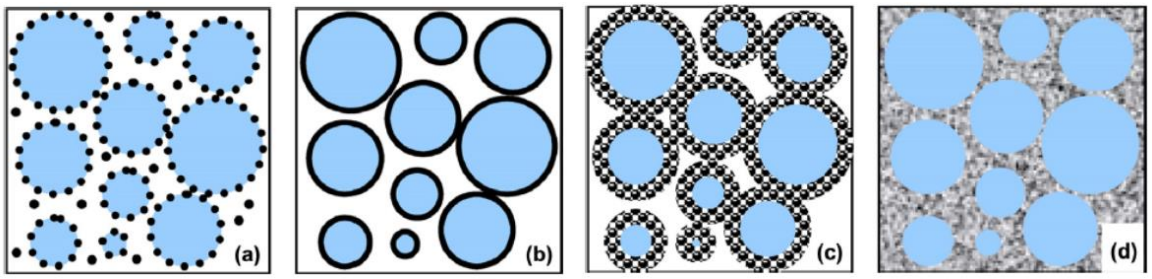

Figure 16: Representation of the gelation process of the waxy emulsions in (a) waxes on the drop of water; (b) waxes covering the drop; (c) solid wax flakes growing in and between the drop; d) water droplets trapped in the waxy network.
(VISITIN *et al*., 2008).

Other studies suggest the asphaltenes as the main stabilizing agents for water and oil emulsions, acting at the interface (SJÖBLOM, 2001; WEI *et al.*, 2016). However, these molecules do not have hydrophilic heads as the surfactants themselves. Asphaltenes consist mainly of hydrophobic portions that are not amphiphilic (CZARNECKI *et al*., 2012). Dynamic measurements of interfacial tension (IFT) between water and organic phases containing asphaltenes are generally analyzed in terms of slow reorganization and interfacial relaxation. One of the arguments that supposedly support this conclusion is that the dynamics of this process is very slow compared to the diffusion time scale calculated from the asphaltenes mass concentrations (LIU *et al*., 2017).

Recently, Jarvis *et al.* (2015) developed a method to isolate interfacial material from crude oil. This method consists of a chromatographic extraction with silica gel column, where an oil/heptol/silica mixture is added, and then eluted with heptol (fraction 1); methanol/toluene (fraction 2); and lastly, alcohol. Results of shear rheology performed by Ligiero *et al*. (2017) in systems using interfacial materials extracted by

the method of Jarvis *et al.* indicate the formation of an elastic film at the interface. This elastic response is stronger when the predominant interfacial compounds have high molecular weight.

The IFT between oil and water plays an important role during production and processing in the petrochemical industry. According to Andersen *et al*. (2017), due to Gibbs adsorption, natural surfactants adhere to the oil/water interface, reducing interfacial tension and in some cases generate an interfacial film. In their studies, Andersen *et al.* evaluated different compositions of interfacial films, removing for example naphthenic acids (NA) and asphaltenes. They observed that oxygenated compounds, carbonyls and a specific type of aromatics are concentrated in the film.

Clingenpeel *et al.* (2017) also used the method of Jarvis *et al*. and found that the extracted fraction containing interfacial material (about 1.0 wt. %) generates a stable emulsion when mixed with water. The fraction without interfacial material did not generate stable emulsions. In addition, the authors performed the characterization of this concentrated fraction of material with interfacial activity by Electrospray Ionization (ESI) and Fourier-Transform Ion Cyclotron Resonance (FT-ICR) mass spectrometry. Thousands of species were identified, and the most abundant contained oxygen, thus suggesting that interfacial activity is directly related to the presence of oxygenated chemical functions. In addition, thousands of dicarboxylic acid species were found. Stability tests with emulsions containing these species revealed extremely stable emulsions.

Valencia-Dávila *et al.* (2016) evaluated seven fractions of NAs of different molecular weights (M_w 451-937) extracted from an acid oil with total acid number (TAN) of 5.3 mgKOH/g. They observed that the stability of emulsions varied according to the molecular weight of the NAs extracted.

Both the stability of the emulsion and the interfacial properties depend on the composition of the crude oil and its native natural surfactants. These compounds encompass species that may even form LC. Studies suggesting the NAs as responsible for the formation of interfacial films and increasing the crude oil emulsion stability (HORVÁTH-SZABO *et al.*, 2001a and 2001b).

Varadaraj and Brons (2007a; 2007b) indicate that the NAs are more interfacially active than the asphaltenes, and still have synergistic effects of interaction with asphaltenes. The studies by Ese and Kilpatrick (2004) suggest that naphthenic acids

and their relative salts (naphthenates) are responsible for forming LC at water and oil interfaces.

2.3.1.1. Naphthenic Acids

Naphthenic acids has a general formula R-COOH, where R represents the cycloaliphatic structure. The term "naphthenic" encompasses all carboxylic acids present in crude oil. Almost all crude oils contain NAs since their formation is linked to the biodegradation of the oil in the reservoir (SJÖBLOM *et al*., 2003).

The NAs molecules contain two basic components: hydrocarbon chains of various sizes (with or without side chains or cycles) and carboxyl groups. It contains 5 to 33 carbons, resulting in molecular weights of approximately 100 to 500 g/mols (CLEMENTE *et al.*, 2003; TAYLOR *et al*., 2005). They have characteristics of surfactants due to their carboxyl functional group that is hydrophilic, and its hydrophobic tail. The petroleum naphthenic acids are considered weak acids with dissociation constants in the range of 10^{-5} to 10^{-6}. The average solubility in water is generally less than 50 mg/L (BRIENT *et al*., 2000). **Figure 17** shows some examples of naphthenic acids structures.

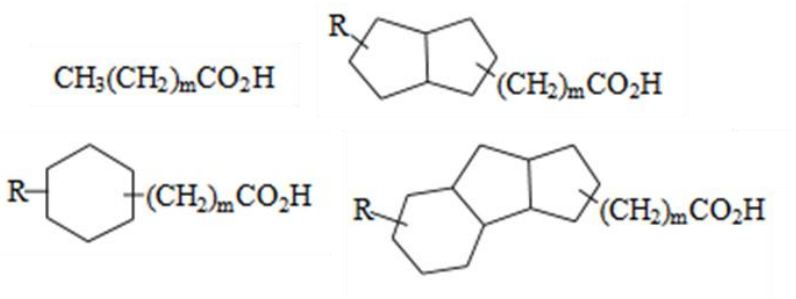

Figure 17: Examples of naphthenic acids structures.

During crude oil production, it is common to find cations of different natures solubilized in the aqueous fractions (mainly sodium or calcium). These cations may have a natural origin or may be injected in the form of hydroxides in order to assist in reducing the interfacial tension between the aqueous and oily phases, favoring the removal of the oil from the rocks (CLEMENTE *et al*., 2003, GAO *et al*., 2010). The alkaline additives react with the NAs, forming the naphthenates (HORVÁTH-SZABÓ *et al*. 2002). According to Brandal *et al*. (2005), the formation of these salts can occur in two ways. The first one suggests that a small part of the total NA of the oil has short

chains, which are soluble in water, and thus the reaction of NAs and alkalis occurs in the aqueous phase. In the second way, it suggests that the formation of naphthenates occurs at the oil-water interface itself since most oil NAs are large molecules, soluble in oil. They accumulate at the interface and react with the alkalis due to the large interfacial areas promoted by the emulsion (SIMON and SJÖBLOM, 2016). Under certain conditions, the naphthenates may also stabilize the emulsions (ACEVEDO *et al*. 1999; BRANDAL *et al*., 2004).

Part of the Brazilian oil reserves consists of oils with high acidity (TEIXEIRA *et al*, 2003; FORTUNY *et al*., 2008). Except for the pre-salt fields, in the last years most of the crude oil reserves discovered in many parts of the world and in Brazil, are composed by unconventional oils with lower API gravity and high total acid number (MARTINS *et al.* 2018). **Figure 18**, extracted from Oliveira *et al.* (2013), shows the variation of the TAN in mgKOH/g of oil as a function of the API gravity for different Brazilian oils in the Campos Basin.

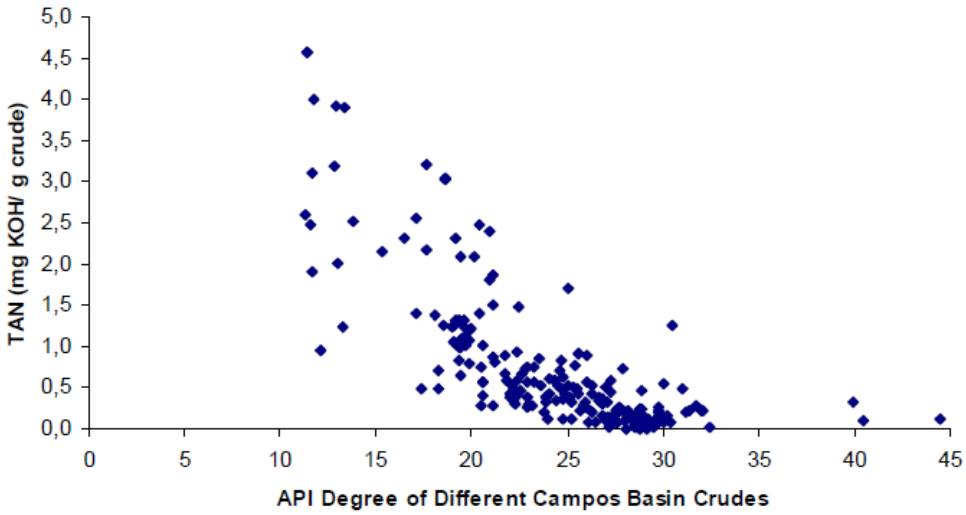

Figure 18: TAN variation *versus* API gravity for 218 oil samples from the Campos Basin. (OLIVEIRA *et al*., 2013).

Although there is no obvious linear correlation between TAN and API gravity, it is possible to identify a tendency between increasing acidity and increasing density. According to Sjöblom *et al.* (2003), heavy oils of geologically young formations have high acid contents, while paraffinic oils generally have a low acid content. In addition, the presence of aromatic compounds, olefins, and dibasic acids also contribute to the increase in the acidity content of the oil (BROWN and ULRICH, 2015).

In summary, it is verified that NAs, which have amphiphilic characteristics, can act at the oil-water interface. The TAN value of an oil is an indication of the total content of these naphthenic acids. Some Brazilian oils have a high acidity index, so they may contain high NAs content. Studies have pointed out that NAs can form lamellar LCs in crude oil emulsions, and may increase the stability of the emulsions. However, stable emulsions are not desirable in the petroleum industry. Until the present moment, there have been no reports of LCs in Brazilian oils. Therefore, the study of liquid crystals in Brazilian crude oil emulsions is of great interest.

2.4. LIQUID CRYSTALS IN CRUDE OIL SYSTEMS

As stated earlier, there are not many papers about LCs in crude oil systems. There are only two research groups in Canada that study this topic (Shaw group and Horváth-Szabó group), and a few isolated papers from other authors. Thus, the publications in this topic are organized in chronological order to show the evolution of the knowledge about LCs in crudes.

In his 1995 paper, Urdahl and Sjöblom isolated interfacial material from crude oil fractions from the North Sea. They formulated two model emulsions of water and n-decane: one containing tetraoxyethylene nonylphenol ether as a model surfactant; and another using interfacial material extracted from the oil. In this proposal to investigate whether the material extracted from the oil was able to stabilize emulsions, they found that not only they were able to maintain stable emulsions, but also that these compounds may be associated with lamellar liquid crystalline phases. This work presented the first indications of liquid crystalline structures in crudes.

Horváth-Szabó *et al*., (2001a) in their first study, used commercial sodium naphthenates with similar characteristics to the naphthenates found in Canadian bitumens, in water. They suggest that if water and surfactant system contains LCs, possibly by adding a third oil phase to the medium, the liquid crystal structures will continue to exist. The LCs visualized by them in that work had a lamellar flat multilayer structure (**Figure 19A**). In their second work, Horváth-Szabó *et al.* (2001b) added toluene to the water-sodium naphthenate system. Emulsions were prepared using 20 shakes of two minutes each within 48 hours. They were then centrifuged for destabilization. **Figure 19B** shows polarized light micrograph of one of the fractions of

these emulsions. In this case, it is possible to note the presence of multilayer of surfactant around the droplets of the emulsion, i.e., lamellar LCs around the micelles. Emulsions in the presence of the interfacial liquid crystalline phase were very stable. The presence of lamellar LC caused higher stiffness of the interface, increasing stability.

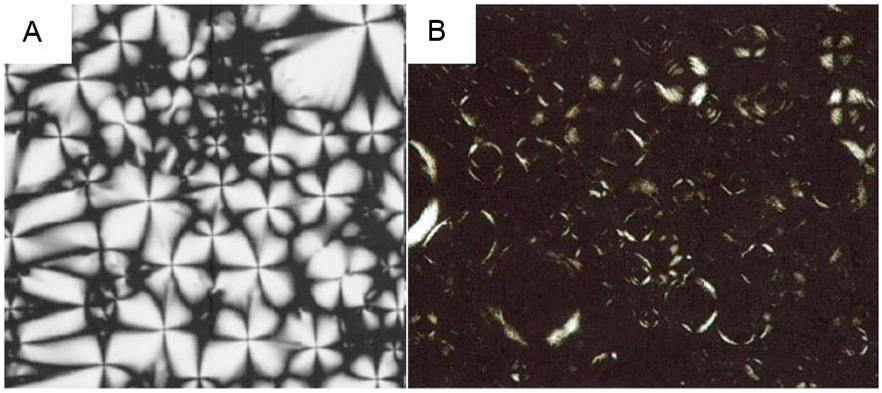

Figure 19: Polarized light microscopy of (A) flat multilayers of lamellar LC in the water-sodium naphthenate system and (B) Maltese cross pattern from lamellar LC around the micelle in water-sodium naphthenate-toluene.
(HORVÁTH-SZABÓ *et al*., 2001a and 2001b).

In the subsequent work of Horváth-Szabó *et al.* (2002), the authors emulsified bitumen (previously dissolved in heptane and toluene) and NaOH solution, with vigorous agitation for 5 minutes and another four days on gentle and constant agitation. Thereafter the emulsion was destabilized by centrifugation. In the bottom phase of the centrifuge tube, i.e. the water-rich phase, it was possible to observe liquid crystal at the interface of bitumen droplets. The drops had the characteristic Maltese cross pattern. The layer composition consisted mainly of sodium naphthenates produced in situ. In addition, they verified that the coalescence of the droplets is made difficult by the mechanism described by Friberg correlations.

According to Horváth-Szabó *et al*. (2003), the first rule of Friberg correlations predicts high values of emulsion stability in the presence of lamellar liquid crystals. According to this rule, the high viscosity of the liquid crystalline phase hinders the process of reducing the interfacial film thickness between the droplets of the emulsion. Thus, coalescence becomes slow. On the other hand, the LC layer improves the interaction between the droplets, favoring flocculation.

Continuing this research, Horváth-Szabó *et al.* (2003) investigated the effects of heptane addition on the phase behavior of its sodium naphthenate-toluene-water

system. They found that the addition of heptane and the increase in temperature adversely affect the formation of lamellar LC in the emulsion while favoring the formation of microemulsions.

In the studies of Sjöblom *et al.* (2003), they suggested that the surfactant bilayers contain layers of intervening water, as represented in the scheme of **Figure 20**.

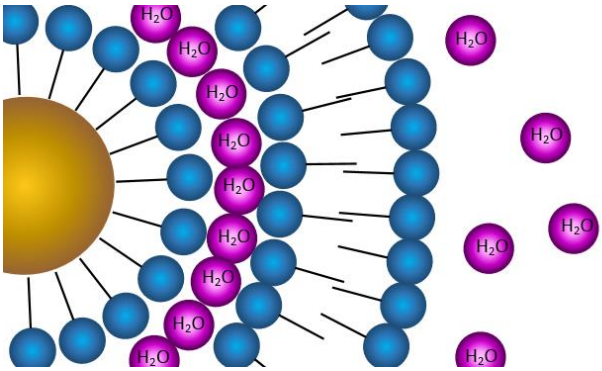

Figure 20: Representation of water intercalated between the surfactant multilayers of a lamellar liquid crystalline structure.

In addition, Sjöblom *et al*. (2003) evaluated the interfacial tension between cyclohexane and aqueous phases with different pHs, and various concentrations of commercial naphthenic acid. The results are shown in **Figure 21**. It is observed that the undissociated form of NA is dominant at low pH. As the pH increases and the acid dissociates, a marked decrease in IFT occurs.

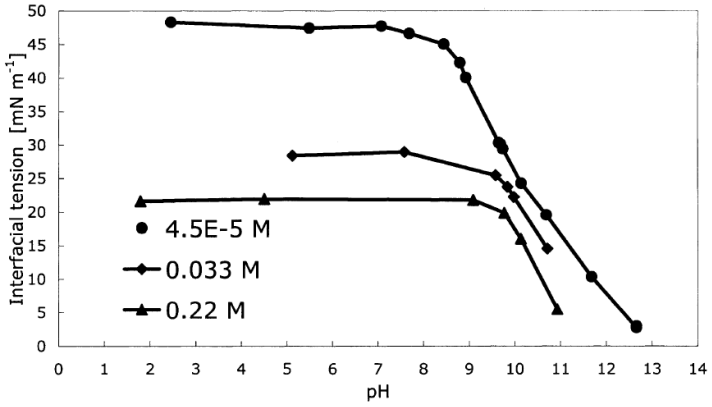

Figure 21: Interfacial tension between cyclohexane and water as a function of pH for three concentrations of commercial NA.
(SJÖBLOM *et al.,* 2003).

Ese and Kilpatrick (2004) analyzed the phase inversion of model emulsions (oil phase composed of toluene and n-heptane), stabilized with three distinct naphthenates, varying pH and concentration of surfactant. They found that at high pH the emulsions formed were the oil-in-water type. At lower pH (pH <10) inversion of the emulsion occurred.

Taylor *et al*. (2005), in partnership with the Horváth-Szabó group, suggest that the interfacial films with lamellar structure are formed step-by-step. The surfactant layers are added gradually, i.e. a new layer is added to an already existing layer, resulting in an increase in the interfacial film thickness.

In the studies of Horváth-Szabó *et al*. (2006) the Friberg correlations are detailed. They used model systems composed of toluene-heptane, aqueous and alkaline solutions, and as surfactants commercial naphthenic acids or NA extracted from bitumen. The authors assume the presence of LCs in acidic and alkaline aqueous fractions systems, through the following justifications: 1) existence of LC in sodium naphthenate-water-toluene and heptane systems; 2) LC at the oil-water interface when NAs are dissolved in the oil phase and NaOH is dissolved in the aqueous phase; 3) NAs are present in oils and bitumen; 4) LC can be observed in bitumen-toluene and heptane-alkaline solution systems; 5) an increase in the stability of bitumen emulsions can be observed above a specific concentration of sodium naphthenates.

Czarnecki *et al.* (2007) and Czarnecki (2009) used emulsions of water and diluted bitumen, without the addition of extra surfactants or oil phases. They observed birefringent material in the emulsion droplets, probably LC. Several water droplets in the oil phase (top fractions of **Figure 22**) and the oil droplets in the aqueous phase (bottom fractions of **Figure 22**) show optical anisotropy on their surfaces. Although the authors do not claim that this anisotropy is due to the liquid crystalline material, even there is strong evidence indicating this possibility.

In the studies of Czarnecki (2009), it was verified by means of mass spectrometry that the composition of the material found in the surfaces of the drops does not match with asphaltenes and resins. Most of the adsorbed species found contain oxygen and sulfur. In addition, this material contains a non-polar fraction with low C/H ratios.

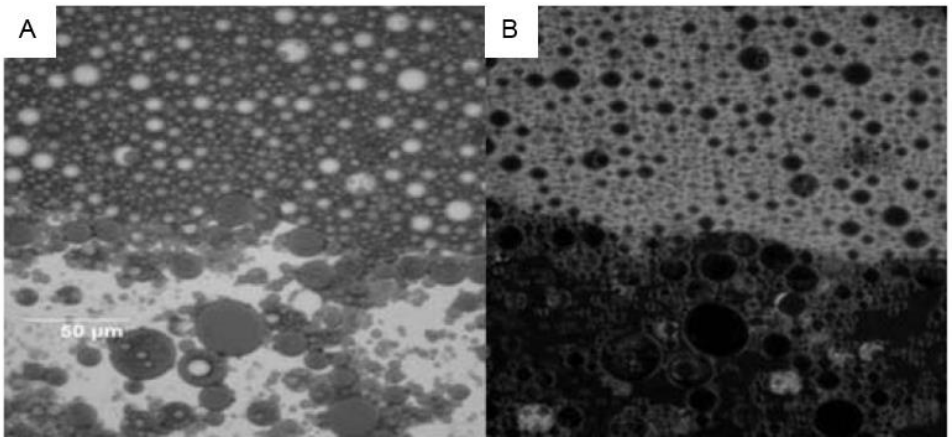

Figure 22: Micrographs from the same coverslip point of diluted bitumen and water emulsion, after centrifugation at (A) bright field and (B) polarized light.
(CZARNECKI *et al*. 2007).

Bagheri *et al.* (2010 and 2012) observed amphotropic LCs (with lyotropic and thermotropic characteristics) in crude oil asphaltic fractions and bituminous sands, extracted with pentane and heptane, that is, they are not emulsions. The structures observed by them were only visible between about 65 and 160 °C, depending on the sample, or at room temperature (25 °C) when exposed to a toluene atmosphere. **Figure 23** shows a polarized light micrograph of one of the isolated asphaltene fractions at 57 °C approximately. The particles have the same Maltese cross pattern relative to the lamellar LCs, however, in this case, its interior is composed of isotropic solid relative to the asphaltene fraction without liquid crystalline organization.

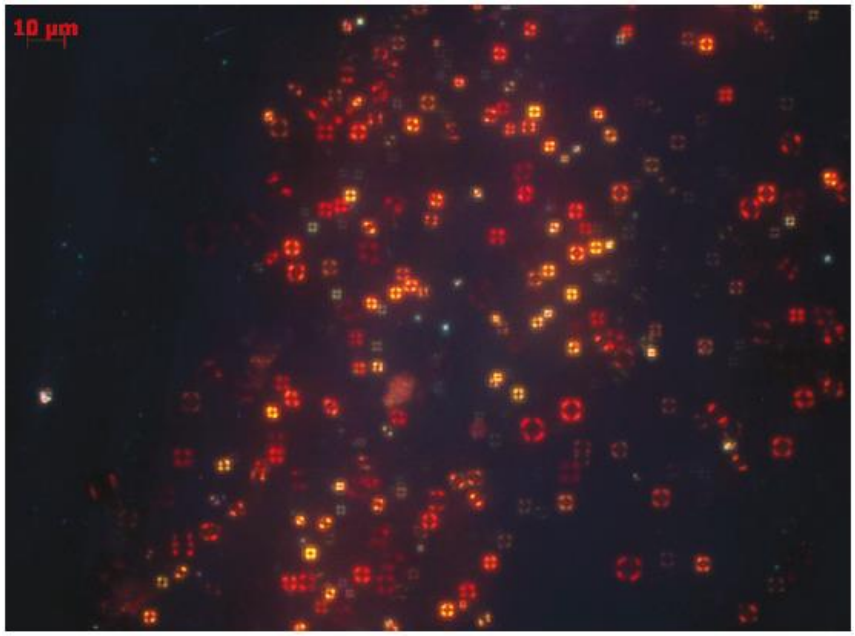

Figure 23: Maltese cross patterns in an isolated asphaltenic fraction at approximately 57 °C.
(BAGHERI *et al*. 2010).

The authors stated that the liquid crystalline material extracted from these fractions comprises more than 10,000 different compounds, the average molecular size of which is smaller than the asphaltenes but has heteroatoms relative to asphaltenes. In addition, Bagheri *et al.* (2010) state that asphaltenes are thin solids at room temperature so these molecules hardly act as LCs in an interface.

In the most recent study, Bagheri *et al*. (2012) evaluated the effect of temperature on the LCs and verified that when they were heated, the structures disappeared and did not reappear after cooling. This happens because the LC remains on the surface, but with the heating, its structure becomes disordered, and cannot be reordered only with cooling. In summary, the LC transition is not reversible. Most lamellar liquid crystal structures are arranged that their polar groups strongly interact with each other, forming some kind of solid like crystal pattern, while the hydrophobic tail organization is much looser and liquid-like, due to the weaker London interactions. Two effects can alter the overall rigidity of these liquid crystals. One is the weakening of polar interactions with other compounds leading to some disparity in the molecular size and shape. The other is the disorder caused by the temperature increase, which increases the molecular motion and reduces the directional forces such as polar interactions (SALAGER and ANTÓN, 1999).

The details of the LC formation process in petroleum emulsion systems are unknown at the present moment. However, as the material must be transported through a viscous medium until it reaches the outer surface, the formation of LC may be coupled to a kinetic control rather than being controlled by an equilibrium process. In addition, Bagheri *et al.* (2012) suggest that the material capable of forming LC possibly prefers to act on small particles rather than on large particles.

According to Qin (2014), in laboratory tests with emulsions prepared with bituminous sands from Canada, spheres of isotropic material, ranging from 5.0 to 50.0 μm in diameter, were involved by liquid crystalline material. However, the emulsions form only with some specific bitumen fractions as the asphaltenic, removed with heptane or with pentane. **Figure 24** shows the polarized light micrograph of the lamellar LCs in water for an emulsion aged for three months. The presence of LCs over a long period further endorses their role in stability.

The transfer mechanisms of the interfacial activity material from the oil phase to the aqueous phase are not yet known, and *in situ* observation remains unfeasible. However, some mechanisms are suggested by Qin (2014): 1) agitation induced by the

evaporation of water through a hydrodynamic mechanism during heating to 200 °C; 2) volatilization of the constituents of bitumen below 200 °C and dragging the molecules responsible for the LCs to the aqueous phase; 3) the transfer takes place during the cooling, below 200 °C, as the water dissolved in the bitumen-rich phase passes to the water-rich phase; 4) the molecules with interfacial activity move to the interface bitumen-water and are transferred by interfacial or thermodynamic phenomena, independent of the transfer of water or light hydrocarbons. None of these plausible mechanisms can be ruled out, but until today, there is no consensus.

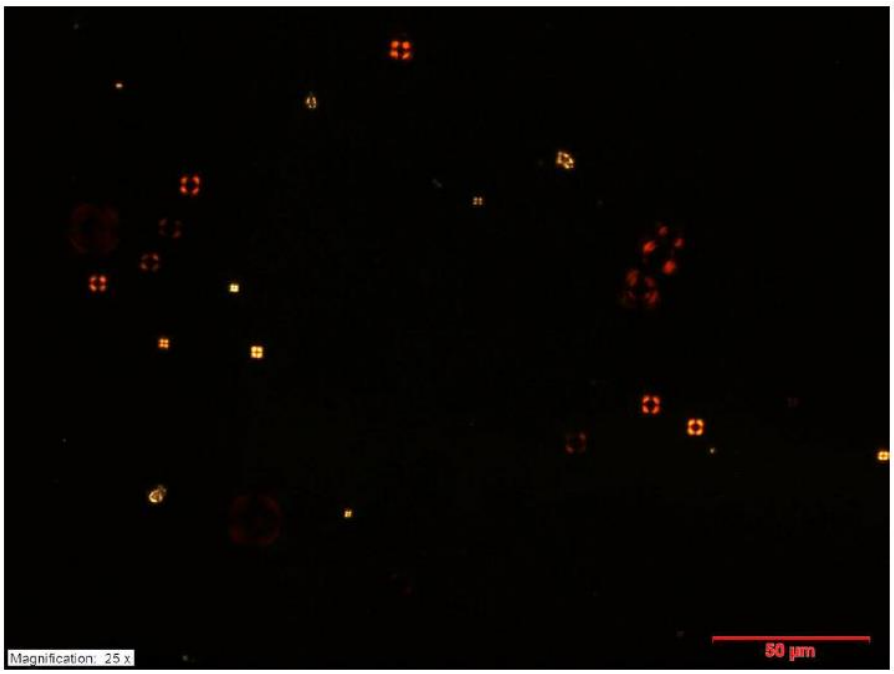

Figure 24: Polarized light micrograph of lamellar LC, in an emulsion aged for three months. (QIN, 2014).

As already discussed, the observation of structures with Maltese cross pattern in emulsions may indicate the presence of lamellar liquid crystals (Bagheri *et al*., 2012). This pattern was detected in Brazilian oil systems for the first time in the bottom fraction of a destabilized emulsion with 5.0 wt. % of deionized water in paraffinic oil, aged for three months, at room temperature (DUNCKE *et al*., 2016). This system was characterized by a color difference between the top and the bottom fraction due to the droplets sedimentation process, as observed in **Figure 25A**. Both fractions were submitted to microscopic analysis. In **Figure 25B,** it is possible to observe Maltese cross patterns, obtained in the bottom phase, rich in water.

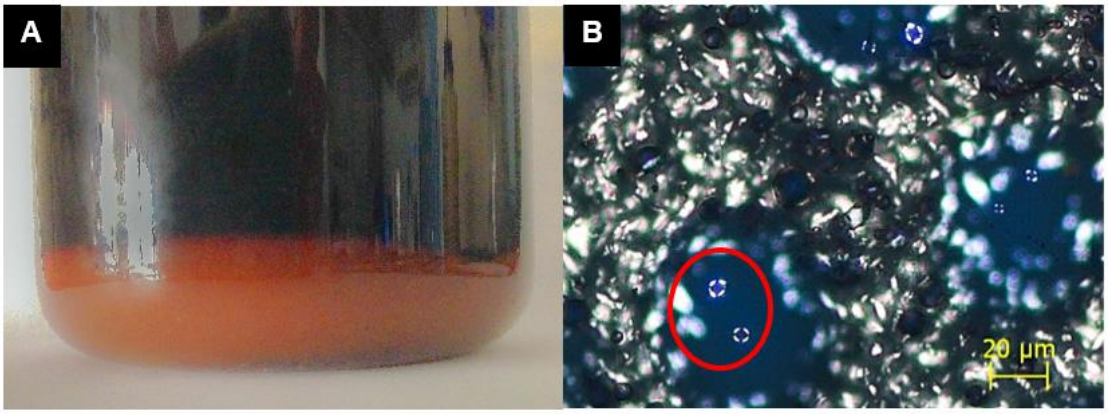

Figure 25: (A) water-oil emulsion with 5.0 wt. % of water, aged for 3 months and (B) polarized light micrograph of the bottom phase, with structures exhibiting Maltese cross optical pattern.

3. ORIGINALITY OF THESIS

The Maltese cross pattern observation may indicate the presence of lamellar LCs. This pattern was observed for the first time in Brazilian crude oil emulsions in this work, and from the doubts generated about this observation, this thesis was originated. The main objective is to investigate the influence of some factors in the LC formation, as wax and salt presence, aqueous phase content, volume and valence of the cation, and crude oil type; as well as to extract and characterize the interfacial material capable to form LC. As observed in the literature reports, there is no investigation about the influence of the factors cited above in the LC formation. Therefore, this thesis presents original content.

4. LIQUID CRYSTAL FORMATION

The presence of liquid crystalline structures in the crude oil-water interface is surrounded by some unanswered questions. This chapter will evaluate the influence of wax presence, salinity, water content, petroleum TAN values, pH and cation volume and valence of the aqueous phase.

4.1. MATERIALS AND METHODS

4.1.1. Materials

4.1.1.1. Crude Oil

Seven crude oils, identified as P1-P7 supplied by Petrobras were selected.

4.1.1.2. Aqueous Phases

Eight aqueous phases were used: deionized water (0.50 µS/cm at 25.0 °C); saline solution with 35.0 g/L of sodium chloride (NaCl), (Sigma Aldrich); alkaline solutions with $1.0x10^{-4}$ mol/L (pH 10.0) and $1.0x10^{-2}$ mol/L (pH 12.0) of sodium hydroxide (NaOH), potassium hydroxide (KOH) and calcium hydroxide ($Ca(OH)_2$), all from Sigma Aldrich.

4.1.2. Physico-Chemical Characterization

4.1.2.1. Density

The density values (ρ) of the crude oils were measured at 20.0 °C on the SVM 3000 (Anton Paar), following the ASTM D7042.

4.1.2.2. API Gravity

By density values, determined following the ASTM D7042, at 20.0 °C, it is possible to obtain the densities at 60.0 °F (15.6 °C) following **Equations 1** and **2**, and

the API gravity following **Equation 3** (BRASIL, 2017). API gravity is the most general classification in the petroleum industry.

$$0.639 \leq \rho_{20°C} \geq 0.931 \rightarrow \rho_{60°F} = 0.0156\rho_{20°C}^2 + 0.9706\rho_{20°C} + 0.0175 \quad (1)$$

$$0.931 \leq \rho_{20°C} \geq 1.055 \rightarrow \rho_{60°F} = 0.0638\rho_{20°C}^2 + 0.8769\rho_{20°C} + 0.0628 \quad (2)$$

$$°API = \frac{141.5}{\rho_{60°F}} - 131.5 \quad (3)$$

4.1.2.3. Viscosity

The crude oil dynamic viscosity (μ) determination was carried out in the Discovery Hybrid Rheometer (DHR) of TA Instruments, equipped with a 40.0 mm parallel plate. A flow ramp test was carried out with the shear rate from 0.1 to 200.0 s^{-1}. The temperature was 25.0 °C and the duration of the test was 8 min.

4.1.2.4. SARA

The saturated, aromatic, resins and asphaltenes (SARA) content for the paraffinic oils (P1-P2 and P7) was obtained by thin layer chromatography with flame ionization detection (TLC-FID) using Iatroscan MK-6 (NTS International). For the oils P3 and P5, the SARA content was obtained by micro distillation cut at 260.0 °C. The micro distillation was carried out using a manual micro distiller, according to an internal procedure from CENPES-Petrobras. The P1-P3, P5 and P7 SARA analyzes were performed at CENPES-Petrobras. For the oils P4 and P6, the ASTM D2549 was used for separation of aromatics and non-aromatics fractions of high boiling oils by elution chromatography, and ASTM D6560 for determination of asphaltenes (heptane insoluble). The P4 and P6 SARA analyzes were performed on LabPetro-UFES.

4.1.2.5. Total Acidity Number

The TAN was determined using titrator Titrando 836 (Metrohm) according to the ASTM-D664 method, with a 0.1 mol/L of KOH solution. A solution containing 495.0 ml

of isopropyl alcohol, 5.0 ml of deionized water and 500.0 ml of toluene was used to dilute the oil.

4.1.2.6. Wax Appearance Temperature

Nano differential scanning calorimeter (DSC), from TA Instruments, was used to determine the wax appearance temperature (WAT) of the oils. Prior to measurements, the samples were homogenized and kept under vacuum for degasification for at least 30 min. Kerosene was used as reference. The following steps were carried out: 1) heating the 300 μL of samples from room temperature to 80.0 °C (2.0 °C/min); 2) conditioning at 80.0 °C for 15 min; 3) cooling from 80.0 °C to 4.0 °C (0.5 °C/min); 4) conditioning at 4.0 °C for 15 min; 5) heating from 4.0 °C to 25.0 °C (2.0 °C/min). The analyses were performed at Labter-EQ-UFRJ.

4.1.2.7. Wax Content

It is possible to obtain the total thermal effect of the wax precipitation (Q) by integrating the area of the exothermic peaks obtained by DSC. With this value, an estimated wax concentration (c_w) can be determined following **Equation 4** (YI and ZHANG, 2011). $\bar{Q}$ is 210.0 J/g, the thermal average wax crystallization enthalpy in crude oils (CHEN *et al*., 2004). WAT is the WAT temperature itself and T_f is the final temperature, in this work, 4.0 °C.

$$c_w = \frac{\int_{T_f}^{WAT} dQ}{\bar{Q}} = \frac{Q}{\bar{Q}} \tag{4}$$

By means of simple math, it is possible to calculate the mass fraction of precipitated waxes (w) as shown in **Equation 5**, where ρ is the sample density, and V is the experimental volume used for the DSC measurement (300 μL).

$$w(\%) = \frac{c_w}{\rho . V_e} . 100 \tag{5}$$

4.1.2.8. Naphthenic Acid Distribution

Fourier-Transform Ion-Cyclotron-Resonance Mass Spectrometry (FT-ICR-MS) obtains the naphthenic acid distribution and the respective average molecular mass of each fraction. The results are provided by Petrobras, and no further information about the technique was provided.

4.1.3. Thermal History Removal

Because of paraffinic oils use (P1-P2 and P7), before the use of these samples, it is essential to remove the thermal history in order to guarantee the total solubilization of pre-existing wax crystals. The thermal history of the oils P1-P2 and P7 was removed by heating flasks of 100 mL of oil for 2 h at 80.0 °C in a circulation oven (400-3ND, from Ethik Technology). According to Li and Zhang (2003) and Pedersen and Rønningsen (2000), this condition is sufficient to dissolve all wax crystals present in the oil.

4.1.4. Emulsion Preparation

The emulsions were prepared using 20.0, 50.0 or 80.0 wt. % of the aqueous phase, with the mechanical agitator PT 3100 (Polytron), at 6,000 rpm for 3 min at 25.0 °C. A total of 150.0 g of emulsion was produced for each procedure.

4.1.5. Emulsion Destabilization

The destabilization of the 20.0 and 50.0 wt. % emulsions prepared (**item 4.1.4**) was carried out in a centrifuge 3-18K (Sigma) at 6,000 rpm at 60.0 °C. The phase separation was evaluated at every 30 min, and the maximum centrifugation time was defined as 2 h. The emulsions prepared with 80.0 wt. % of aqueous phase were characterized by the spontaneous separation of phases, therefore not been subjected to centrifugation.

4.1.6. Water Content Determination

The top phases (rich in oil) separated after the destabilization step, were titrated with Karl Fisher reagent in potentiometric titrator Titrando 836 (Metrohm), with double Pt-wire electrode, in order to measure the residual water content.

4.1.7. pH Determination

The bottom phases (rich in water) separated after the destabilization step, were submitted to pH analysis in order to verify the aqueous phases pH changes after the emulsification. The pH analysis was carried out on the potentiometric titrator Titrando 836 (Metrohm).

4.1.8. Optical Microscopy

During all the experiments steps, microscopic analyses were carried out in parallel in order to follow the variations suffered in each system. The Axiovert 40 MAT (Carl Zeiss) inverted optical microscope equipped with the Axiocam MRc digital camera was used. Two lighting techniques were used: polarized light and bright field. The polarized light technique allowed characterizing the anisotropic optical behavior of crystalline material. The bright field technique was used to visualize non-birefringent emulsion components, such as water or oil droplets.

4.1.9. Interfacial Tension

4.1.9.1. Drop Method

The IFT using the drop method, between the oily and the aqueous phases were evaluated on goniometer Tracker-H (Teclis). An analysis interval of 3 h was used. The temperature was kept constant at 25.0 °C. The oil droplets volumes were the largest as possible for each system, ranging from 30.0 to 60.0 μL.

4.1.9.2. Wilhelmy Plate Method

The IFT using the Wilhelmy platinum plate was carried out on the K100 tensiometer (Krüss). The total time of analysis was 3 h, with one point per min. The temperature was kept constant at 25.0 °C.

4.1.10. Interfacial Rheology

Interfacial rheology tests were carried out in the goniometer Tracker-H (Teclis). In these tests, the crude oil samples were inserted in a syringe coupled to a U needle, which was immersed in the aqueous phase. The measurements were performed by the drop profile. Oscillatory volume tests were used, which provide drop volume variations *versus* time. The value of the total elastic modulus was determined by the response of the interfacial tension to the sinusoidal variations of the interfacial area and consequently of the volume of the drop. For that, 30 series of 30 cycles were used without oscillation (to organize the interface) plus 5 oscillatory cycles. Each cycle lasts 10 s. The tests had a total duration of 3 h. The maximum droplet sizes were about 30.0 to 60.0 µL (depending on the system). According to Alves *et al.* (2014), the droplet volume effect is small on the interfacial tension values. The oscillation amplitude of the droplets was 6.0 % of the maximum droplet volume, because of the nearly constant elasticity modulus is in this range. The viscoelastic modulus is less sensible in high amplitudes of the interfacial area than at lower oscillations (SZTUKOWSKI and YARRANTON, 2005b). The oscillation frequency selected was 0.1 Hz. The frequency of oscillation influences the elasticity values. For low frequencies, the surfactants have sufficient time for diffusion; on the other hand, for high frequencies, the diffusion is less important and the instantaneous elasticity is calculated (ALVES *et al.*, 2014)

4.2. RESULTS AND DISCUSSIONS

4.2.1. Physico-Chemical Characterization

The physico-chemical characterizations for the seven oils (P1-P7) are

presented in **Table 1**. It can be seen that the densities and the API gravity values are in agreement with the expected values for Brazilian crudes. In December 2018, the average API gravity of Brazilian oil was 27.2, with 37.4 % of the production considered light oil (≥ 31 °API), 49.0 % of medium oil (22 ≤ °API < 31) and 13.6 % of heavy oil (> 22 °API) (ANP, 2019). The terms light, medium and heavy oils, are related to the density, but the measure to which it is directly related to oil production and which must be taken into consideration is viscosity. The viscosity is the property that governs petroleum productivity (Anglo-Persian Oil Company, 2011). According to Cornelius (1987), oils with viscosities greater than 0.30 Pa.s are less fluid. Only the samples P4 and P7 show viscosities less than 0.30 Pa.s. The values presented in **Table 1** are the averages between the shear rate from 10.0 to 100.0 s^{-1}. P1-P7 exhibit viscosities independent of shear rate, i.e. all oils are considered Newtonian fluids. P3 present the highest viscosity (2.66 Pa.s).

Table 1: Crude oil physico-chemical characterization.

		P1	P2	P3	P4	P5	P6	P7
ρ (g/cm^3)		0.912 ± 0.004	0.910 ± 0.006	0.953 ± 0.012	0.919 ± 0.006	0.939 ± 0.005	0.943 ± 0.009	0.884 ± 0.002
API		23.1	23.4	16.4	22.1	18.6	17.9	28.0
μ (Pa.s)		0.47 ± 2.2x10^{-3}	1.07 ± 3.3x10^{-3}	2.66 ± 6.2x10^{-4}	0.24 ± 7.5x10^{-4}	0.59 ± 6.0x10^{-4}	0.93 ± 6.3x10^{-4}	0.06 ± 9.6x10^{-5}
Sat. *(wt.%)*		53.1	40.4	25.3 ± 0.6	51.5 ± 0.5	26.0 ± 0.7	39.2 ± 0.1	54.0
Aro. *(wt.%)*		25.6	16.2	44.8 ± 0.1	33.8 ± 0.4	48.4 ± 0.4	46.3 ± 0.5	24.0
Res. *(wt.%)*		21.1	42.7	21.1 ± 0.4	10.8 ± 0.1	15.6 ± 0.2	12.2 ± 0.1	22.0
Asp. *(wt.%)*		<0.17	0.65	8.70 ± 0.2	3.97 ± 0.1	10.0 ± 1.0	2.27 ± 0.1	<0.50
Wax content *(wt.%)*		2.19 ± 0.01	4.67 ± 0.01	0.13 ± 0.01	0.89 ± 0.01	0.24 ± 0.01	0.06 ± 0.01	3.09 ± 0.01
WAT *(°C)*	1st ev.	42.1 ± 0.3	52.2 ± 0.2	19.2 ± 0.4	42.1 ± 0.4	60.9 ± 0.6	19.0 ± 0.4	46.8 ± 0.2
	2nd ev.	23.5 ± 0.1	29.4 ± 0.2	--	17.6 ± 0.2	18.7 ± 0.4	--	25.6 ± 0.1
TAN (mgKOH/g)		0.64 ± 0.02	2.05 ± 0.01	3.04 ± 0.01	0.85 ± 0.01	2.76 ± 0.02	2.88 ± 0.01	0.33 ± 0.03

The saturated content for P3, P5, and P6, obtained by the SARA test, were the lowest of the six oils. These oils also had the lowest wax content (obtained by DSC baseline integration). It should be noted that the SARA techniques used were different (P1-P2 and P7 by TLC-FID; P3 and P5 by internal procedure; P4 and P6 by ASTM D2549 and D6560), so the comparison between the samples may not be ideal. In

addition, the wax content obtained only considers the waxes precipitated up to 4.0 °C, that is, waxes with lower crystallization points were not accounted for. The paraffinic oils P1, P2, and P7 show 2.2, 4.7 and 3.1 wt. % of precipitated wax respectively.

All samples present TAN values higher than 0.5 mgKOH/g, except the paraffinic oil P7 (0.33 mgKOH/g). According to Qian *et al.* (2001), the crude oils are classified as acidic when the TAN is higher of 0.5 mgKOH/g. In general, samples that have low acidity are originate from reservoirs with non-biodegradable oils. On the other hand, samples with high acidity have more biodegraded oil (MARTINS *et al.,* 2018). It is important to highlight that some Brazilian crude oils have high acidity, especially due to the presence of naphthenic acids. The samples P3, P5, and P6, whose are the heaviest (API gravity < 19), present TAN values of 3.04, 2.76 and 2.88 mgKOH/g, respectively.

4.2.2. Considerations about Liquid Crystal Observation

4.2.2.1. Crude Oils

The first LC observation on the Brazilian panorama was in an aged emulsion with only 5.0 wt. % of water (DUNCKE *et al.,* 2016). Considering this low water content, scanning of all the crude oil samples was carried out, in order to evaluate if there are liquid crystalline structures in the absence of water. **Figure 26** shows the polarized light micrographs for all dehydrated oils at 15 °C.

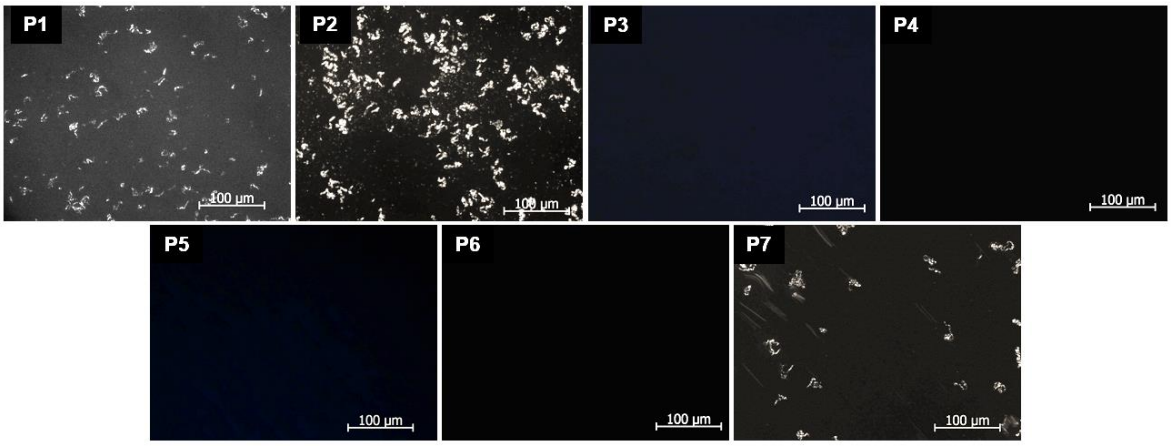

Figure 26: Polarized light micrographs for dehydrated oils P1-P7 at 15 °C.

As can be seen, no Maltese cross pattern was observed. Therefore, the liquid crystalline material is directly related to the presence of water in the system. This behavior is expected due to the lyotropic features of the lamellar LCs (as explained on **item 2.1.**).

Another characteristic observed in **Figure 26** is the wax crystal presence in the paraffinic oils. It is possible to note the highest precipitated wax content on the P2 (which have 4.7 wt. % according to the DSC integration baseline). The non-paraffinic oils (P3-P6) do not show any birefringent material at 20 °C, even having some wax content. Possibly the few waxes present are not precipitated at 20 °C, or the crystals are still too small to be seen under a microscope.

4.2.2.2. Top Emulsion Fraction

After three months, the emulsion (in which the first LCs were seen) present phase separation (as previously shown in **Figure 25A**). Both fractions (top and bottom) were analyzed by optical microscopy and the LCs were visualized only at the bottom fraction, i.e. the water-rich phase.

Immediately after the preparation of all emulsions in this study, they were homogeneous, showing no visible phase separation (except systems containing 80.0 wt. % of aqueous phase). **Figure 27** shows the bright field and polarized light micrographs of the fresh emulsion composed by the non-paraffinic P5 and 80.0 wt. % of deionized water, and the top fraction of that after destabilization.

It is clearly possible to note a large number of droplets on the bright field microscopy of the fresh emulsion. However, when the polarized light was used, no Maltese cross pattern was observed, i.e. no LC is present. After de destabilization, few droplets are observed, which indicates a good destabilization efficiency.

Figure 28 shows the bright field and polarized light micrographs of the fresh emulsion composed by the paraffinic oil P7 and 50.0 wt. % of deionized water, and the top fraction of that after destabilization.

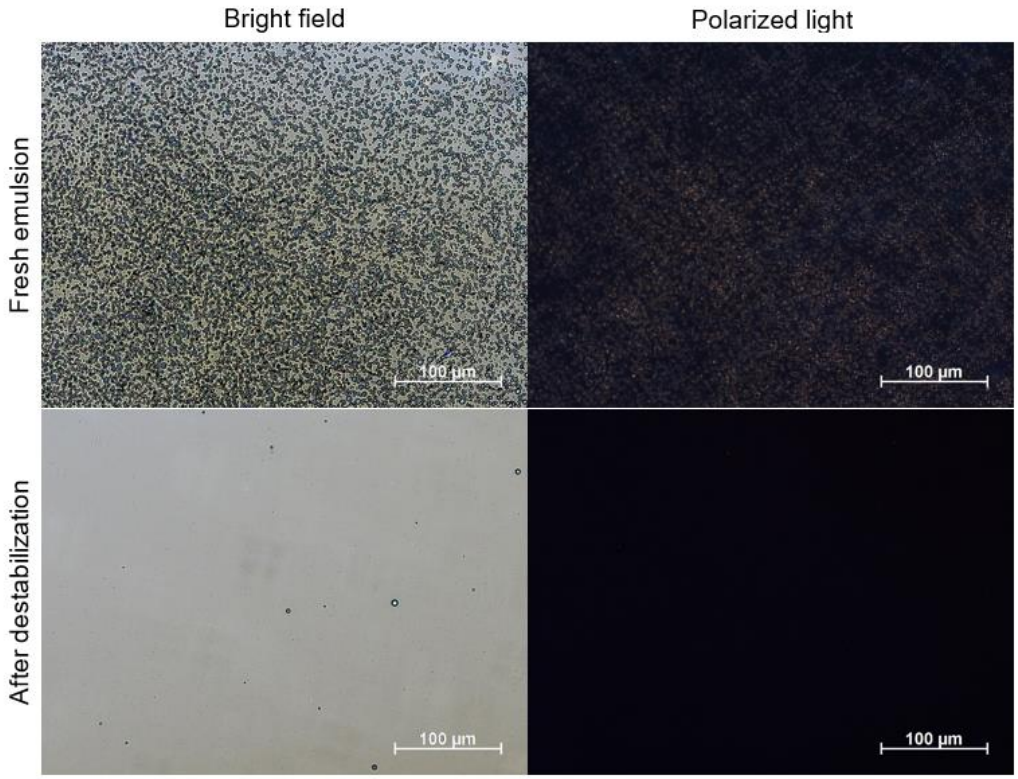

Figure 27: Bright field and polarized light micrographs of the top fraction of P5 and 80.0 wt. % of deionized water before (fresh emulsion) and after destabilization.

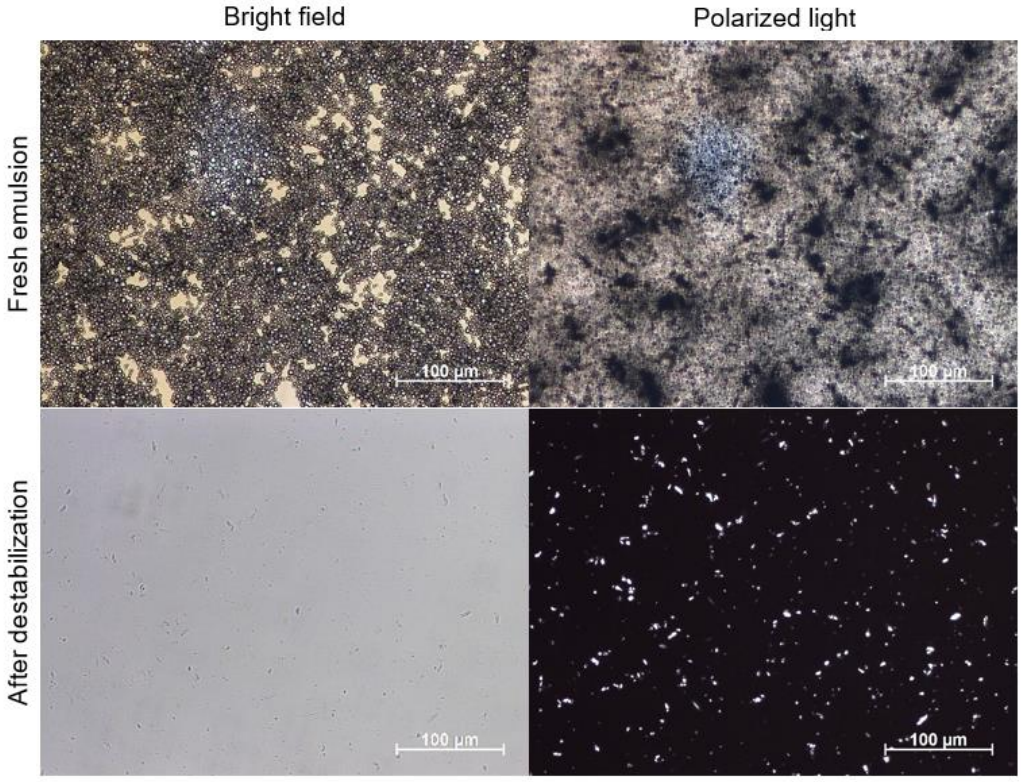

Figure 28: Bright field and polarized light micrographs of the top fraction of P7 and 50.0 wt. % of deionized water before (fresh emulsion) and after destabilization.

As in **Figure 27**, it is observed droplets on the bright field microscopy of the fresh emulsion in **Figure 28**, but, when the polarized light was used, birefringent material was observed. However, this birefringence is not in Maltese cross shape. The birefringence on polarized light, in this case, can be attributed to the wax crystals present, which can surround the droplets (as explained on **item 2.3.1.**). After the destabilization, none droplets are observed; however, it is possible to note wax crystals, which are evidenced on the polarized light micrograph.

Top fractions of all emulsions after destabilization step were submitted to the Karl Fisher titration. Insignificant water contents were found for all systems, proving destabilization efficiency.

Figure 27 and **Figure 28** show none Maltese cross pattern, i.e. no liquid crystalline structures, being thus attested that the LC appearance is visible in water-rich fractions, i.e. the bottom fractions. Considering that LCs are formed by NA and the respective naphthenates, Horváth-Szabó *et al*. (2001b) suggest that the solubility of naphthenates is low in oil; thus, they fail to balance in small drops of water in a continuous oil phase.

4.2.2.3. Bottom Emulsion Fraction

Considering that no liquid crystalline structure could be observed in the top fractions of the destabilized emulsions, the bottom fractions received more attention. Because of the density difference between the aqueous phases (about 1.0 g/cm^3) and the oil phases (about 0.9 g/cm^3), the bottom fractions are composed of dispersed oil droplets in the aqueous phase. Unlike the top fraction, which after destabilization had insignificant water contents, the bottom fractions presented dispersed oil, visible even to the naked eye.

Figure 29 shows the bottom fraction bright field and polarized light micrographs of the same point of the coverslip, for the system composed by P2 and 80.0 wt. % of water.

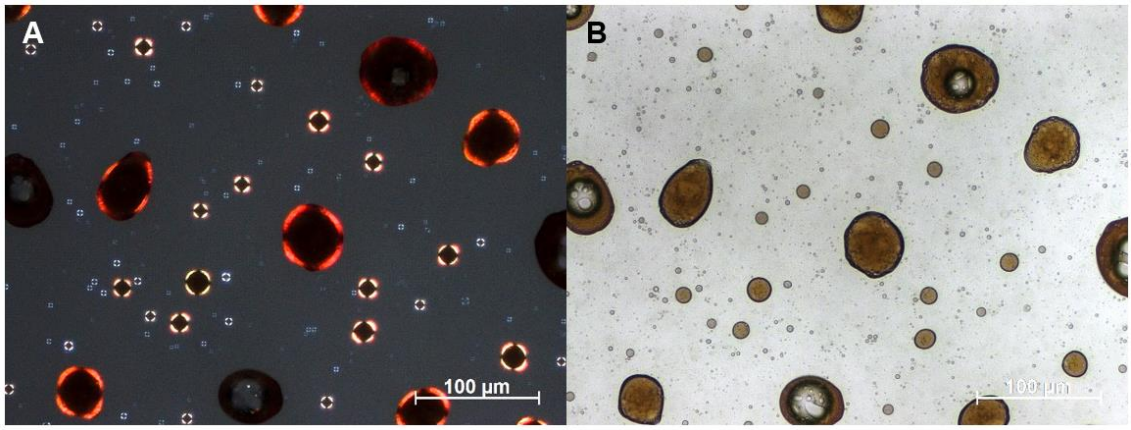

Figure 29: A) Polarized light and B) bright field micrographs of the bottom fraction at the same coverslip point of the system P2 and 80.0 wt. % of water.

On polarized light (**Figure 29A**), it is clearly observed a Maltese cross pattern, indicating the LC presence. The droplets of the bottom fraction of the emulsions are oily due to their brown coloration (**Figure 29B**), characteristic of the crude oil. In addition, in some drops, it is possible to note something like a multiple emulsion, containing water droplets dispersed into the oil droplets, which are dispersed in the continuous aqueous phase.

Based on all the considerations stated in these last three topics (**items 4.2.2.1, 4.2.2.2** and **4.2.2.3**), it is clear the formation of LC around oil or multiple emulsion droplets, only in the bottom fractions of the emulsions. No LCs are observed in dehydrated oil or oil-rich top fraction.

4.2.3. Wax Presence

Right after the first observation of liquid crystals in Brazilian crude oil systems (reported at the end of **item 2.4**, which gave rise to this research), nothing was known about these structures. Initially, it was not known whether the Maltese cross observed from the bottom fraction of the aged emulsion (**Figure 25B**), composed by paraffinic oil, was related to the presence of wax, which also has crystalline characteristics such as birefringence. Therefore, the first factor evaluated on LC formation was the presence of wax. **Figure 30** shows the polarized light micrographs of the emulsions bottom fractions obtained after the destabilization process, prepared with 50.0 wt. % of deionized water as aqueous phase and the oils P1, P4, P6, and P7 with different

wax contents (2.19; 0.89; 0.06 and 3.09 wt. % of waxes respectively).

It is found that both paraffinic and non-paraffinic oils are characterized by the presence of Maltese cross patterns. Therefore, it is believed that the presence of liquid crystals is not conditioned to the paraffinic composition of the oil. Waxes are non-polar molecules and do not have hydrophilic parts, that is, they do not act as surfactants. Thus, it is expected that the presence of wax does not affect the interface.

When comparing the images of **Figure 30**, it is possible to note that P7, which has the lowest TAN value (0.33 mgKOH/g), shows less amount of LC structures than the other oils, suggesting that the acidity content may be related to the LC formation. However, it is important to state that the microscopy technique, as used, is qualitative as it was not possible to standardize the amount and thickness of the sample in the coverslip. Therefore, the largest amount of liquid crystals in the image of oil P1 may be a local phenomenon and may not represent the whole sample.

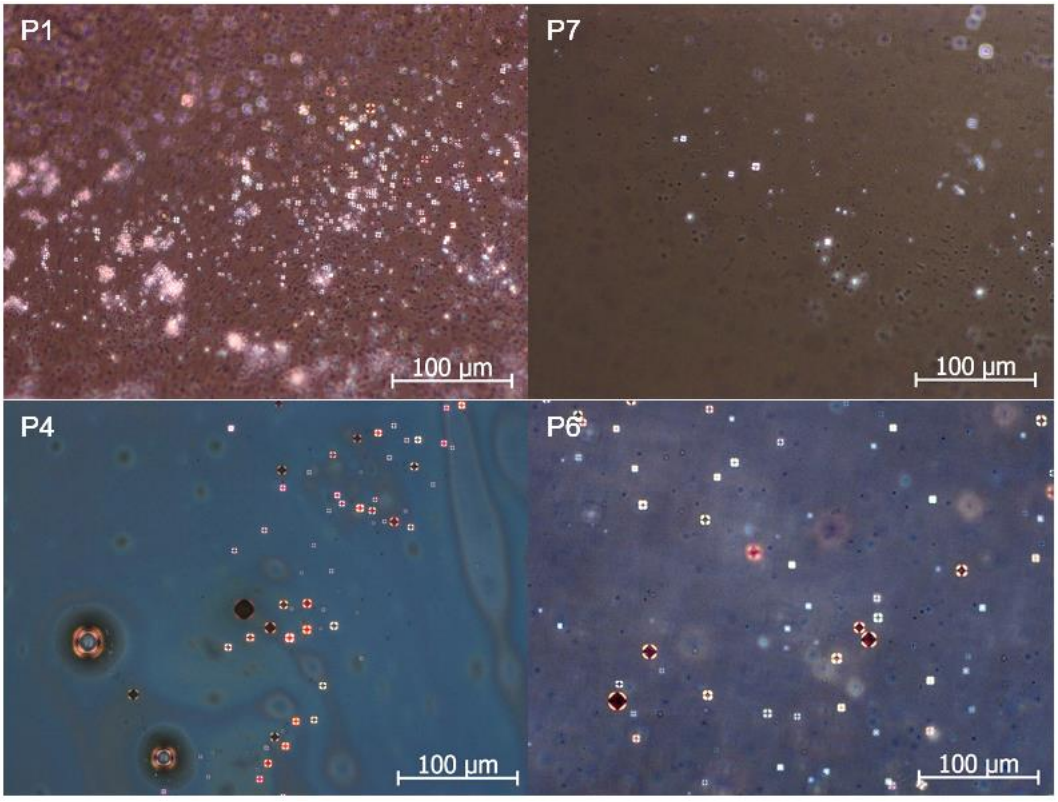

Figure 30: Polarized light microscopy of the emulsions bottom fraction prepared with 50.0 wt. % of deionized water and the oils P1, P4, P6, and P7.

4.2.4. Salinity

Another variable evaluated in the LC formation was the presence of salts in the aqueous phase. The emulsion stability can be disturbed by adding salt (HU *et al*., 2018). This disturb can be evaluated by variations on the interfacial tension between the oil and aqueous phase (McCLEMENTS, 2004). According to Alves *et al.* (2014), the addition of salt to water-surfactant-crude oil systems promotes an increase in the stability of the emulsion due to the formation of a more elastic interface.

Table 2 presents the interfacial tension values (obtained by Wilhelmy plate method) between the oils P1, P4, P6 and P7, and the phases: deionized water and NaCl solution (35.0 g/L). The average values relative to the stability interval of the IFT curve, after about 2 h of the test, are shown. As can be seen, the salt addition increases the IFT between the water and oil phases. Lashkarbolooki *et al.* (2014) also observe this IFT increase in the presence of salinity. The addition of cations by means of concentrated salt solutions can create “bridges” and ‘‘crosslinks’’ with the surfactant molecules, increasing the interfacial tension (HU *et al*., 2018).

Table 2: IFT values between P1, P4, P6, P7 and deionized water and NaCl solution.

Oil	**IFT** (mN/m)	
	H_2O	NaCl (35.0 g/L)
P1	16.48 ± 0.16	19.17 ± 0.05
P4	13.92 ± 0.06	15.66 ± 0.02
P6	19.63 ± 0.10	23.11 ± 0.01
P7	12.88 ± 0.02	15.54 ± 0.01

Figure 31 presents the bright field and polarized light micrographs of the bottom fraction emulsions prepared with P4 and 20.0 wt. % of deionized water and NaCl solution (35.0 g/L). For both aqueous phases, it is observed the occurrence of Maltese crosses, i.e. lamellar LC. Therefore, the presence of the salt (NaCl up to 35.0 g/L) is not relevant for the formation or inhibition of liquid crystalline structures.

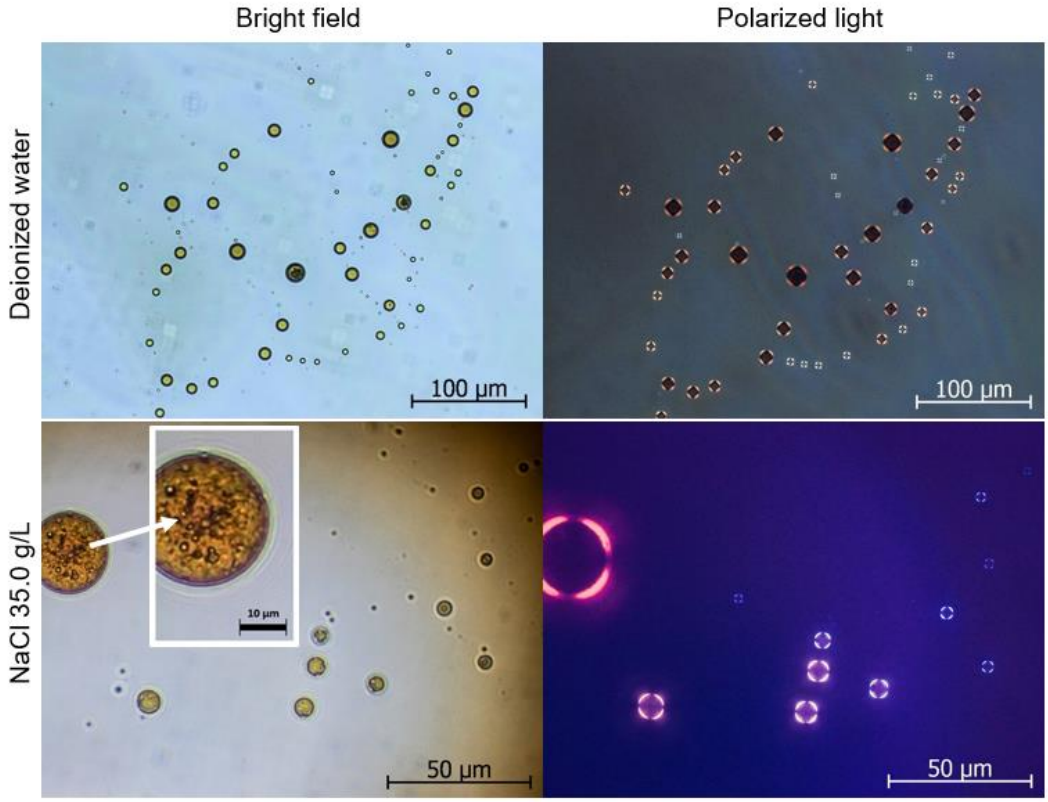

Figure 31: Bottom fraction micrograph of the emulsions prepared with P4 and 20.0 wt. % of deionized water NaCl solution (35.0 g/L).

It is interesting to observe in **Figure 31** (the detail from the bright field micrograph for NaCl solution) the presence of small droplets inside a larger droplet. This observation, in accordance with observed in **Figure 29**, suggests that the nuclei of LCs can be formed by multiple emulsion. Thus, despite of the literature suggestions about LC structures coating oil droplets, strong evidence indicates that multiple emulsions may also form the interior of the droplet.

4.2.5. Aqueous Fraction

Another factor evaluated in the LC formation in crude oil systems was the water content. The evaluation of this factor was motivated by the initial observation of LC in a water-rich phase. **Figure 32** illustrates the influence of the aqueous phase content employed in the preparation of the emulsion with the petroleum P7, in the emergence of the crystalline liquid structures.

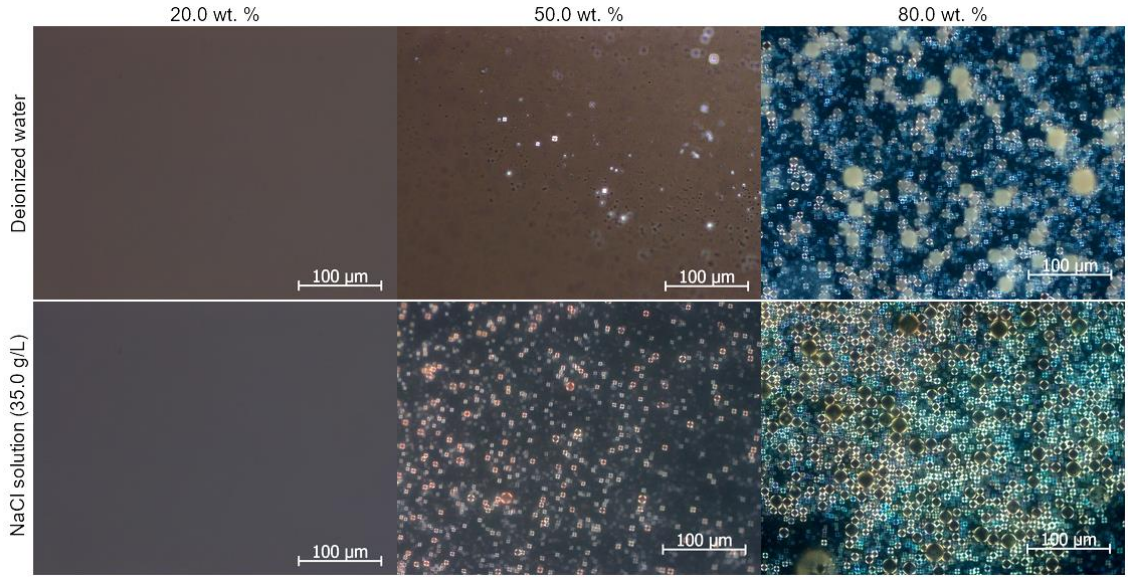

Figure 32: Emulsion bottom fraction micrograph of P7 and 20.0, 50.0 and 80.0 wt. % of water and NaCl solution.

It is noted that, regardless of the dispersed phase (deionized water or saline solution), there is a significant increase for liquid crystals as the volume fraction of the aqueous phase increases. Thus, it is suggested that the aqueous phase content is a determining factor for the appearance and observation of liquid crystals. Probably, this behavior is related to the greater affinity of the crude oil native surfactants with water. This behavior is valid to the other evaluated oils too. Considering that the formation of LC is favored at high levels of the aqueous phase, this aqueous-oil phase proportion will be adopted as the standard i.e., from this point, system containing 20.0 and 50.0 wt. % will no longer be shown.

4.2.6. Total Acid Number

Sjöblom *et al.* (2003) affirm that there is a significant relation between TAN values and the naphthenic acids content, and Ese and Kilpatrick (2004) suggest that NAs are related to the LC formation in crude oil systems. **Figure 33** shows the bottom fraction emulsion formed by P1-P5 and P7 with 80.0 wt. % of deionized water (pH 6.3). P6 was not shown in **Figure 33** because of the similar TAN value with P5 (2.88 for P6 and 2.76 mgKOH/g for P5).

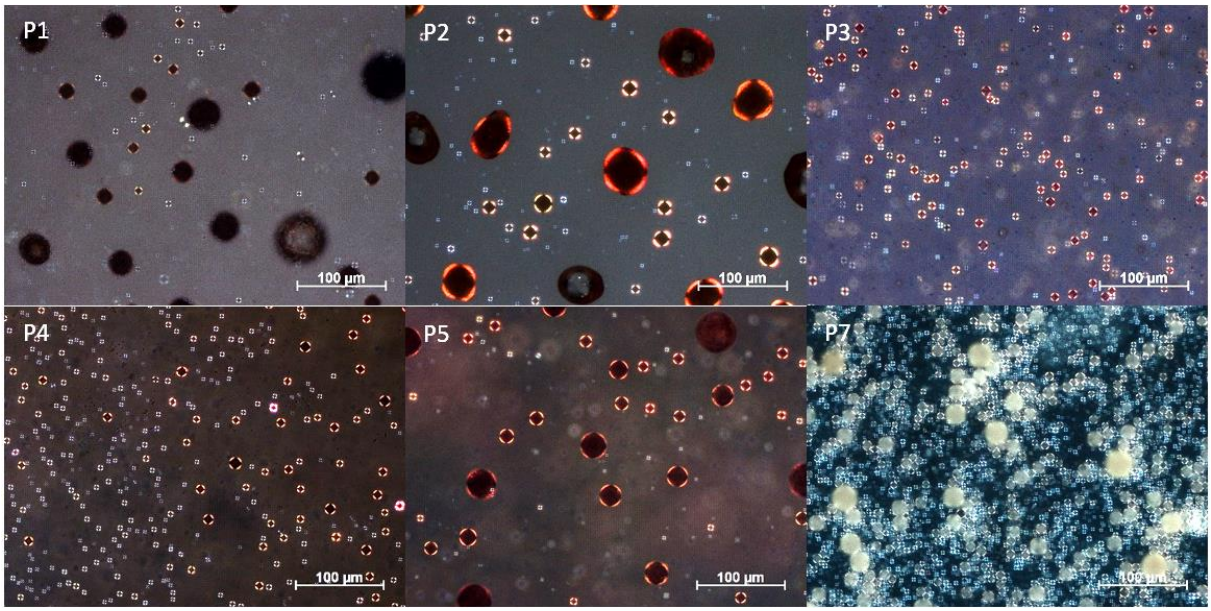

Figure 33: Polarized light micrographs of bottom fraction emulsion formed of P1-P5 and P7, with 80.0 wt. % of deionized water.

Initially, it is not possible to notice any relation between the different TAN values and the LC formation, considering that P7 has the lowest TAN value (0.33 mgKOH/g) and the highest amount of LC. P1 has the second lowest TAN (0.64 mgKOH/g) and present the lowest amount of LC in water. The P2-P5 oils, considered the most acidic (2.05, 3.04, 0.85 and 2.76 mgKOH/g, respectively), showed no significant differences in the amount of LC observed by the micrographs. However, it will be shown later (**item 4.2.7**) that the TAN has a role in the LC formation. To explain the behavior shown in **Figure 33**, it is necessary consider the oil viscosities. P7 (the least acid) has the lowest viscosity (0.06 Pa.s), while P3 (the most acidic) exhibits a viscosity 44.3 times higher (2.66 Pa.s). This oil viscosity difference may favor or hinder the interaction between the oil and water and consequently can favor or hinder the LC formation. Comparing the oils P1 and P5 that present similar viscosities (0.47 Pa.s for P1 and 0.59 Pa.s for P5), and different TAN values (0.64 mgKOH/g for P1 and 2.76 mgKOH/g for P5), it is possible to note more LC structures for P5 system. In summary, the viscosity of the oil influences the formation of the liquid crystalline structures.

The naphthenic acid distribution and the average molecular mass (M_w) of the naphthenic acid fraction of P1-P2 and P7 are shown in **Table 3**. The results were obtained by FT-ICR-MS that offers a higher mass resolution, mass resolving power, and mass accuracy, which enable the analysis of complex petroleum mixtures on a

molecular level (DIAS *et al*., 2014).

Table 3: Naphthenic acid distribution and respective average molecular mass of P1-P2 and P7.

	P1		P2		P7	
	wt. %	M_w *(g/mol)*	wt. %	M_w *(g/mol)*	wt. %	M_w *(g/mol)*
Linear	39.5	392.6	56.0	340.6	92.2	--
1 ring	15.0	445.1	15.5	388.1	7.8	344.3
2 rings	11.2	447.5	8.9	371.2	0	--
3 rings	9.1	432.9	6.5	374.5	0	--
4 rings	9.3	450.1	7.0	426.5	0	--
Complex	15.9	461.9	6.1	452.4	0	--

The three oils show a naphthenic acid distribution predominantly linear. Possibly these can be related to the amount of LC present in **Figure 33**, owing the less amount of LC structures in P1 (39.5 wt. % of linear NA), intermediate amount of LC in P2 (56.0 wt.% of linear NA) and the higher LC amount in P7 (92.2 wt. % of linear NA).Therefore, the linearity of the NA can promote the LC organization.

4.2.7. pH

Enhanced oil recovery (EOR) by alkaline flooding was proposed as an inexpensive way to reduce the interfacial tension between the aqueous and oily phases, favoring the removal of oil from the reservoir (SALAGER and ANTÓN, 1999). In addition, in reservoirs with high CO_2 content, the pressure decrease after the extraction of the oil promotes the release of this gas leading to an increase in pH of the produced water (BRANDAL *et al*., 2005). Thus, the influence of pH of the alkaline phases on the LC formation was analyzed. **Figure 34** shows the bottom fractions formed from emulsions of P1 and P3-P5 and deionized water (pH 6.3) and NaOH alkaline solutions (pH 10.0 and 12.0).

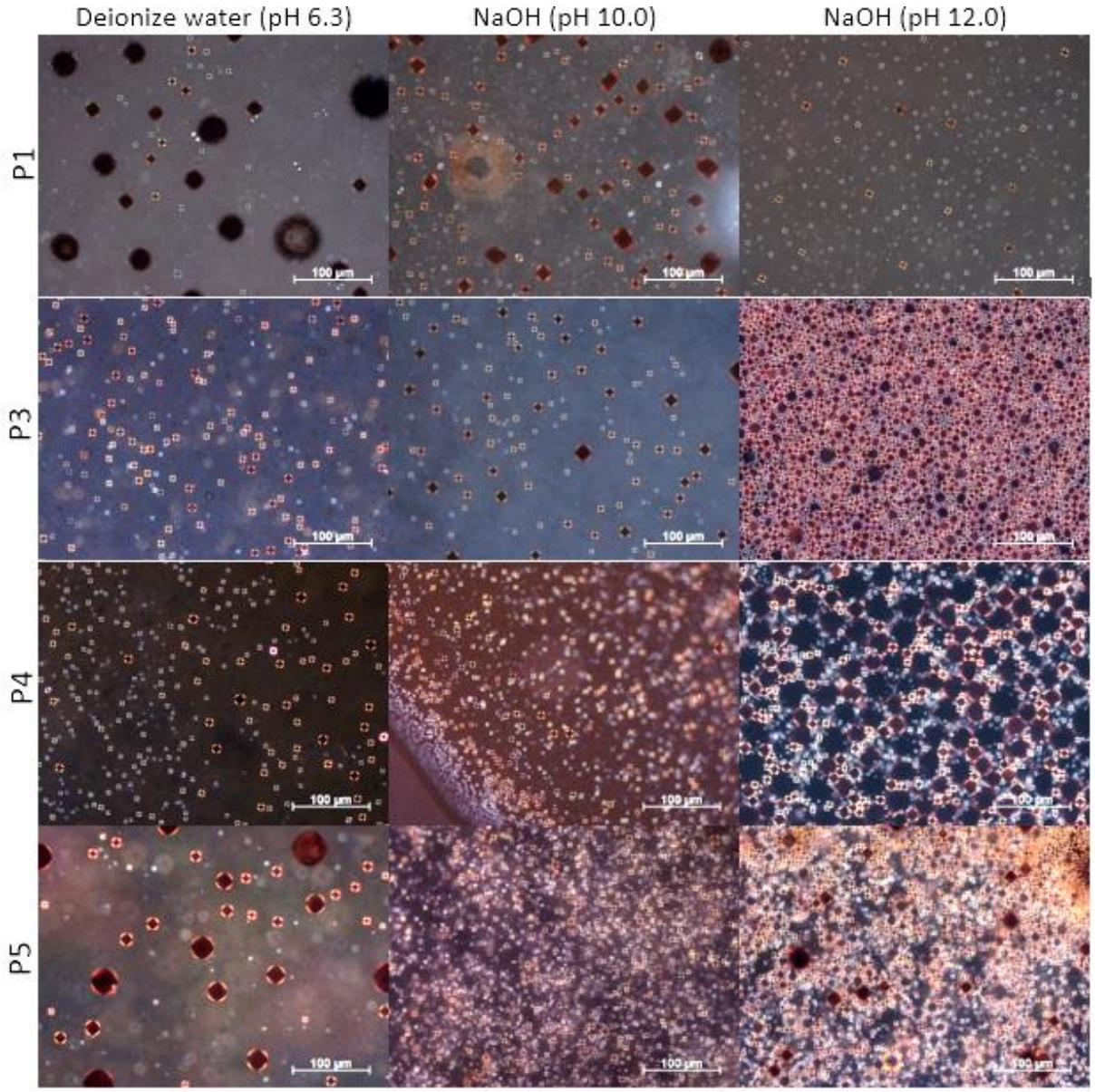

Figure 34: P1 and P3-P5 with deionized water (pH 6.3) and NaOH solutions (pH 10.0 and 12.0).

As can be seen, practically all the droplets are covered by LC and there are less LC structures for deionized water than in the presence of alkaline solutions, especially for the sample P3-P5, which present higher TAN values. The crude oil P1 (TAN value 0.64 mgKOH/g), showed almost no change in the amount of LC *versus* pH.

The NAs are carboxylic acids and are considered weak acids, whose K_a are around 10^{-5}, and they do not dissociate completely in water. Carboxylic acids with less than six carbons are soluble in water; with six or more they became partially or not soluble, on the other hand, their respective metal salts (naphthenates) are generally completely soluble (McMURRY, 2009). Therefore, most NAs remains in the oil phase.

This may be a plausible justification for the observation of less LC structures in systems using only deionized water. In addition, the carboxylic acids can make hydrogen bonds with other NAs (**Figure 35**), which may result in a reduction of molecules available for LC formation when the aqueous phase is deionized water.

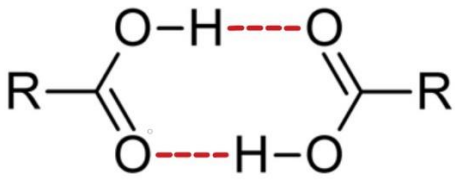

Figure 35: Hydrogen bond of carboxylic acids.

The NAs are considered as Bronsted–Lowry acids because they can donate a proton. **Figure 36** expresses the acid-base mechanism reaction responsible for the naphthenates formation. In the petroleum industry, this reaction occurs because of the interaction between natural naphthenic acids of the crude oil and the hydroxyl anions present in the alkali solutions injected in the reservoir.

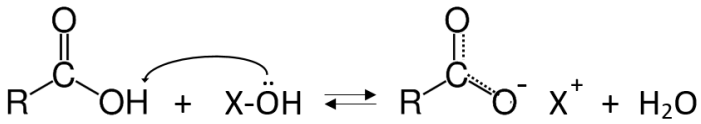

Figure 36: Acid-base reaction between NA and alkali forming naphthenate.

The amount of LC structures increases with the increase of pH (**Figure 34**) for samples P3-P5 (characterized by higher TAN values), thus, the ionization of the NA in high pH and/or the formation of naphthenates possibly are related to the LC formation. The equilibrium between the naphthenic acids (with the proton – NAH) and naphthenates (without the proton – NA^-) in water can be expressed by the **Equation 6**, and the equilibrium constant is expressed in **Equation 7**.

$$NAH \leftrightarrows NA^- + H^+ \tag{6}$$

$$K_a = \frac{[NA_w^-][H_w^+]}{NAH_w} \tag{7}$$

Thus, the relative amounts of the naphthenates and the naphthenic acids depends on the pH according to **Equation 8**.

$$\frac{[NA_w^-]}{[NAH_w]} = \frac{K_a}{[H^+]} \quad (8)$$

The dissociated (ionic) and undissociated (nonionic) species are likely to selectively partition or fractionate between water and oil. It can generally be assumed that the amount of dissociated salt in oil $[NA_o^-]$ is negligible, whereas the amount of undissociated acid in water $[NAH_w]$ is to be taken into account as it appears in the dissociation equilibrium (SALAGER and ANTÓN, 1999). The partition coefficient (P_a) of the undissociated acid between oil and water is defined by **Equation 9**.

$$P_a = \frac{[NAH_o]}{[NAH_w]} \quad (9)$$

For long-chain naphthenic acids, P_a can be in the 100-1000 range, i.e. neglecting the amount of acid present in the oil phase would be equivalent to neglecting most of it (SALAGER and ANTÓN, 1999).

After the emulsification and destabilization processes, the pH of the aqueous bottom fractions were evaluated by titration. pH values for P1 and P3-P5 are presented in **Table 4**. It is observed that the greater reduction in the pH of the bottom aqueous phases is generated from P3, possibly related to the naphthenic acid content suggested by the high TAN value (3.04 mgKOH/g). This relationship is also manifested for the other oils, with P1 (0.64 mgKOH/g) being the lower pH variation in the bottom phases, followed by P4 and P5 (0.85 and 2.76 mgKOH/g, respectively). It is clear the influence of the acidic compounds on the pH reduction.

Table 4: pH values of bottom fractions for P1 and P3-P5.

	H_2O	**NaOH**	
Oil	pH 6.3	pH 10.0	pH 12.0
P1	5.71 ± 0.20	9.48 ± 0.03	11.87 ± 0.16
P3	5.14 ± 0.17	5.52 ± 0.19	11.12 ± 0.22
P4	5.32 ± 0.02	7.63 ± 0.16	11.76 ± 0.02
P5	5.20 ± 0.06	6.00 ± 0.03	11.36 ± 0.07

From the pH **Equation** (**10**), it was obtained the concentration of dissociated H^+ in the deionized water (pH 6.3) and in the bottom fractions of this respective aqueous phase (based on the values of the first column of **Table 4**). **Table 5** shows the estimated values of H^+ (acid concentration) in the water phase. The H^+ value in oil is about 100-1000 times higher than in water, considering that the partition coefficient suggested by Salager and Antón (1999).

$$pH = -\log[H^+] \tag{10}$$

By converting the TAN values, originally in mg of KOH/g of petroleum to mol of KOH/L of petroleum, and considering that the acid-base reaction of this titer has a 1:1 ratio, which is possibly untrue due to the presence of polyprotic acids, sulfonates, aromatics, olefins, etc. which are capable of interfering on the acidity (BROWN and ULRICH, 2015), we have a simplistic estimate of the acidic compounds content in the crude oil (NA_o) (**Table 5**).

Table 5: $[H^+]$ and $[NA_o]$ estimated in the water phase from P1 and P3-P5.

Oil	$[\boldsymbol{H_w^+}]$ *mol/L*	$[\boldsymbol{NA_o}]$ *mol/L*
P1	1.9 x 10^{-6}	1.0 x 10^{-2}
P3	7.2 x 10^{-6}	5.2 x 10^{-2}
P4	4.8 x 10^{-6}	1.4 x 10^{-2}
P5	6.3 x 10^{-6}	4.6 x 10^{-2}

Considering that the naphthenic acid content obtained by **Equation 9** is 100-1000 times the value of $[H_w^+]$ of **Table 5**, we have a concentration range of 10^{-4} to 10^{-3}, which is in the range of the value obtained by converting the TAN (10^{-2}). As stated, this

difference is possibly related to the low dissociation of the NA, and to the other compounds with the capacity to alter the acidity.

4.2.7.1. Removal of Acidic Compounds

In order to observe the possible NA removal by the aqueous phases, the top fractions of the crude oils P4 and P5 (rich in oil) were submitted to new emulsification and destabilization processes for two more times, with the respective aqueous phase. The pH values of the bottom fractions after first, second and third emulsifications for oils P4 and P5 are presented in **Table 6**. **Figure 37,** and **38** show the micrographs for these steps for P4 and P5, respectively.

Table 6: pH values for the bottom fraction of destabilized emulsions of P4 and P5.

Emulsification	P4			P5		
	H_2O	NaOH		H_2O	NaOH	
	pH 6.3	pH 10.0	pH 12.0	pH 6.3	pH 10.0	pH 12.0
1st	5.32 ± 0.02	7.63 ± 0.16	11.76 ± 0.02	5.20 ± 0.06	6.00 ± 0.03	11.36 ± 0.07
2nd	5.97 ± 0.03	7.92 ± 0.02	11.14 ± 0.03	5.32 ± 0.04	6.40 ± 0.03	11.92 ± 0.06
3rd	6.11 ± 0.09	8.44 ± 0.19	11.85 ± 0.10	5.55 ± 0.14	6.66 ± 0.08	11.46 ± 0.18

It is possible to observe in all systems that the pH of the aqueous phases after the first emulsification was the lowest, and after the third, the values were the highest, i.e., closer to the pH of the original aqueous phase (**Table 6**). Possibly this behavior is related to the transfer of the acidic compounds from the crude oil to the aqueous phase. In the first emulsification, most of the soluble acidic compounds are transferred to the water. Thus, in the following emulsions steps, fewer compounds are available and therefore the pH does not suffer such a marked reduction. However, there is no significant difference between the micrographs (**Figures 37** and **38**) for the first and the third emulsification steps it thus suggests that even with increasing pH between the subsequent emulsions steps, it is not sufficient to reduce the amount of LC.

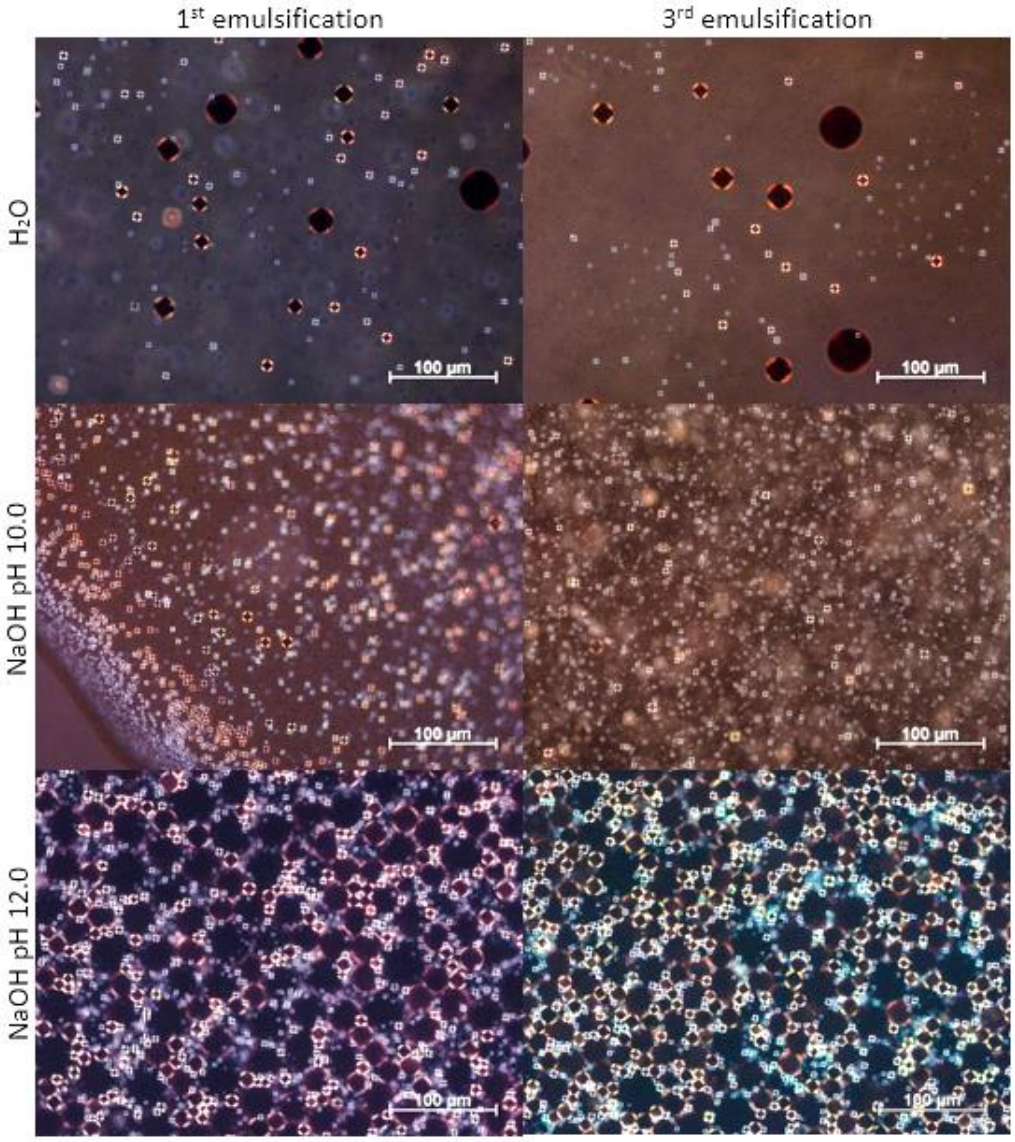

Figure 37: P4 bottom phase after first and third emulsification processes.

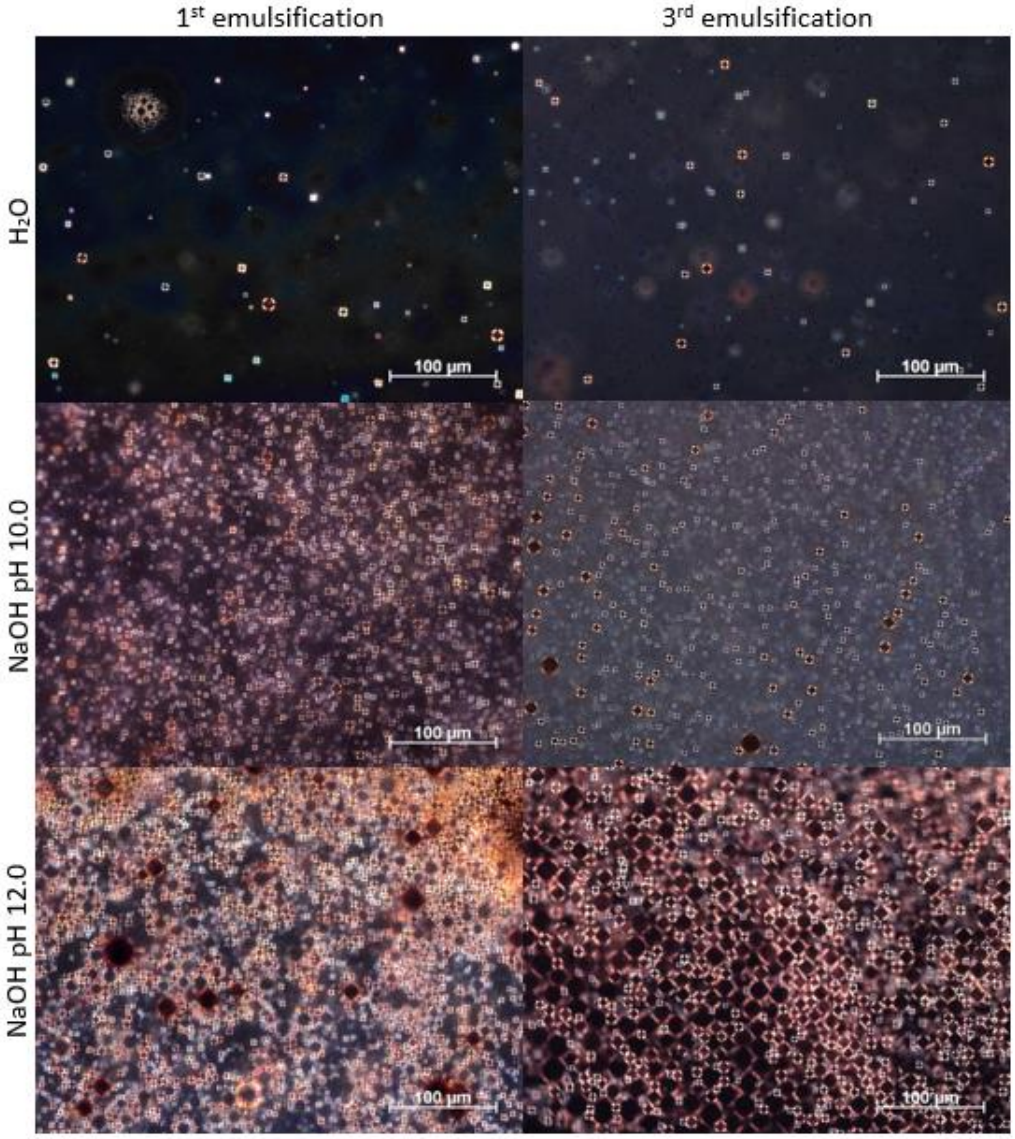

Figure 38: P5 bottom phase after first and third emulsification processes.

Some of the top fractions of the systems (oil-rich) after the emulsification process were subjected to a new TAN evaluation. The TAN values for the P5 as received and after first emulsification with deionized water and alkaline solutions, and after three emulsifications with NaOH solution at pH 12.0 are shown in **Table 7**.

Table 7: P5 TAN values as received and after emulsification.

Oil	**Original TAN**	**TAN after 1st emulsification** *(mgKOH/g)*					**After 3rd emulsification**
		H_2O	NaOH pH 10.0	NaOH pH 12.0	KOH pH 12.0	$Ca(OH)_2$ pH 12.0	NaOH pH 12.0
P5	2.76 ± 0.02	2.36 ± 0.01	2.30 ± 0.01	1.02 ± 0.02	1.26 ± 0.01	1.49 ± 0.01	0.52 ± 0.03

It is observed that TAN values obtained after the first emulsification were lower than the original TAN. However, there was no significant variation between emulsification with water and the solution with pH 10.0. Alkaline solutions at pH 12.0 showed the most significant reductions in TAN (about 54.4 % of reduction over the original TAN). Among them, the NaOH solution was the one that most reduced the TAN value (63.0 % of reduction). The evaluation of the TAN after three consecutive emulsifications presented a reduction of 81.2 % than the original value.

After this discussion, it is evident that the pH of the aqueous phase and the cation plays an important role in the LC formation. According to Salager and Antón (1999), ionic surfactants (as naphthenates) generally lead to liquid crystals structures at ambient temperature, rather than microemulsions. The next topic (**item 4.2.8**) addresses in more detail the influence of cations on the LC formation.

4.2.8. Cation

In order to observe the influence of volume and valence of the cation, the effect of different aqueous alkaline solutions composed by sodium, potassium, and calcium was analyzed on the LC formation.

Figures 39, **40** and **41** show the bottom fractions of the emulsions formed by P1 and P3-P5, with NaOH, KOH and $Ca(OH)_2$ alkaline solutions (pH 10.0 and 12.0). For NaOH systems (**Figure 34**, repeated in **Figure 39** to facilitate the comparison), the number of LC structures, in general, is higher for pH 12.0 than pH 10.0 for P3-P5. For KOH systems, it is observed similar behavior. However, fewer structures were present in KOH for P1 and P3. The Na^+ and K^+ have the same valence, but the atomic volume of the K^+ is 45.7 cm^3/mol, almost two times the atomic volume of Na^+ (23.7 cm^3/mol). This larger volume for K^+ can be responsible for less LC structures compared with Na^+ systems because the volume can disturb the organization of the molecules and consequently the LC formation. According to Brandal *et al* (2005), the interaction between the cation and the water molecules decreases with the cation size and valence. For oils P4 and P5, the LC content for NaOH and KOH is almost the same. In these cases, the K^+ volume was not a factor that affected the LC formation. Possibly this behavior is related to the type of the structure of the acidic molecules that can

interact with both Na^+ and K^+, and are different in each petroleum.

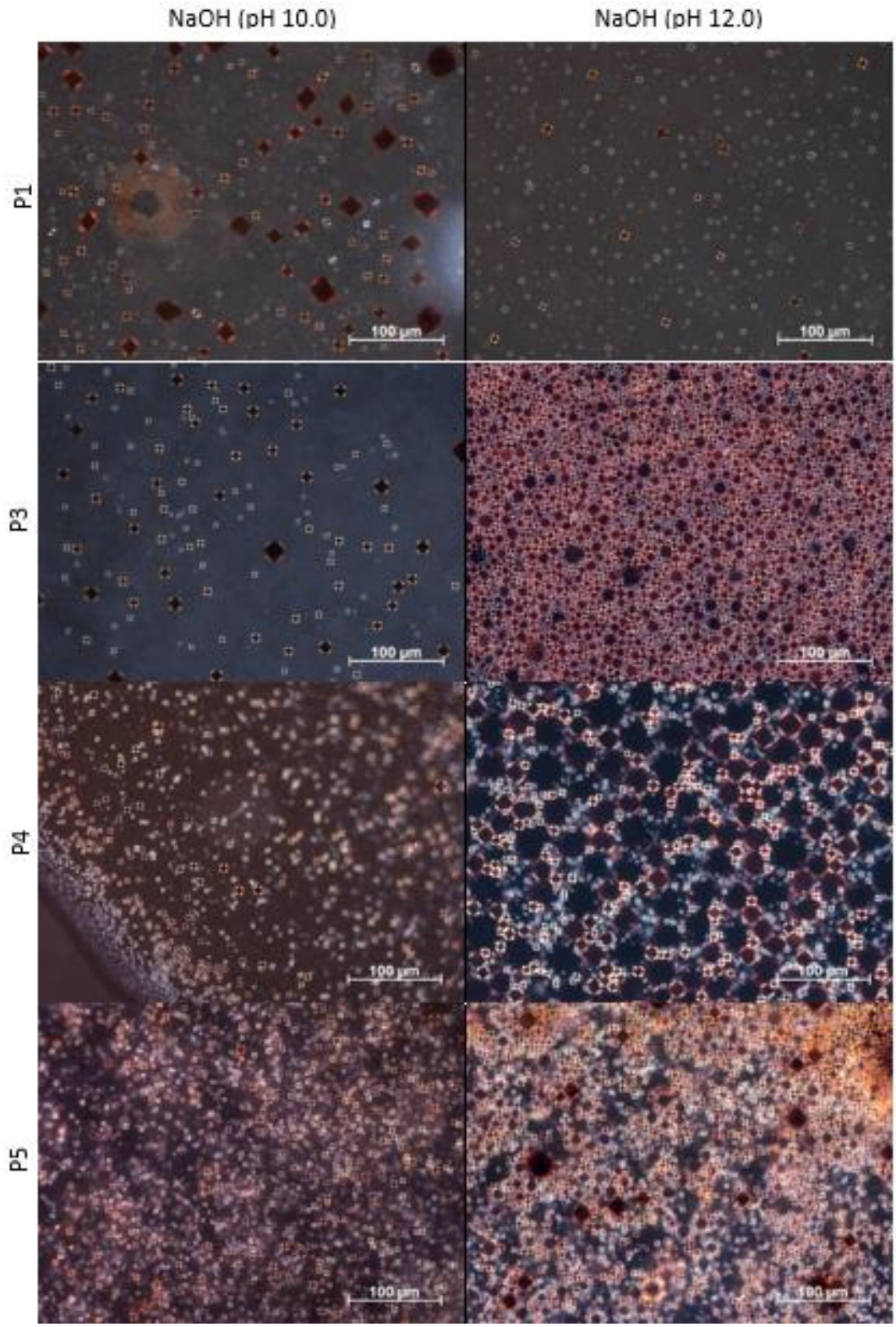

Figure 39: Bottom fractions of the emulsions formed by P1 and P3-P5, with NaOH solutions at pH 10.0 and 12.0.

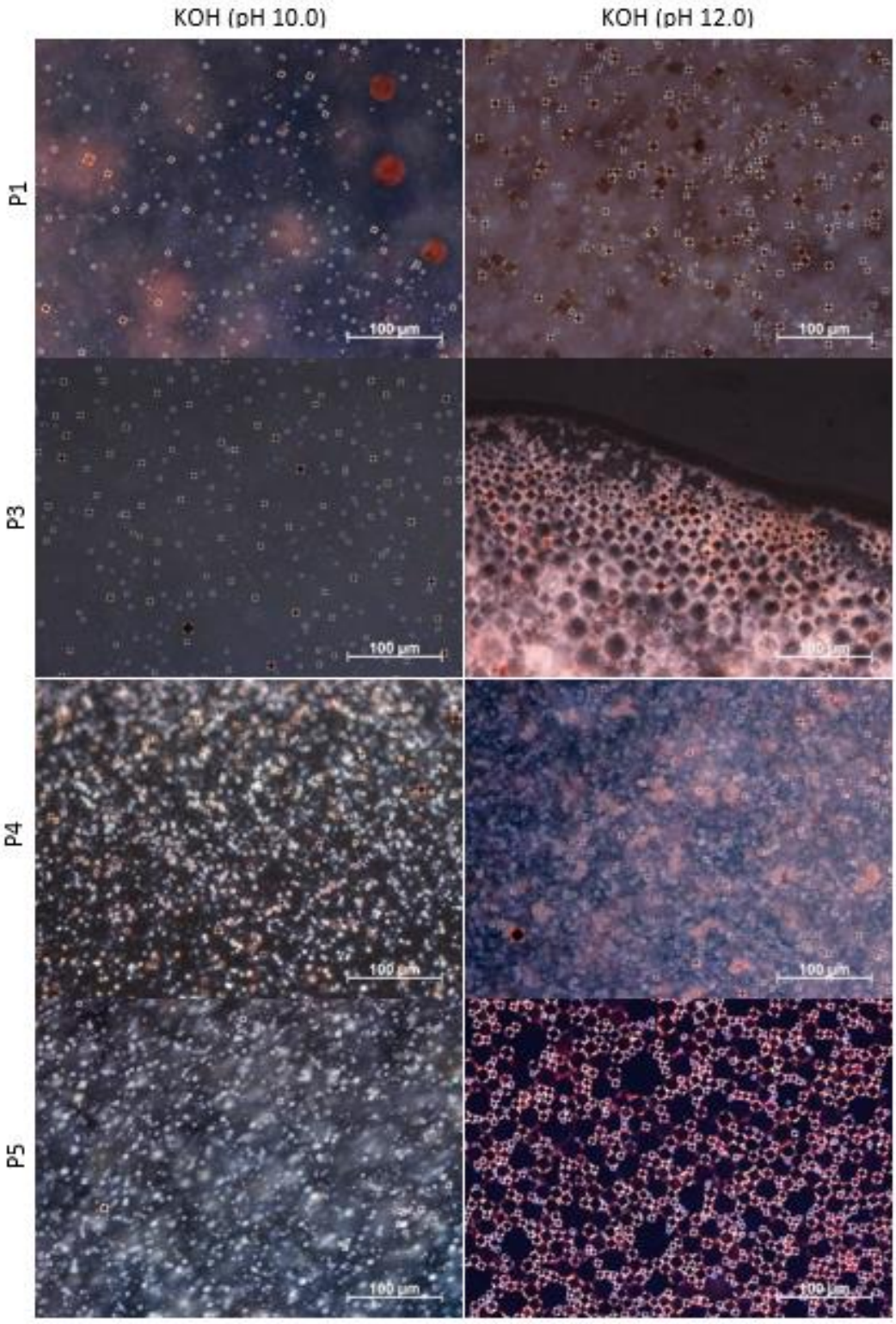

Figure 40: Bottom fractions of the emulsions formed by P1 and P3-P5, with KOH solutions at pH 10.0 and 12.0.

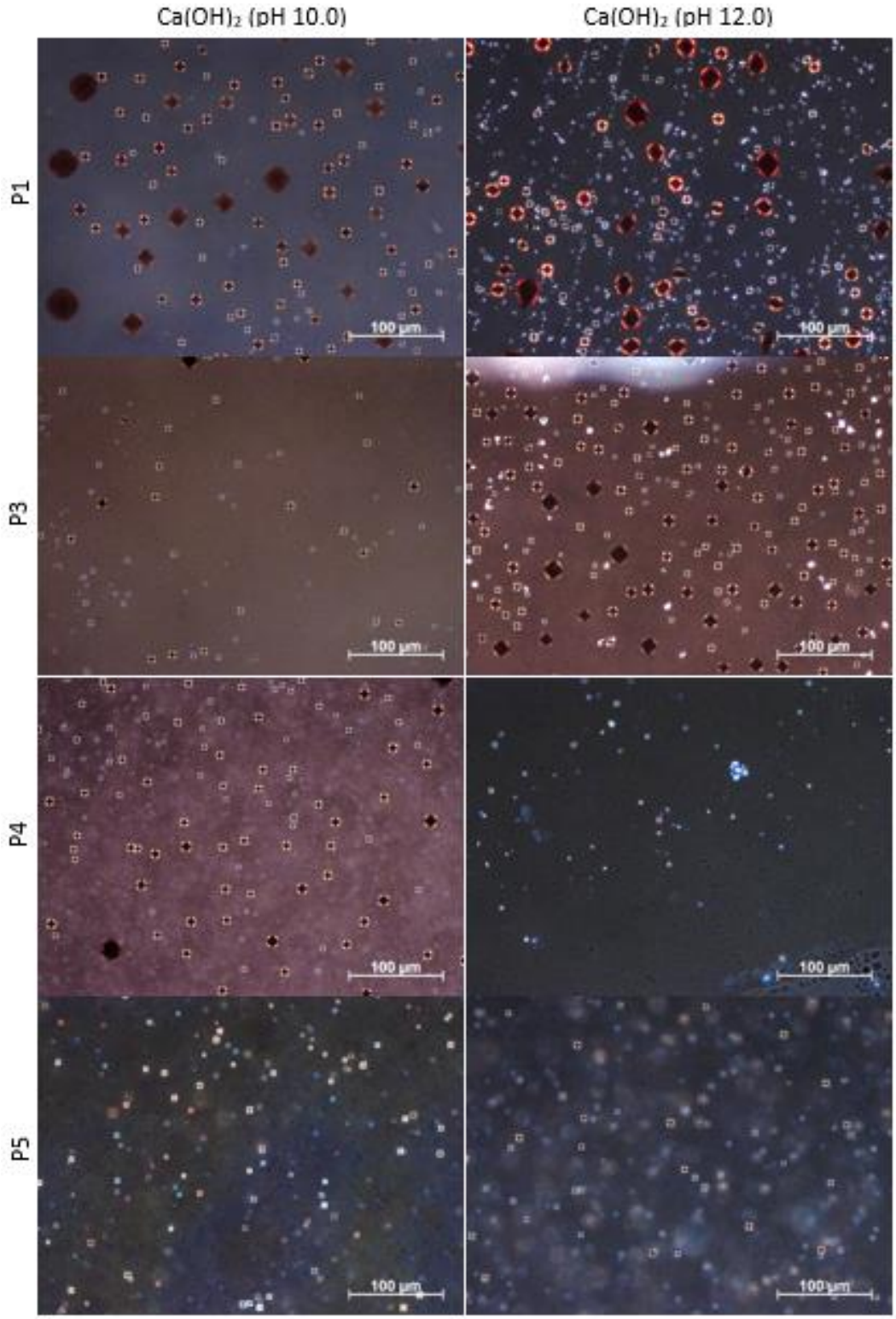

Figure 41: Bottom fractions of the emulsions formed by P1 and P3-P5, with $Ca(OH)_2$ solutions at pH 10.0 and 12.0.

Comparing the systems composed by cations of different valence (Na^+ and Ca^{2+}) and similar volumes (23.7 cm^3 for Na^+, and 25.9 cm^3 Ca^{2+}), it is possible to note that, in general, for the monovalent Na^+ more LC were observed. The bivalent Ca^{2+} was not too efficient on the LC formation. According to the solvation theory, the higher the charge of the solvated molecule the greater the interaction with a polar solvent and the more charge will be stabilized (BRUICE, 2006).

The relations between LC appearance and the cations volume and valence possibly are related to the structures of the acidic molecules, which are different in each oil. Some structures may have mono-, di-, tri- or tetra- acids sites. Only a more in-depth analysis of the acid molecule structures of each oil could clarify the structure/cation relationship with LC formation.

4.2.8.1. Interfacial Tension

Another characteristic analyzed was the interfacial tension between the aqueous and oily phases. The IFT can be explained in terms of the Van der Waals forces acting on the molecules of a liquid. In the bulk, the molecules are exposed to balanced forces coming from all directions. However, on the surface, the molecules are subjected to unbalanced forces (**Figure 42**), leading them to be pulled towards the bulk and cause contraction of the surface.

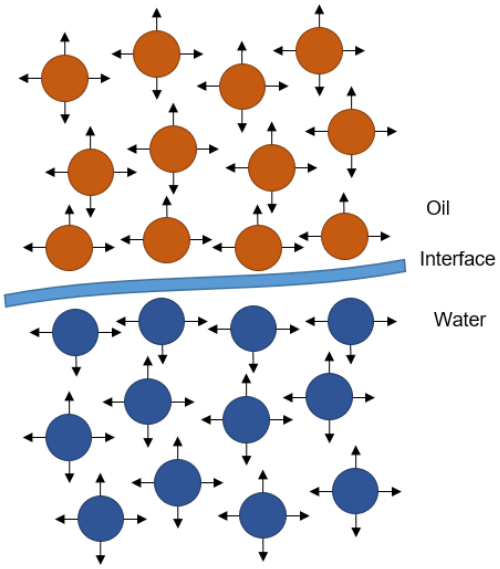

Figure 42: Attraction forces on the surface and bulk of the liquids.

The IFT between alkaline solution and the oil phase is strongly time-dependent. The organic acids (naphthenic acids) present in the oil have amphiphilic characteristics and act by adsorbing or desorbing at the water/oil interface, where it is converted into a carboxylic salt (naphthenates) with surfactant properties such as interfacial tension lowering (SALAGER and ANTÓN, 1999, HORVÁTH-SZABÓ *et al.* 2002). If the adsorption rate is greater than the desorption rate, the interfacial tension decreases. At the moment when the adsorption and desorption achieve the equilibrium, the interfacial tension reaches a steady or constant value. **Figure 43** shows the IFT behavior for the oils P1 and P3-P5, and the aqueous systems (H_2O pH 6.3, NaOH, KOH and $Ca(OH)_2$ pH 10.0) *versus* time, before the emulsification process (oil as received), and between the dehydrated oil after the emulsification process.

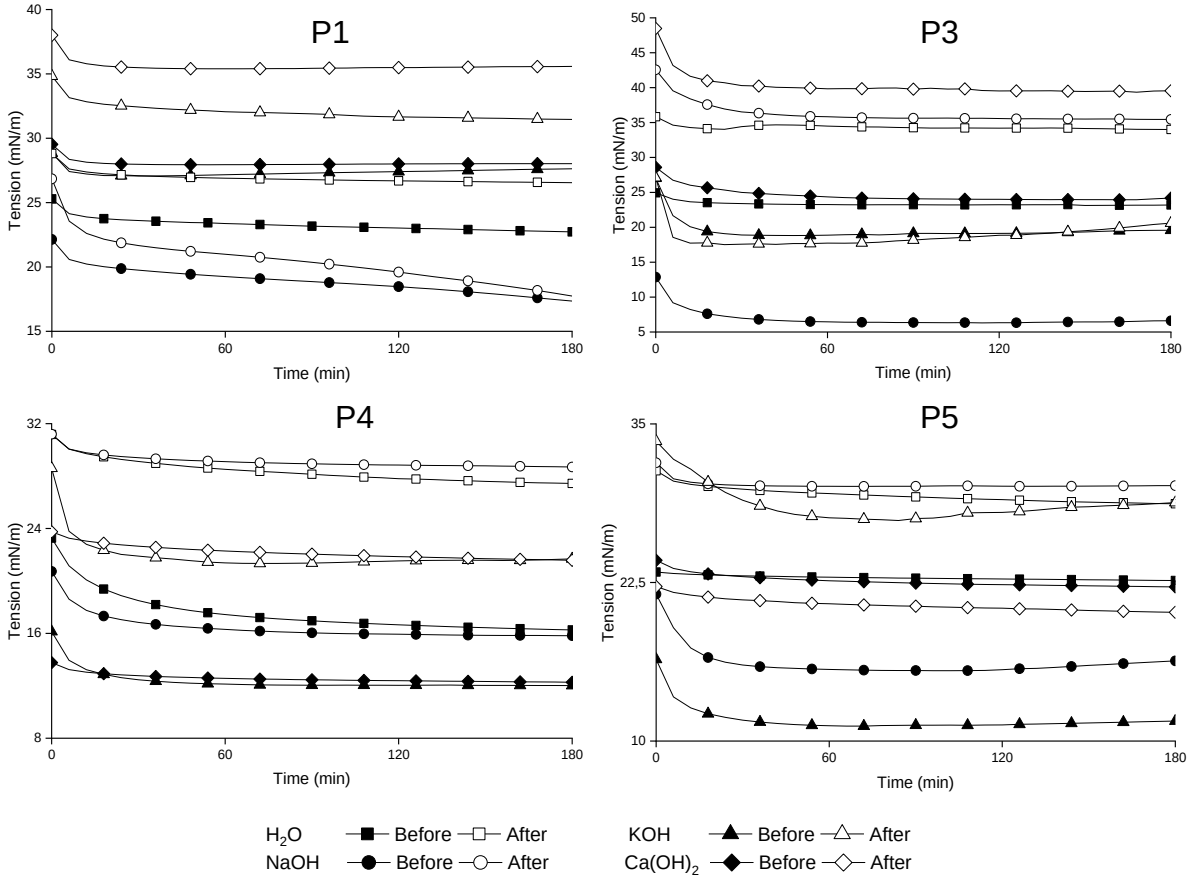

Figure 43: IFT *versus* time for P1 and P3-P5 and H_2O, NaOH, KOH and $Ca(OH)_2$ solutions (pH 10.0), before and after emulsification process.

The kinetics of interface formation, that is, the time necessary to achieve the equilibrium point, varies according to the type and content of natural surfactants in the

oil, and the characteristic of the aqueous phase. In the analyzed systems is possible to note that all systems reached the equilibrium in about three hours. In general, the systems composed by the crude oil as received, i.e. before the emulsification processes present faster stabilization kinetics than systems that used dehydrated oil after emulsification. For P1 the stabilization kinetics of the IFT and NaOH solutions was the slowest. This behavior is also observed for oils P3-P5 and KOH after the emulsification process. As the petroleum is a very complex multicomponent matrix, the structures of its natural surfactants are not known, as well as the kinetics of stabilizing the interfaces of these molecules. Thus, it was not possible to establish a relationship between the equilibrium velocities of adsorption and desorption of the molecules at the interface and the type of aqueous solution.

Table 8 presents the IFT values between the deionized water, NaOH, KOH and $Ca(OH)_2$ solutions at pH 10.0, and P1-P5, before and after the emulsification process. The IFT values presented are an average from the last hour of the experiment, where the adsorption/desorption equilibrium was reached or almost reached.

Table 8: IFT between P1-P5 and deionized water, NaOH, KOH and $Ca(OH)_2$ solutions at pH 10.0 before and after the emulsification process.

		P1	P2	P3	P4	P5
H_2O pH 6.3 *(mN/m)*	Before	22.85 ± 0.30	15.30 ± 0.46	26.96 ± 0.29	16.42 ± 1.08	22.71 ± 1.56
	After	26.61 ± 0.10	19.73 ± 0.10	34.12 ± 0.08	27.59 ± 0.85	28.83 ± 0.06
NaOH pH 10.0 *(mN/m)*	Before	15.49 ± 1.73	10.80 ± 2.10	6.47 ± 0.05	15.86 ± 0.18	16.00 ± 0.16
	After	18.62 ± 0.05	19.61 ± 0.02	35.50 ± 1.30	28.77 ± 0.11	30.11 ± 0.04
KOH pH 10.0 *(mN/m)*	Before	27.53 ± 0.24	15.34 ± 0.18	19.37 ± 0.16	12.03 ± 0.12	11.44 ± 0.24
	After	31.55 ± 1.62	17.13 ± 0.54	20.00 ± 1.70	21.59 ± 0.75	28.48 ± 0.09
$Ca(OH)_2$ pH 10.0 *(mN/m)*	Before	28.02 ± 0.03	14.73 ± 0.22	24.00 ± 0.44	17.87 ± 0.06	22.23 ± 0.03
	After	35.54 ± 2.35	19.96 ± 0.04	39.50 ± 0.32	21.70 ± 0.03	20.29 ± 0.18

The IFT values obtained before the emulsification, i.e. the crude oil as received and the aqueous solutions, present lower tensions in all cases (except for P5 and $Ca(OH)_2$) than that obtained from the oil after the emulsification and centrifugation. This behavior is expected as more material with interfacial activity is present in the oil

before the emulsification. After emulsification, part of the interfacial material is removed and higher IFT are observed. By observing the IFT variation ($\Delta\sigma$) between the before and after, we can notice the lower $\Delta\sigma$ values for the paraffinic oils P1 and P2. This lower variation indicates that less material with interfacial activity was removed from these oils after emulsification.

Comparing the IFT results before the emulsification (**Table 8**) and the LC micrographs at pH 10.0 (**Figures 39** to **41**), which represent the first contact between the petroleum (as received) and the alkaline solutions, is noted that for each oil, the systems with higher LC amounts observed were the ones that presented the lowest tensions. For example, for P1 the lowest IFT value among the alkaline solutions was obtained with NaOH (15.49 ± 1.73 mN/m), and the microscopy of this system was the one with the highest LC presence (**Figure 39**). P3 presented the same characteristic of P1, being the largest number of LC (**Figure 39**) and its lowest IFT (6.47 ± 0.05 mN/m) obtained with NaOH. P4 and P5 presented the lowest tensions in systems with KOH, and as can be seen in **Figure 40**, the content of LC is higher as with NaOH that also present low IFT values. This behavior can be related to the structure of the carboxylic acids native from each oil and their interaction with the cations.

The IFT for solutions with pH 12.0 was not evaluated on the drop method because it was not possible to form the drop. Thus, some values from pH 12.0 solutions were obtained from the Wilhelmy plate method. For P3 and NaOH, for example, the IFT value obtained was 1.24 ± 0.01 mN/m, for P5 and KOH the IFT value was 0.78 ± 0.02 mN/m.

4.2.8.2. Interfacial Modulus

The interfacial film formed by the crude oil surfactant molecules is able to withstand compression deformations and exhibit elasticity and viscosity. The dilatational rheology, which evaluates the variation of interfacial tension as a function of a drop volume or area variation during the interface compression/expansion, can be a very useful tool in evaluating the elasticity/viscosity of the film. According to the Gibbs elasticity equation (**11**), the interfacial layers are compressible, where ε is defined as interfacial modulus, i.e. the resistance to the creation of gradients in surface/interfacial

tension and *A* represents the area (FULLER and VERMANT, 2012).

$$\varepsilon = \frac{d\sigma}{dlnA} \tag{11}$$

The elasticity can be broken down into two components: one real (ε'), which represents the elastic modulus; and an imaginary one (ε"), which represents the viscous modulus (**Equation 12**).

$$\varepsilon = \varepsilon' + \varepsilon'' \tag{12}$$

Figure 44 presents the viscous and the elastic modulus of the P4 and H_2O, NaOH, KOH and $Ca(OH)_2$ at pH 10.0 before the emulsification process.

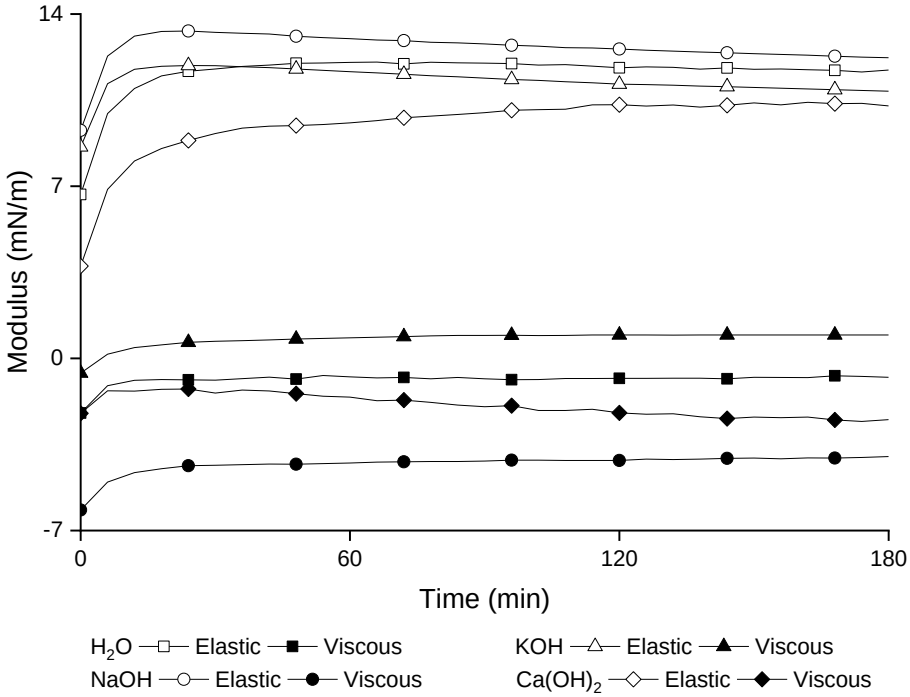

Figure 44: Elastic and viscous modulis of P4 and H_2O, NaOH, KOH and $Ca(OH)_2$ at pH 10.0 before the emulsification process.

The elasticity of the interfacial film can vary considerably over time because of the rearrangement, displacement, interfacial transport and consequent consolidation of the film (VERRUTO *et al*., 2009). For P4, the elasticity of the interfacial film variates

during the first 30 min of analyses; after that, both ε' and ε'' do not show significant variations, i.e. the film reached the consolidation. It is also possible to notice that the interfacial module is essentially governed by the elastic component as its values are high when compared to the viscous component, which presents values close to zero or even negative. Therefore, the interfacial film has elastic behavior.

The average of the last hour of analyses of the elastic modulus (ε') for P1-P2 and P4-P5 and H_2O, pH 10.0 alkaline solutions made with NaOH, KOH and $Ca(OH)_2$ is presented in **Table 9**. Typically, after one hour, the curve of interfacial tension becomes nearly constant with time and then a value of the interfacial tension for a specific volume is recorded. The study of the oscillation amplitude is performed by analyzing the constant region of the elasticity in the function of time for oscillations of different fractions of the interfacial area (ALVES *et al*., 2014).

Table 9: Elastic modulus (ε') between P1-P2 and P4-P5 and deionized water, NaOH, KOH and $Ca(OH)_2$ solutions at pH 10.0 before and after the emulsification process.

		P1	P2	P4	P5
H_2O pH 6.3 *(mN/m)*	Before	12.68 ± 0.66	5.12 ± 1.90	11.79 ± 0.35	8.12 ± 0.34
	After	2.35 ± 0.25	2.57 ± 0.11	4.83 ± 0.30	3.86 ± 0.24
NaOH pH 10.0 *(mN/m)*	Before	14.86 ± 1.27	36.96 ± 1.28	12.37 ± 0.18	13.75 ± 0.29
	After	4.01 ± 0.41	2.81 ± 0.10	1.05 ± 0.38	12.97 ± 0.06
KOH pH 10.0 *(mN/m)*	Before	7.08 ± 0.17	6.45 ± 0.94	10.96 ± 0.23	17.15 ± 0.79
	After	4.29 ± 0.24	4.26 ± 0.53	10.51 ± 0.04	12.98 ± 0.35
$Ca(OH)_2$ pH 10.0 *(mN/m)*	Before	6.39 ± 0.38	9.88 ± 0.19	10.32 ± 0.06	5.44 ± 0.02
	After	3.02 ± 0.29	3.32 ± 0.28	9.75 ± 0.28	6.21 ± 0.37

Because of the synergism, a mix of surfactants can provide better performance than single surfactant systems (ROSEN and KUNJAPPU, 2012). Attractive interactions between molecules of different surfactant change the concentration of surfactant required to give a certain surface tension, surface pressure, or cross-sectional molecular area (ISHIZUKA *et al*., 2011). The surfactant films behavior of molecular packaging is closely related to their bending elastic properties (SZLEIFER *et al*., 1990; CANTOR, 1999). As the surfactant molecules are more tightly packaged, the elasticity

of the film increases because of the increase in the bending constant. The bending constant is also related to phase behavior and structure (ISHIZUKA *et al*., 2011). Except for P5 and $Ca(OH)_2$, it is observed a decrease in the elastic modulus data from the system composed of crude oil as received (before) and the systems composed by the dehydrated oil after one emulsification process. Possibly, a more diverse range of surfactant molecules is present in the petroleum as received. After emulsification, part of this material is removed (as already shown in the IFT reduction), therefore, a reduction in the elastic modulus also occurs.

Moreover, the highest ε' value for the systems before emulsification process was obtained with NaOH, except for P5 which present the high ε' with KOH, indicating the formation of more rigid interfaces with NaOH system. In general, the $Ca(OH)_2$ systems present the lower values.

Interfaces with large elastic modulus experience a relatively large increase in energy when the interfacial area increases or surfactants such as asphaltenes are spread more thinly on the interface. Therefore, a droplet with an elastic film is less likely to deform during a collision with another droplet (SZTUKOWSKI and YARRANTON, 2005b).

The elastic modulus for P3 could not be determined. The values obtained were below of the equipment detection limits, possibly because of the high viscosity presented by this petroleum as received (2.66 Pa.s) and after emulsification and demulsification. The viscosities of the dehydrated P3 after demulsification process were 3.43 ± 0.01 Pa.s for water, 4.03 ± 0.01 Pa.s for NaOH, 4.40 ± 0.01 Pa.s for KOH, and $3.58 \pm 3.3 \times 10^{-3}$ Pa.s for P3 and $Ca(OH)_2$. According to Rötger (1974), for material at a constant temperature, there are many relaxation times, but only one viscosity. Where only a single relaxation time is involved, the viscosity is directly connected with the elastic modulus. The relaxation time of the P3 is governed by the viscosity and not by the elastic modulus. In addition, ε' is not always measurable.

4.3. PARTIAL CONCLUSION

In the absence of water, the crude oil samples as received do not present liquid crystalline structures. The LC in crude oil emulsions systems is directly related to the

presence of water. This behavior is expected due to the lyotropic features of the lamellar LCs. Immediately after the preparation of the emulsions containing 20.0 and 50.0 wt. % of water, there is no visible phase separation. The micrographs shows a large number of droplets on the bright field. However, in the polarized light no Maltese cross was observed, i.e., no LC is present. After emulsion destabilization, few or none water droplets were observed on the top oily phase. These droplets do not present LC. However, the microscopy of the bottom phases of the emulsion, that is composed of dispersed oil or multiple emulsion droplets in the aqueous phase, present LC structure in almost all droplets.

It is found that bottom fractions of emulsion composed by both paraffinic and non-paraffinic oils are characterized by the presence of Maltese cross patterns. The presence of the salt (NaCl up to 35.0 g/L) is also not relevant for the formation or inhibition of liquid crystalline structures. Therefore, it is believed that the presence of liquid crystals is not conditioned to the paraffinic composition of crude oil and even to the salt concentration an aqueous phase. However, the aqueous phase content is a determining factor for the appearance and observation of liquid crystals. The LC is favored at high levels of the aqueous phase. The TAN values and the viscosity of petroleum are also related to the LC formation. The low viscosities may favor the interaction between the oil and water and thus form more LC.

The pH of the aqueous phase is another important factor related to the LC presence. Less LC structures were observed for deionized water than in the presence of alkaline solutions, and in general, the amount of LC structures increase with the increase in the pH. Thus, the ionization of the NA in high pH and/or the formation of naphthenates possibly are related to the LC formation.

The presence of different alkaline solutions composed by cations with different volume and valence can also affect the LC formation. In some cases, the larger volume for K^+ can be responsible for less LC structures compared with Na^+ systems because the volume can disturb the organization of the molecules and consequently the LC formation. However, in other cases, the LC presence does not show differences between Na^+ and K^+. Possibly this behavior is related to the type of the structure of the acidic molecules that can interact with both Na^+ and K^+, and are different in each oil. Comparing the systems composed by different cation valence (Na^+ and Ca^{2+}) and the

same volume it is possible to note that, in general, for the monovalent Na^+ more LC were observed. The bivalent Ca^{2+} was not too efficient on the LC formation.

As the petroleum is a very complex multicomponent matrix, the structures of its natural surfactants are unknown, as well as the kinetics of stabilizing the interfaces of these molecules. Thus, it was not possible to establish a relationship between the equilibrium velocities of adsorption and desorption of the molecules at the interface and the type of aqueous solution. However, in general, the systems composed by the petroleum as received, i.e. before the emulsification processes present a faster IFT stabilization kinetics than systems that used dehydrated oil after emulsification. The IFT values obtained before the emulsification, present lower tensions in all cases than that obtained from the oil after the emulsification and centrifugation. This behavior is expected since more material with interfacial activity is present in the oil before the emulsification. After emulsification, part of the interfacial material is removed and higher IFT were observed.

The interfacial modulus is essentially governed by the elastic component since its values are high when compared to the viscous component. The elasticity of the interfacial film reached the consolidation after around 30 min. Due to synergism, interactions between molecules of different surfactant can be organized in more tightly packaged, and then the elasticity of the film increases. In general, it is observed a decrease in the elastic modulus data from the system composed of crude oil as received (before) and the systems composed by the crude oil after one emulsification process. Possibly, a more diverse range of surfactant molecules is present in the crude as received. After emulsification, part of this material is removed and a reduction in the elastic modulus occurs.

The interfacial material removal by the aqueous phases was observed on the pH analyses, on the IFT values increase and the elastic modulus decrease between the oil before and after emulsification process. Possibly this behavior is related to the transfer of the acidic compounds from the oily to the aqueous phase. In the first emulsification, most of the soluble acidic compounds are transferred to the water, thus, in the following emulsions steps, fewer compounds are available.

5. EXTRACTION AND CHARACTERIZATION OF INTERFACIAL MATERIAL

Based on the fact that the oil emulsification process removes part of the material with interfacial activity (as discussed in **Chapter 4**), it was decided to use aqueous phase extraction (emulsification) to remove the interfacial material that can be related to the LC formation.

5.1. MATERIALS AND METHODS

5.1.1. Materials

5.1.1.1. Crude Oils

Five of the seven oils assessed in **Chapter 4** were used. They were identified as P1-P5, all supplied by Petrobras.

5.1.1.2. Aqueous Phases

Deionized water and three alkaline solutions with $1.0x10^{-2}$ mol/L (pH 12.0) of sodium hydroxide (NaOH), potassium hydroxide (KOH) and calcium hydroxide ($Ca(OH)_2$), all from Sigma Aldrich, were used.

5.1.1.3. Model Emulsion

Mineral oil (0.86 g/cm^3 at 20.0 ºC) was used as the oil phase. A commercial naphthenic acid (0.92 g/cm^3 at 20.0 ºC, yellow/light brown liquid) was used as surfactant. Both are from Sigma Aldrich. The emulsion preparation procedure is the same as described on **item 4.1.4**.

5.1.2. Aqueous Phase Extraction

The aqueous phase extraction is based on emulsification of 20.0 wt. % of crude oil (30.0 g) and 80.0 wt. % of aqueous solutions at pH 12.0, totaling 150.0 g. The biphasic system (**Figure 45A**) is then mixed at 6,000 rpm for 3.0 min in Polytron PT

3100 at room temperature (**Figure 45B**) (as described in **item 4.1.4**). After the emulsification, the system is kept at rest for 24 h to favor the natural separation of the phases (**Figure 45C**). The aqueous phase (bottom fraction), rich in LC structures, were removed with a syringe and transferred to a new becker. Then the aqueous phase was subjected to a heating process in a C-MAG HS7 plate (IKA). The temperature of heating was around 50.0 and 60.0 °C, for water evaporation and concentration of the liquid crystalline material. Because of the presence of oil in this aqueous phase, during the heating, the residual oil sticks on the walls of the becker, being removed with a spatula. At the end of the process, the precipitate salt appears on the bottom of the becker and is collected.

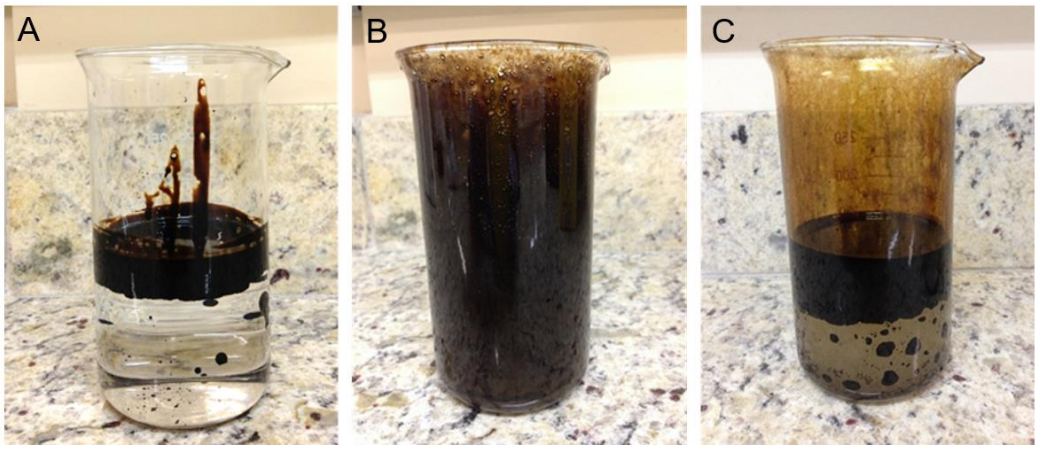

Figure 45: Process of aqueous phase extraction of material with interfacial activity (A) before stirring, (B) shortly after stirring and (C) 24 h after stirring.

5.1.3. Characterizations

5.1.3.1. SAXS

The interfacial material was submitted to small angle X-ray scattering (SAXS) at Laboratório Nacional de Luz Síncrotron (LNLS) in Campinas-SP. The aqueous bottom fraction, rich in LC, of P5 and deionized water and NaOH pH 12.0 solution, were analyzed. The SAXS1 light line was used, operating at a fixed energy of 8.0 keV. The distance between the sample and the detector was 1.0 m. This experiment allows determination of structural parameters such as distances present in the molecules, spinning radius, mass, morphology, state of aggregation, etc., with dimensions ranging

between 1.0 and 100.0 nm.

5.1.3.2. FT-IR

The salt collected from each extraction described above (**item 5.1.2**) was characterized by FT-IR with attenuated total reflectance (ATR) and 60 scans, 4.0 cm^{-1} of the resolution, on Frontier FT-IR/FIR (Perkin Elmer). The analyses were carried out on LAPIN laboratory on Instituto de Macromoléculas Eloisa Mano (IMA) at Federal University of Rio de Janeiro. The commercial naphthenic acid was characterized by FT-IR with ATR by Nicolet 6700 (Thermo Scientific) at Engepol laboratory.

5.2. RESULTS AND DISCUSSIONS

5.2.1. SAXS

The SAXS method requires a Synchrotron light source that is generated from a particle accelerator. This light beam irradiates the sample and X-ray scattering at small angles (θ <10 °) is then analyzed (DONG and BOYD, 2011). For this purpose, a detector and an analyzer that registers the SAXS measurements *(I(q)*) as a function of the scattering vector modulus (*q*) (GLATTER and KRATKY, 1982) are used. **Figure 46** shows a hypothetical curve of a SAXS analysis.

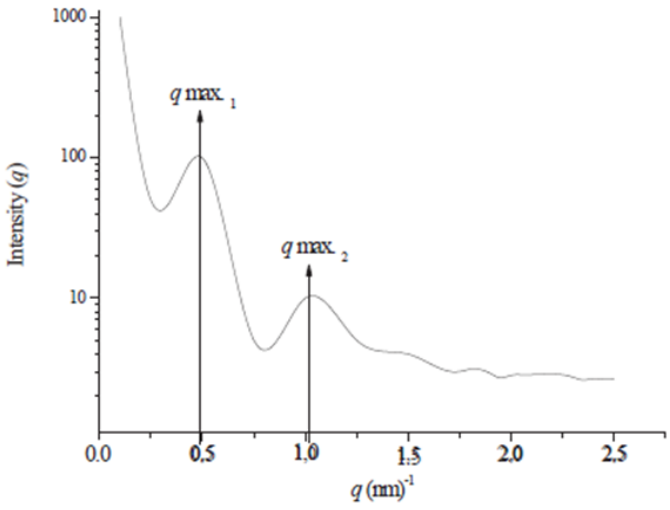

Figure 46: SAXS hypothetical curve for LCs: intensity x scattering vector (CHIARI *et al*., 2012)

The peaks shown in **Figure 46** are known as Bragg peaks, which provide information on the diffractive effects of the material with crystalline characteristics. These peaks are directly related to the scattering of X-rays that affect the sample. The structure of the crystalline or liquid crystalline material has a periodicity, that is, there are planes of atoms separated by a fixed distance in the different directions (DANIELSSON, 1976). **Figure 47** shows the diffraction, the optical path difference between X-rays.

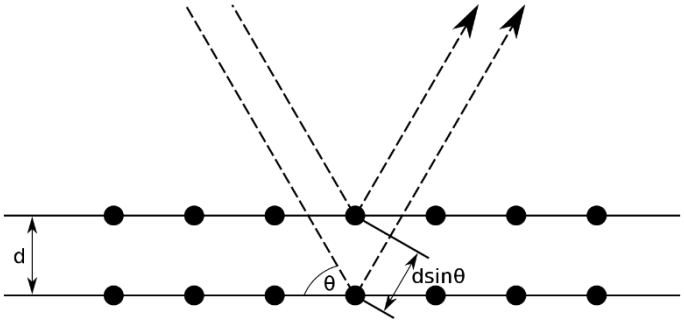

Figure 47: Optical path difference between two rays, where *d* is the distance between the considered planes and θ is the angle of incidence.
(https://pt.wikipedia.org/wiki/Lei_de_Bragg)

This diffraction occurs according to the Bragg Law and is described by **Equation 13**, which establishes the relationship between the diffraction angle and the distance between planes. In this equation, *n* is an integer, λ is the wavelength of the X-rays, *d* is the interplanar distance and θ is the diffraction angle.

$$n\lambda = 2d\ sen\theta \tag{13}$$

The value obtained in a SAXS analysis represents this distance between the particles capable of spreading X-rays. The relationship between the values obtained indicates the type of arrangement found in the system (GLATTER and KRATKY, 1982; ALEXANDRIDIS *et al*., 1998; CRAIEVICH, 2002). For lyotropic systems, the position and intensity of the Bragg peaks allow determining the crystallographic symmetry. This analysis is given by the relative distances of the peaks. For the lamellar phases, the *q* values of the Bragg peaks exhibit the ratios 1: 2: 3: 4... (CAMPOS *et al*., 2012). In the case of the hypothetical curve shown in **Figure 46**, the ratio *d1*/*d2* would result in 2, which describes lamellar structures (ALEXANDRIDIS *et al*., 1998).

Figure 48 presents SAXS curves for the aqueous bottom fractions of the systems composed by P5 and H_2O and NaOH. The P5 and deionized water curves are very noisy, indicating that there are no objects on the SAXS scale. The curve of this sample is identical to a pure water curve. Possibly the oil droplets surrounded by LC of this system coalesced or adhered to the glass of the bottle during transportation since the phase was completely clear before the SAXS analyses. The inclination of the P5 and NaOH curve indicates the formation of very large objects, which are probably the droplets of the emulsions; however, there are no Bragg peaks. According to Bagheri *et al*. (2012) and Engels *et al*. (1995), lamellar LCs dispersed in an emulsion can be analyzed by SAXS as they are able to disperse the X-ray beams; however, emulsions with submicron droplet sizes are not detectable. The average droplet size for the system P5 and NaOH, determined through microscopy analyzes, was 4.57 ± 0.47 µm of diameter, and an LC thickness of 1.77 ± 0.14 µm, which are values that can be identifiable by SAXS. The absence of Bragg peaks, in this case, can be related to the complex matrix that is the petroleum itself, which may contain crystalline compounds interfering in the SAXS analysis.

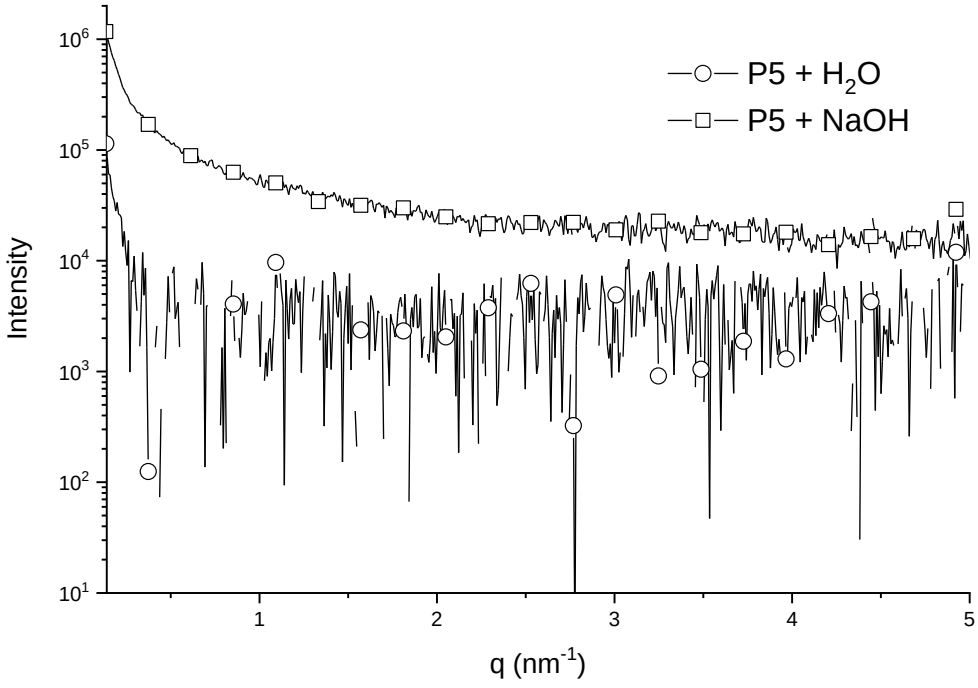

Figure 48: SAXS curves for aqueous bottom fractions of the systems composed by P5 and H_2O and NaOH.

5.2.2. Coffee Ring Effect

The coffee ring effect is an interesting phenomenon in colloid science. When a colloidal emulsion is dried on a solid surface, the dispersed particles or droplets move to the edge of the droplet and deposit in a ring shape, the coffee ring effect (YUNKER *et al*., 2011).

The liquid crystal domains in the water-rich phase of crude oil are mobile both in the bulk and on the edges of a droplet and tend to concentrate on the border of the sessile aqueous drops. **Figure 49** presents some polarized micrographs of this effect.

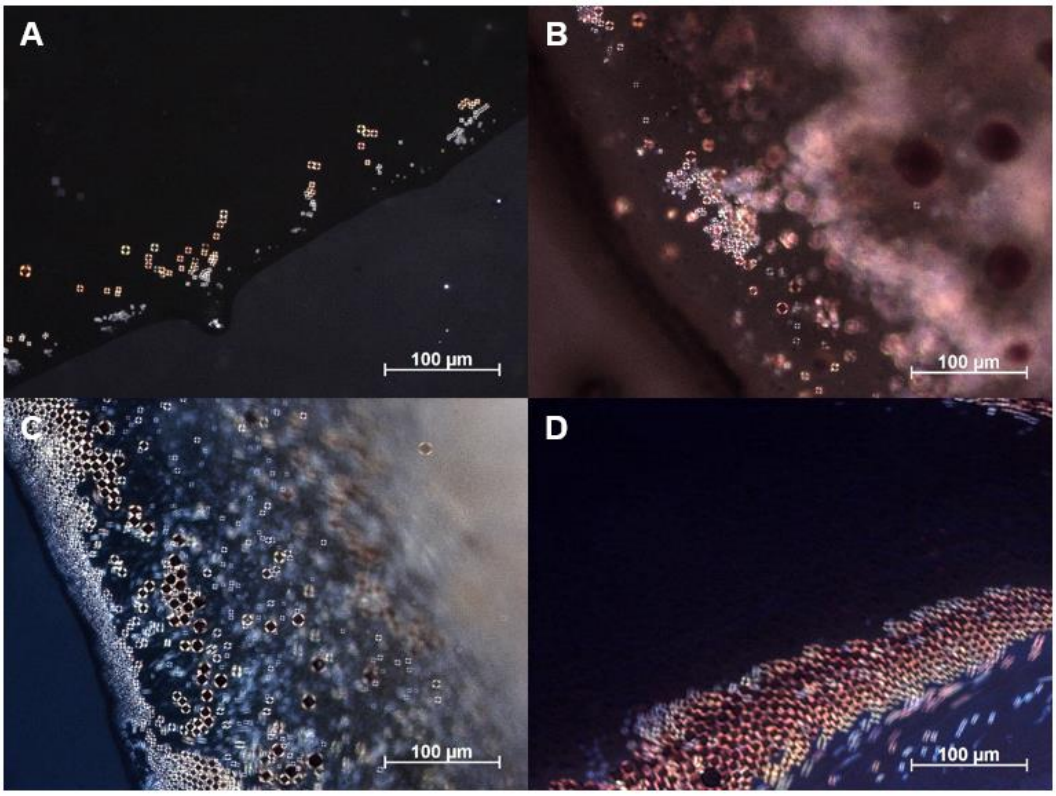

Figure 49: Coffee ring effect on (A) P5 and H_2O; (B) P3 and $Ca(OH)_2$; (C) P4 and NaOH and (D) P5 and KOH.

According to Qin (2014), this effect is accentuated as the sessile aqueous drops evaporate. While the water evaporates, the size of the contact line of the droplet does not change. The evaporation leads only to a contact angle decrease ($\beta_1>\beta_2>\beta_3$) Induced by the evaporation, the outward capillary flow carries the LC from the center to the edges of the sessile droplet (RUSSEL, 2011). **Figure 50** shows a schematic illustration of this behavior.

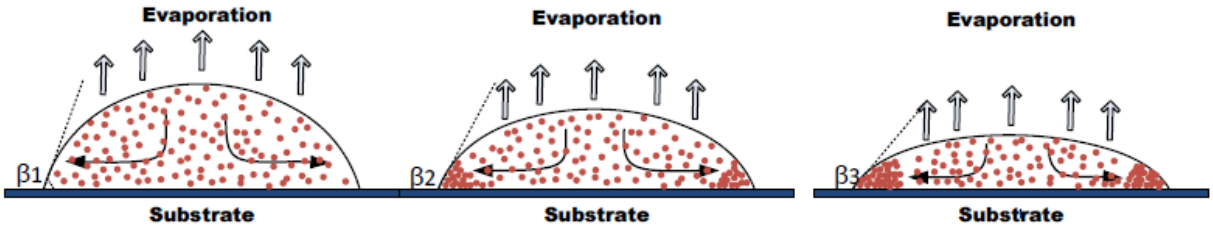

Figure 50: Coffee ring effect during sessile aqueous droplet evaporation. (QIN, 2014)

During the water evaporation, the oil droplets surrounded by liquid crystal lose their structures, coalesce, and form a film in the water-free residue. Thus, the material responsible for the LC layer, deposits on the edges of the sessile droplet.

Figure 51 presents polarized light micrographs of the deposits obtained by QIN (2014) from Shell Peace River bitumen emulsion; and **Figure 52** presents the 24 h dry edges of the sessile droplets for systems composed by P4-P5 and H_2O, and NaOH, KOH, $Ca(OH)_2$ at pH 12.0. It is possible to note that Qin sample is similar to that obtained on this present thesis.

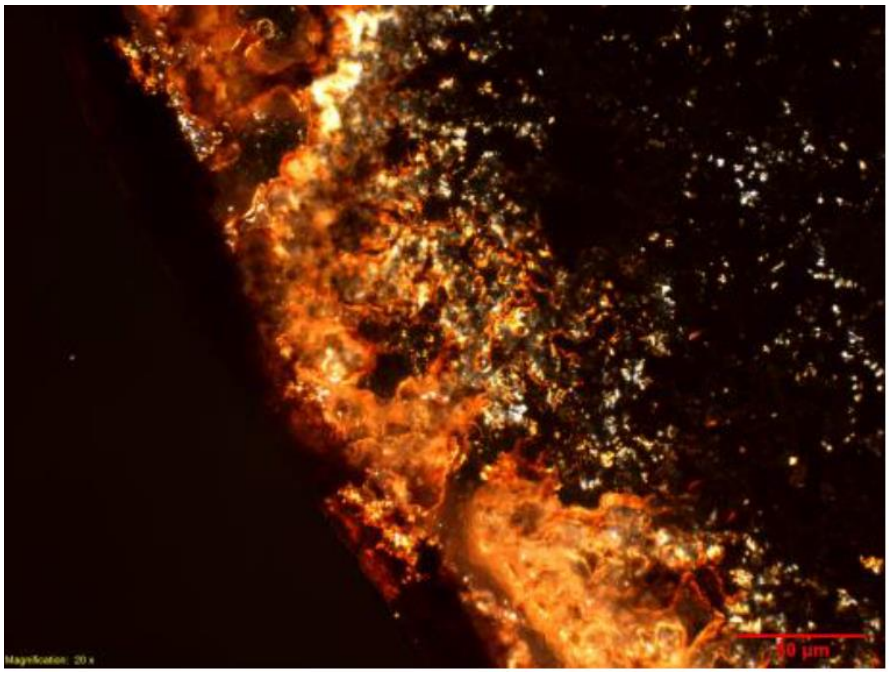

Figure 51: Polarized light micrograph of water free residue from Shell Peace River. (QIN, 2014)

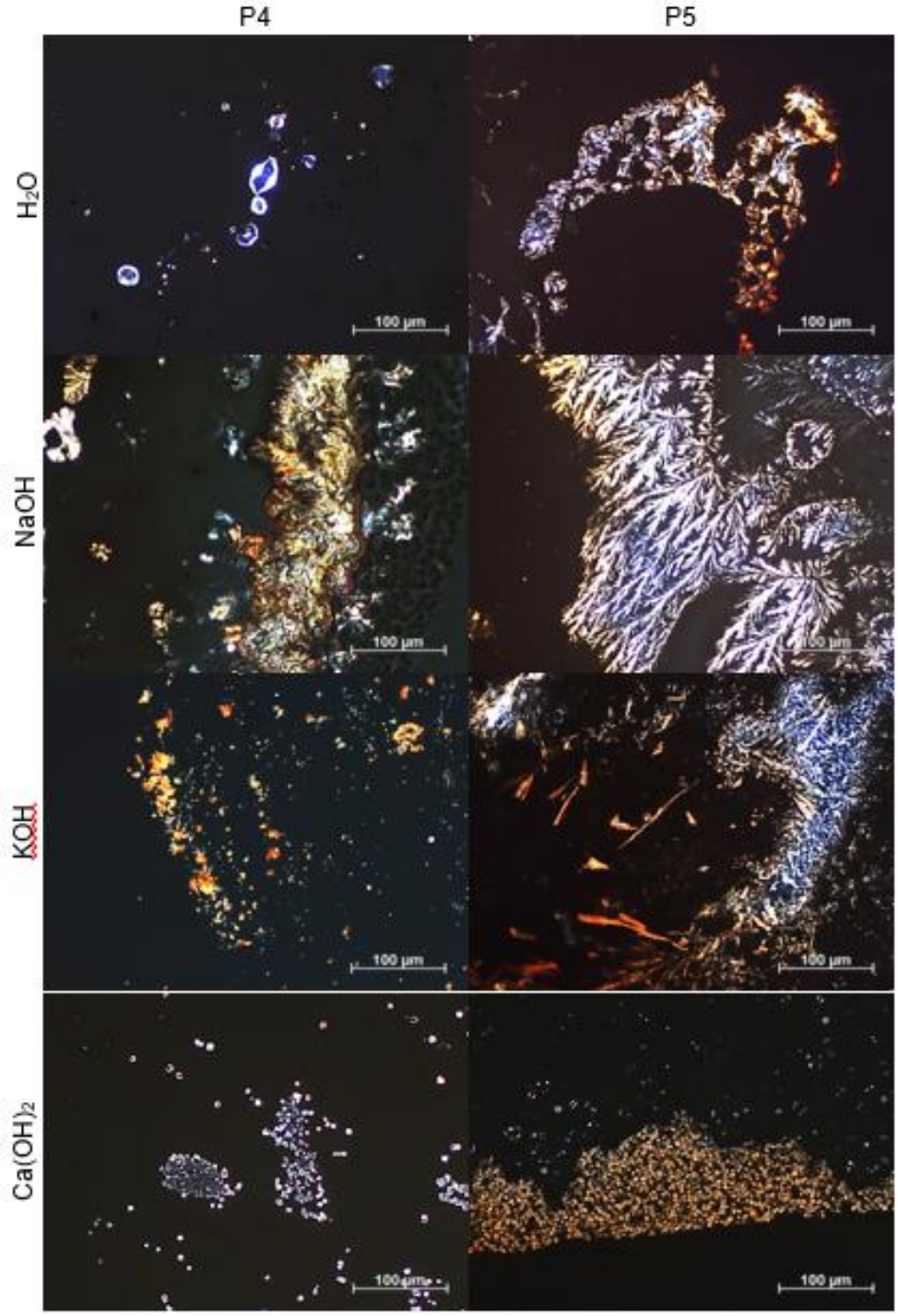

Figure 52: Polarized light micrographs of the dry edges for systems composed by P4-P5 and H_2O, and NaOH, KOH, $Ca(OH)_2$ at pH 12.0.

5.2.3. Aqueous Phase Extraction

Because of the possibility of LC concentration on the edges of the sessile droplets, the aqueous phase extraction methodology was proposed. The extraction is

based on the liquid crystalline material concentration at the edge of droplets during the evaporation process. Thus, a larger volume of solution containing LC was placed in a becker and heated to about 50.0 to 60.0 °C to speed up the process. It is known that LC are lyotropic structures that need water to be formed, i.e. without water, the liquid crystalline structure ceases to exist. In addition, is also known that due to the alkaline solutions and the acidic compounds of the oil, an acid-base reaction occurs forming metal salts (as described in **item 4.2.7**). Thus, the material deposited on the bottom of becker after water evaporation (**Figure 53**) is possibly related to naphthenates and not to the LC itself. In addition, this evaporation residue can contains salts and excess of alkali (e.g. NaOH, KOH and $Ca(OH)_2$).

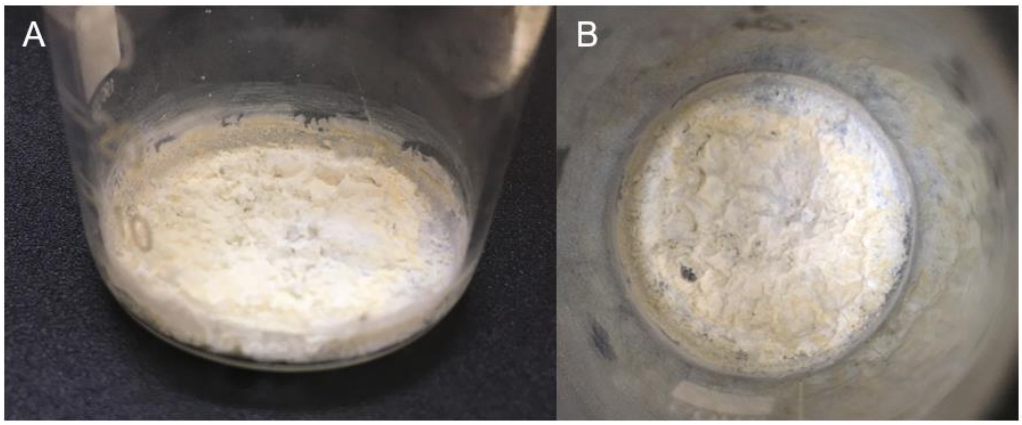

Figure 53: Extracted saline material after water evaporation.

The total amount of saline material extracted from systems composed by P1-P5 and pH 12.0 alkaline solution made with NaOH, KOH and $Ca(OH)_2$ are presented in **Table 10**. These masses are related to 90.0 to 120.0 g of original petroleum. **Figure 54** presents the photograph of each saline material extracted.

Table 10: Mass of saline material collected after water evaporation.

	NaOH	**KOH**	**$Ca(OH)_2$**
P1	0.0869 g	0.1263 g	0.0655 g
P2	0.1060 g	0.1220 g	0.0211 g
P3	0.0817 g	0.0846 g	0.0153 g
P4	0.3748 g	0.2637 g	0.0234 g
P5	0.5605 g	0.7186 g	0.1133 g

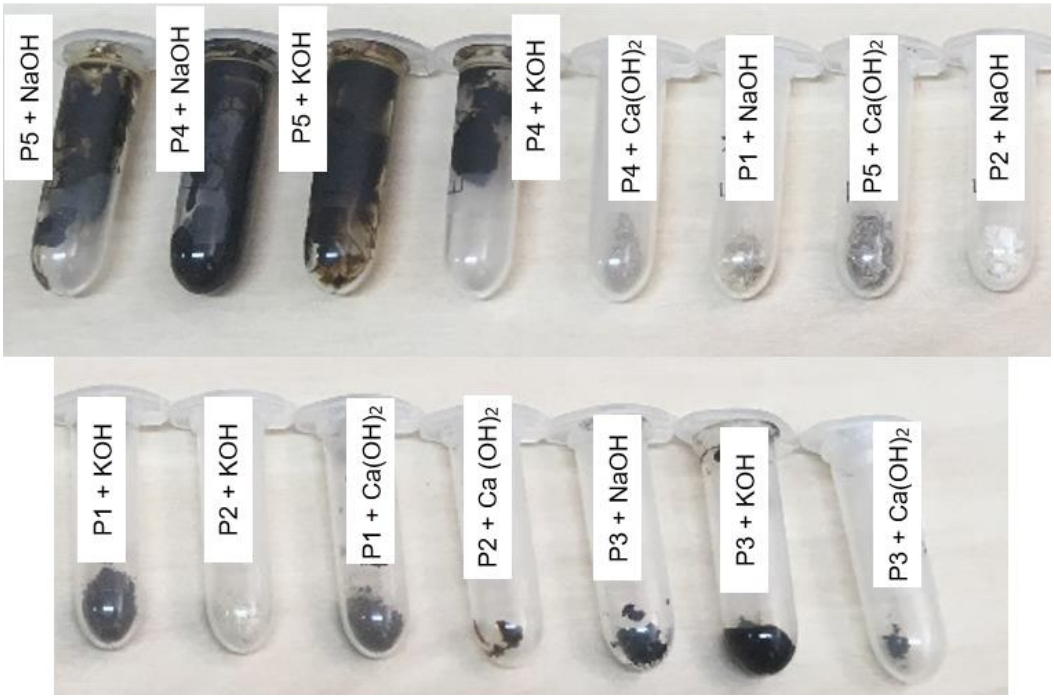

Figure 54: Extracted salt material from P1-P5 and NaOH, KOH and $Ca(OH)_2$.

Observing **Figure 54** is noted that not all samples provide white salts. Some of them are yellow or brown and others are like a viscous paste. No relationship can be observed between the colorations of the extracted materials and the respective compositions of the systems (crude oil and alkaline solutions). These color and aspects characteristics can be related to the oil composition and to the acid-basic reaction. The acidic matrix of each oil is different in composition and in content, therefore it is expected that the product of the acid-base reaction was different. In addition, other compounds may have been extracted together, such as asphaltenes that are solid particles at 25.0 °C (QIN, 2014). In general, the material extracted from the paraffinic petroleum P1 and P2 are more similar to a salt, with crystalline appearance, and these oils have the lowest levels of asphaltenes.

In order to verify if the salt material extracted can form a structured interfacial film, IFT and interfacial rheology was performed (according to the method described in **items 4.1.9.1** and **4.1.10,** respectively). **Figure 55** present the IFT between an aqueous solution (2.44 g/L of the collected salt material from P2 and KOH) and mineral oil, and the IFT of pure deionized water and mineral oil as the reference of absence of salt material. **Figure 56** presents the elastic modulus for both systems.

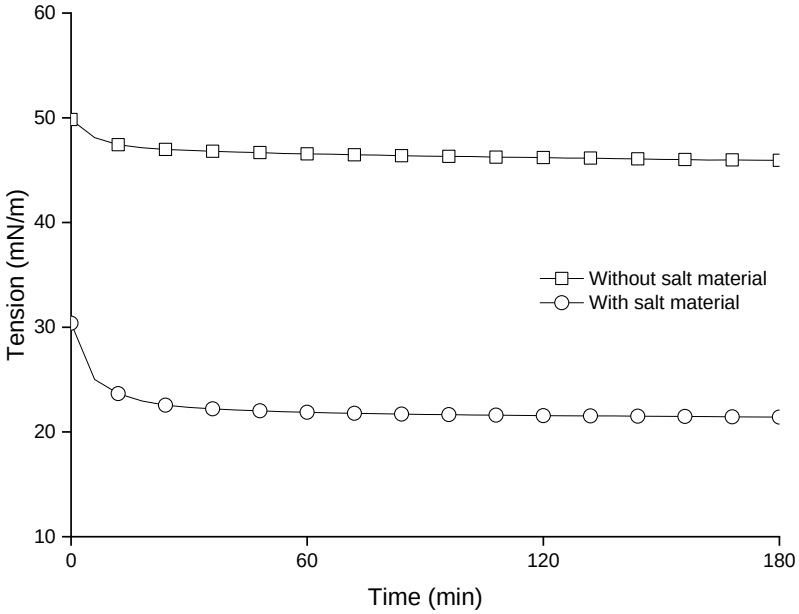

Figure 55: IFT between water and mineral oil with and without P2 and KOH collected salt material.

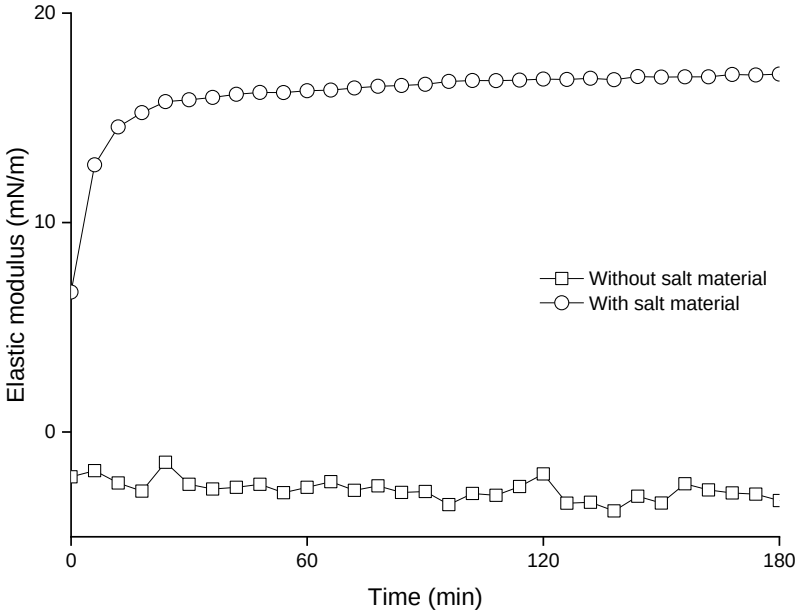

Figure 56: Elastic modulus between water and mineral oil with and without P2 and KOH collected salt material.

It is possible to observe that (**Figure 55**), as expected, the IFT between pure water and mineral oil (46.0 ± 0.1 mN/m average of the last hour) was higher than that with the salt material in the aqueous phase (21.5 ± 4.5x10^{-2} mN/m average of the last hour). This behavior confirms that the salt material posses interfacial activity. This

interfacial activity can be noted on the interfacial elastic modulus (**Figure 56**). The system with the salt material presents an elastic modulus of 16.9 ± 0.1 mN/m and, for the system without the salt material the modulus was negative (-3.0 ± 0.5 mN/m), i.e. out of the equipment detection limit because of lack of organized interface.

5.2.3.1. FT-IR

The FT-IR spectra of the previously collected salt materials are shown in the next figures. **Figures 57** shows the salt material form system composed of P2-P5 and NaOH solutions. It is possible to note that P2 respective salt material is white (**Figure 54**) and the FT-IR spectra do not show good peaks. The peaks from this system were relatively weak and poorly resolved. In addition, it is observed the absence of a peak at approximately 3000 cm-1, which is relative to –OH from carboxylic acid (PAVIA *et al*., 2001). Possibly, this absence of –OH peak could be related to high reaction conversion, i.e. the acid-base reaction converted all the acid into salt. The P3-P5 extracted salt materials are brown (**Figure 54**) and their respective spectra present the –OH peak, with P5 having the best-defined peaks.

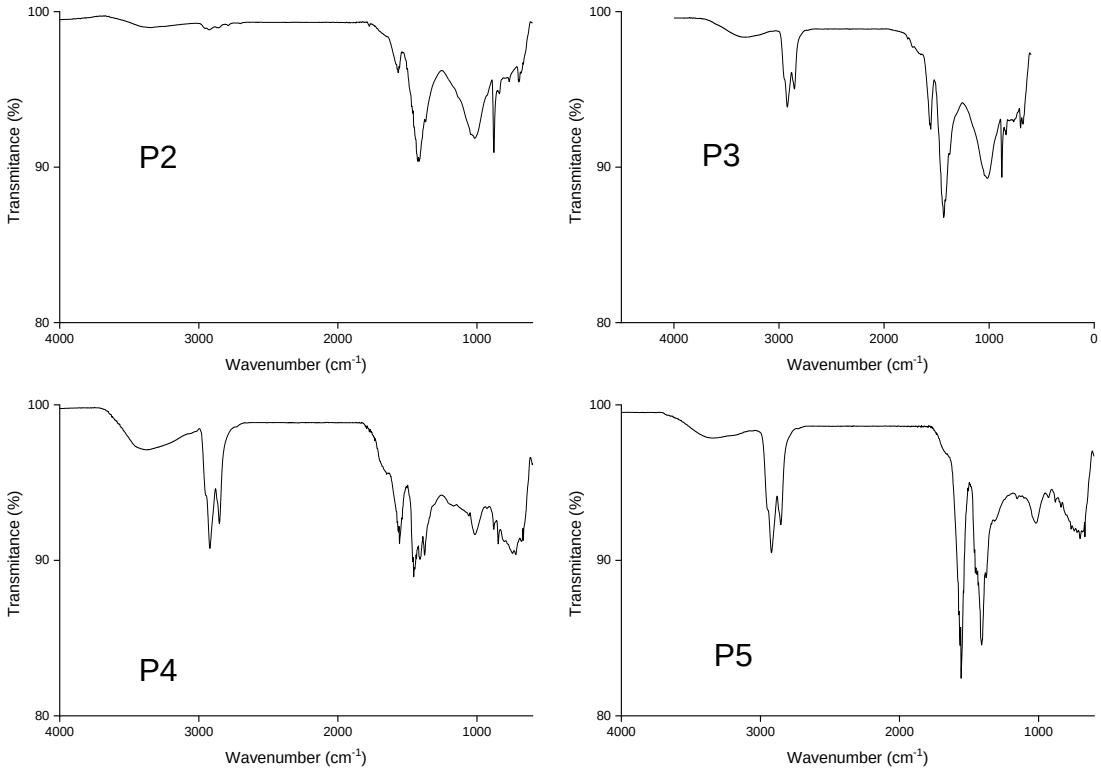

Figure 57: FT-IR spectra from salt material collected from P2-P5 and NaOH.

Figure 58 presents the P1 and P5 FT-IR spectra from the respective extracted salts from the KOH solution. To the KOH respective salts, all FT-IR spectra present the –OH peak; however, the resolution of peaks below 1800 cm^{-1} was not good from P1. Peaks below 1800 cm^{-1} are related to –C=O, –C-O, $–CH_2$, $–CH_3$ and –OH out of the molecule plane. The P5 spectra present a better peak resolution below 1800 cm^{-1} compared to the other samples.

Figure 59 presents the spectra from extracted salt material from P2 and P5 and $Ca(OH)_2$. The $Ca(OH)_2$ extracted salt materials show the lowest resolution spectra for all samples. In these cases, no peak can be correctly identified. **Figure 60** presents the FT-IR of commercial naphthenic acid.

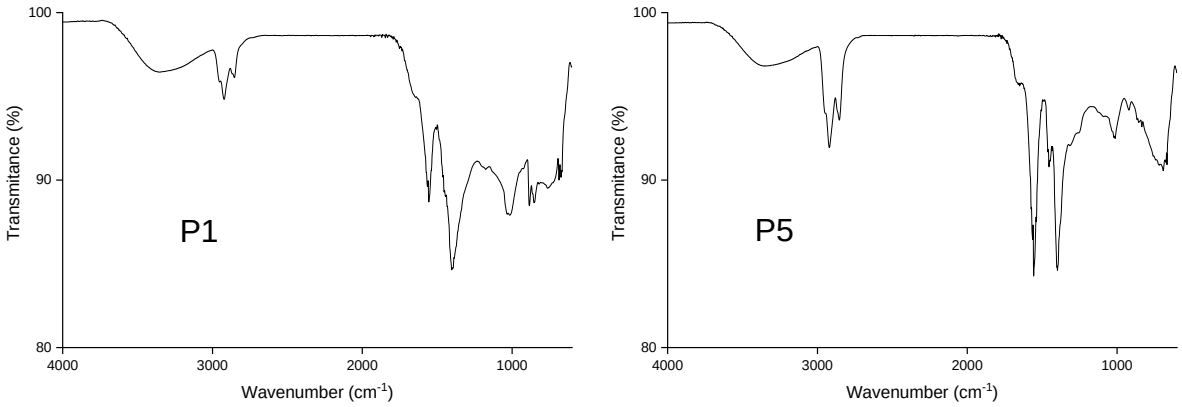

Figure 58: FT-IR spectra from salt material collected from P1 and P5 and KOH.

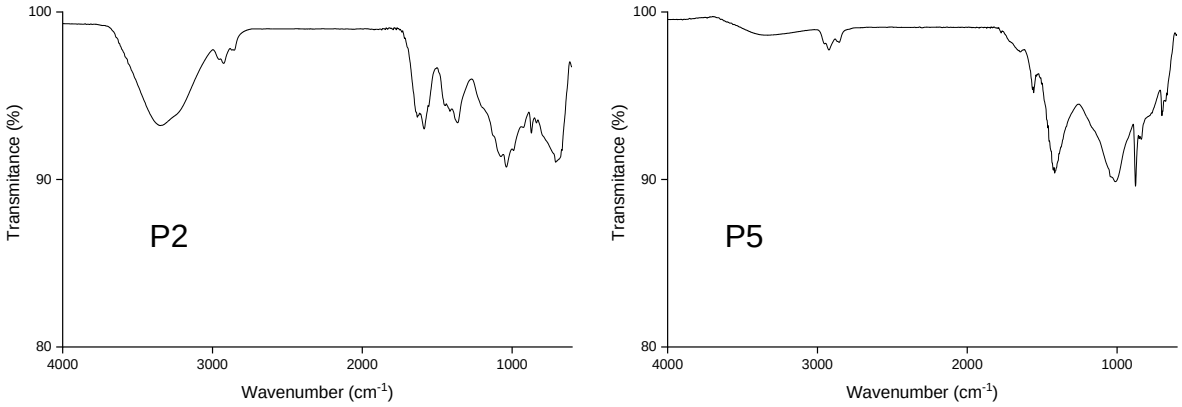

Figure 59: FT-IR spectra from salt material collected from P2 and P5 and $Ca(OH)_2$.

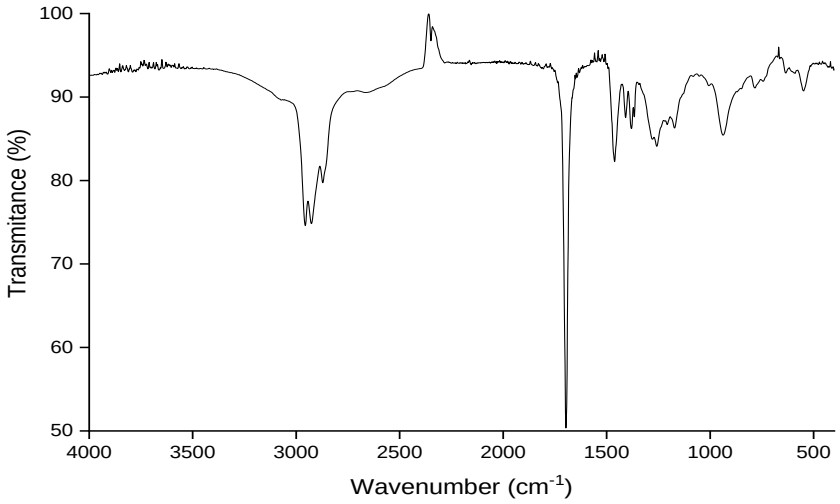

Figure 60: FT-IR spectra of commercial naphthenic acid.

The FT-IR spectrum of commercial naphthenic acid shows a broad duplet in 2950-2920 cm^{-1}, and a peak at 2870 cm^{-1} attached. According to Pavia *et al*. (2001), the FT-IR spectra of –OH from carboxylic acid has broadband between 3400 and 2400 cm^{-1}, generally, overlap –CH peak at 3000 cm^{-1}. The salt material extracted to the P5 and NaOH (best spectral resolution) (**Figure 57**) present the peak at 2920 cm^{-1}.

Carboxylic acids have strong bands between 1730 and 1700 cm^{-1} for –C=O of single aliphatic chains, but if there is –C=C or phenyl group this band can be shifted down (PAVIA *et al*., 2001). The commercial NA present a strong and sharp peak at 1697 cm^{-1} that could be related to –C=O of single aliphatic chains, and probably there is –C=C or phenyl group. The spectra of P5 and NaOH (**Figure 57**) did not present this peak. The commercial NA show a weak and sharp peak at 1467 cm^{-1}, referring to $–CH_2$ (1465 cm^{-1}). The P5 and NaOH did not present peak ate 1465 cm^{-1}, however present peaks at 1556 and 1409 cm^{-1} that could be related to –C-O vibrations in the –COOR group, bending vibrations –COH in-plane bending vibrations respectively (KARIMI *et al*., 2016).

According to Pavia *et al*., (2001), the –C-O peak from carboxylic acids occurs between 1320 and 1210 cm^{-1} and has medium intensity. Broadband at 930 cm^{-1} is characteristic of –OH outside the plane of the molecule. The commercial NA present weak and wide peaks at 1260 and 930 cm^{-1}. The P5 and NaOH (**Figure 57**) did not show these peaks. The peak of $–CH_2$ from an open chain with more than four carbons are present at 720 cm^{-1} (PAVIA *et al*., 2001). The commercial acid does not have a

peak at 720 cm^{-1}, thus it should not have more than four linear carbons in the chain. However, the P5 and NaOH (**Figure 57**) possess a peak at 702 cm^{-1} that could be related to $–CH_2$ from the open chain.

With this FT-IR information, it is possible to note some similar characteristics between the commercial NA and the salt material extracted from the P5 and NaOH. However, it is not possible to attest that the P5 and NaOH salt material is an NA. Because of that, a model emulsion composed by the commercial NA was prepared and analyzed by optical microscopy in an attempt to observe the LC Maltese cross pattern.

5.2.4. Liquid Crystal in Model Emulsion System

Because of the indications that naphthenic acids are responsible for the LC formation in petroleum emulsions, an emulsion containing 20.0 wt. % of mineral oil, water, and 3.33 wt. % of commercial naphthenic acid was prepared. **Figure 61** shows the polarized light microscopy of the bottom fraction of this emulsion. It is possible to observe the pattern of the characteristic Maltese cross of LC. This observation is another evidence linking LCs with naphthenic acids.

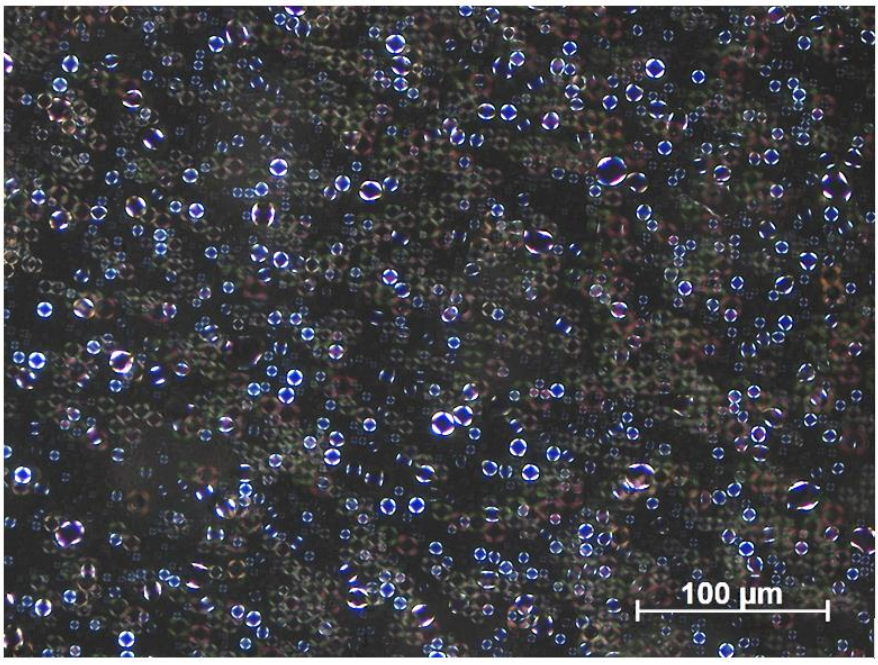

Figure 61: LC from O/W model emulsion made with commercial NA and mineral oil.

5.3. PARTIAL CONCLUSION

The SAXS analysis of the water-crude oil emulsion containing lamellar LC stabilizing the oil droplets did not present the periodicity of the Bragg peaks, possibly due to the complex matrix that is the petroleum itself, which may contain crystalline compounds interfering in the SAXS analysis.

Taking advantage of the coffee ring effect, which is the accumulation of the emulsion droplets on the edges of a sessile droplet over a coverslip, the extraction of the interfacial material was carried out about of 0.18 g of salt material extracted from each system. The salt material present differences in color and aspects characteristics possibly related to the petroleum composition and to the acid-base reaction. The FT-IR spectra these salts in almost all cases did not present good resolution of the peaks and bands. However, the comparison of the salt extracted from the system composed by P5 and NaOH, with FT-IR of a commercial NA presented similarities. There are strong indications that naphthenic acids are responsible for the LC formation in petroleum emulsions. The emulsion prepared with the commercial NA present LC, further corroborating these indications.

6. ADDITIONAL CONSIDERATIONS

The topic of LC in petroleum systems still has many unanswered questions. In addition to the factors that may contribute to its formation (**Chapter 4**) and the attempt of extraction and characterization (**Chapter 5**), it is propose an explanation for the observation of LC only in oil-in-water systems. In addition, the LC is known in the cosmetics industry for its high stability, but there is no evidence of the stability of such structures in petroleum systems. Therefore, some observations about stability and a simplified proposal of LC formation mechanism are presented.

6.1. FORMATION MECHANISM

As noted in **item 4.2.2** in **Chapter 4**, the Maltese cross pattern related to LC was only observed in the bottom phases of the emulsified systems, i.e. oil droplets dispersed in water. **Figure 62** depicts a drop of petroleum encased in multi-layers of surfactant. These multi-layers may be arranged in the form of LC as discussed above. In addition, according to Sjöblom *et al.* (2003), it may contain intercalated water between the layers. In this representation, the petroleum, whose largest fraction is of saturated chains, is surrounded by its natural surfactants that, because they are amphiphilic, have interfacial activity. Even small amounts of surfactant are able to stabilize a drop.

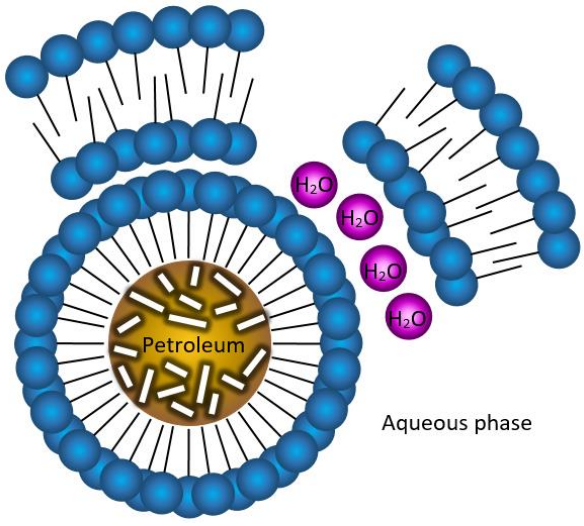

Figure 62: LC formation around a petroleum droplet.

Figure 63 represents the opposite situation as shown in **Figure 62**. In this case, a water drop is stabilized by natural crude oil surfactants. As in the continuous phase, there are a large number of nonpolar molecules and these molecules may have small sizes and consequently have high mobility, they end up interacting with the nonpolar parts of the surfactant molecules in the film, preventing the formation of other layers of surfactant and consequently the LC forming. Both suggested mechanisms are representations based on the LC appearance only in oil-water systems and their absence in water-oil systems.

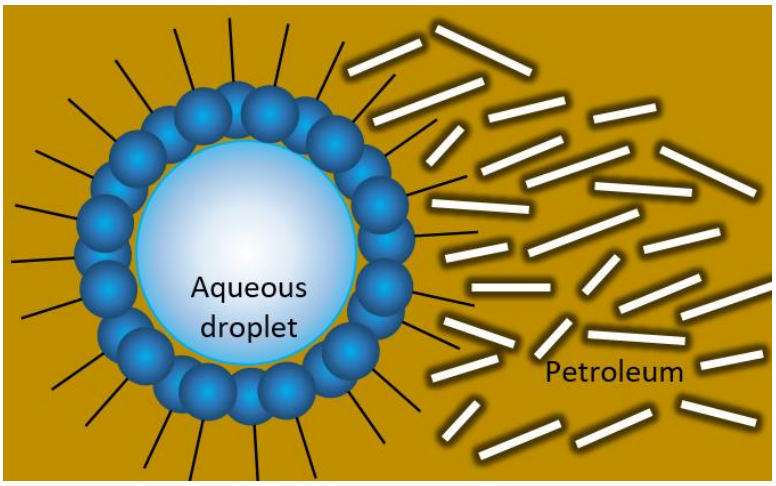

Figure 63: Aqueous droplet in a petroleum continuous phase.

6.2. STABILITY

Water-in-oil emulsions are very common during petroleum production. However, oil-in-water systems are mostly found in production waters. Water is usually separated from the oil by electro-coalescence methods. **Figure 64** shows the polarized light microscopy of a sample of the produced water from an electro-coalescence pilot plant. The original emulsion was prepared with 10.0 wt. % of water and 1.0 wt. % of surfactant. The sample was collected after the application of the destabilization electric field. It is clear the presence of liquid crystalline structures, that is, even after processes of electro-coalescence the LC remain organized. The oil content in this produced water was not available.

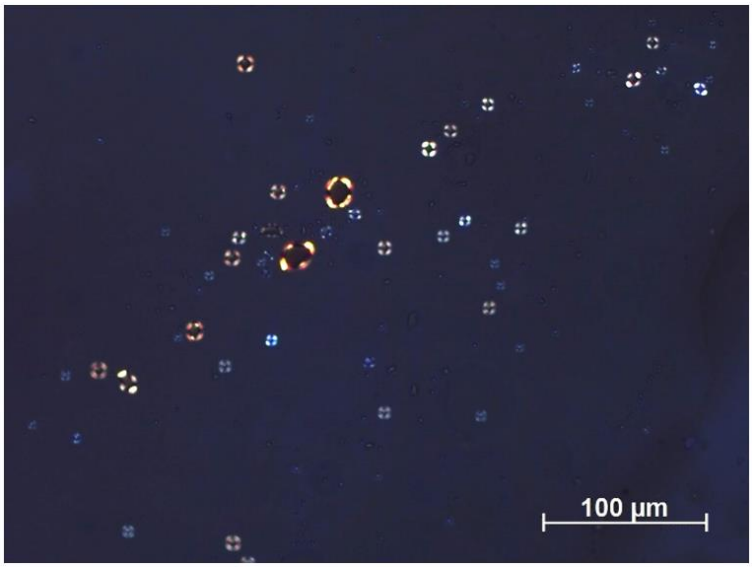

Figure 64: LC presence in a produced water from electro coalescing pilot plant.

Further evidence about the stability of LC structures is shown in **Figure 65** that presents polarized light microscopy of a sample of produced water from a Brazilian refinery, aged for about ten years. Once again, the liquid crystalline structures are present, so it is possible to attest to the great stability of the LC in emulsified systems involving crude oil.

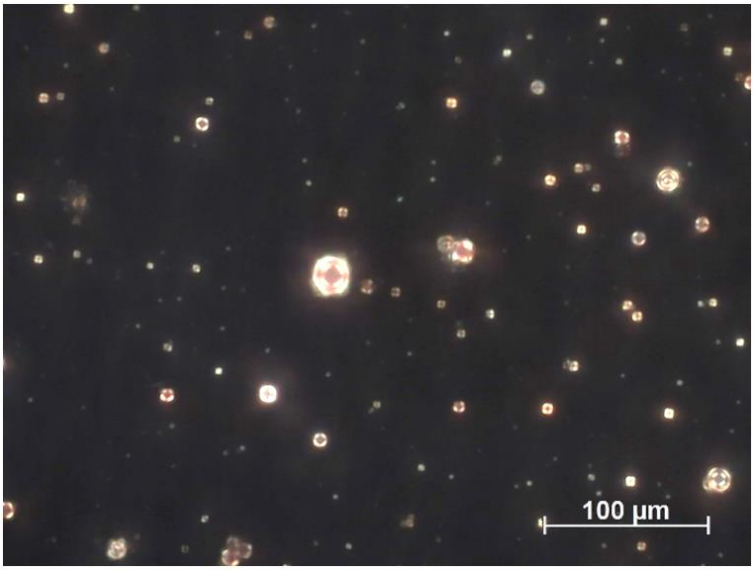

Figure 65: LC presence in a produced water from Brazilian refinery.

According to Produced Water Society (2017), the physicochemical properties of the produced water vary considerably depending on the geographic location, geologic

formation and the type of petroleum. The crude oil presence on the produced water can be found in different physical forms. As free oil in the form of large droplets, that is readily removable by gravity separation methods. As dispersed oil, in the form of small droplets, that could be somewhat difficult to remove and is probably the LC cases. Finally as dissolved oil, in the form of hydrocarbons and other similar materials dissolved in the water stream that is very challenging to eliminate.

Currently, regulations require the total oil and grease content of the effluent water to be reduced to levels ranging from between 15.0 and 50.0 mg/L. Brazilian regulation CONAMA 393/2007 require a maximum monthly average of 29.0 mg/L, which can reach a maximum of 42.0 mg/L ppm per day. Disposal of produced water into onshore surface waters is generally prohibited by environmental regulations. Onshore disposal typically requires the produced water effluent to be injected into saltwater disposal well (STEWART and ARNOLD, 2011).

6.3. PARTIAL CONCLUSION

Because of the appearance of LC only in oil-in-water systems, a mechanism is suggested based on the composition of the oil and the characteristics of the molecules present in the crude oil. This proposition considers that even small amounts the surfactants, which are amphiphilic and have an affinity for water, are capable of stabilize the oil drops. In water-oil systems, the nonpolar molecules present in the oil end up interacting with the nonpolar parts of the surfactant molecules in the film, preventing other layers of surfactant to form LC.

Strong evidences about the LC stability in produced water from petroleum systems were found. The LC structures were present in the produced water of an electrocoalescence pilot plant and in produced water from a Brazilian refinery aged for about ten years.

7. CONCLUSION

Because of the lyotropic features of the lamellar LCs, the presence of water is fundamental. In the absence of water, the petroleum samples as received do not present liquid crystalline structures. The micrographs of the bottom phases of the separated emulsion, that is composed of dispersed oil or multiple emulsion droplets in the aqueous phase, present LC structure in almost all droplets. A proposition of formation mechanism suggests that in water-oil systems the nonpolar molecules present in the oil end up interacting with the nonpolar parts of the surfactant molecules in the film, preventing other layers of surfactant to form LC.

It is believed that the presence of liquid crystals is not related to the paraffins and even to the salt concentration in the aqueous phase. However, the LC is favored at high aqueous phase content because of the migration of certain acidic species from oil to water, that can be organized in LC and stabilize the oil droplets. TAN values and viscosity of crude oil are also related to the LC formation. Low viscosities promotes the migration of acid from oil to water and thus form more LC. The ionization of the NA in high pH and/or the formation of naphthenates possibly are related to the LC formation, because of the amount of LC increasing with the pH increase. The presence of cations with different volume and valence can also affect the LC formation. In some cases, the larger volume for K^+ can be responsible for less LC structures compared with Na^+ systems. In addition, the monovalent Na^+ presents more LC than the bivalent Ca^{2+}, possibly because of molecular structure of the native acid compounds from the crude oil.

As the petroleum is a very complex multicomponent matrix, the structures of its natural surfactants are unknown, as well as the kinetics of stabilization of the interface in these systems. Thus, it was not possible to establish a relationship between the equilibrium velocities of adsorption and desorption of the molecules at the interface and the nature of the aqueous solution. However, in general, the systems composed by the oil as received, i.e. before the emulsification processes present a faster IFT stabilization kinetics than systems that used dehydrated oil after emulsification. The IFT values obtained before the emulsification were lower, while elastic modulus was higher. For the systems composed by the oil after one emulsification process, the IFT was higher and the elastic modulus was lower. This behavior is expected as more

diverse range of surfactant molecules is present in the crude oil as received. After emulsification, part of this material is removed and a decrease in IFT values and a reduction in the elastic modulus occurs

The FT-IR spectra of the extracted salt material in almost all cases did not present good resolution of the peaks and bands. However, the comparison of the salt extracted from the system composed by P5 and NaOH, with an FT-IR of a commercial NA present similarities. There are strong indications that naphthenic acids are responsible for the LC formation in petroleum emulsions. The emulsion prepared with the commercial NA presents LC, further corroborating these indications.

Strong evidences about the LC stability in produced water from petroleum systems were found. The LC structures were present in the produced water of an electrocoalescence pilot plant and in produced water from Brazilian refinery aged for about ten years.

8. REFERENCES

ACEVEDO, S.; ESCOBAR, G.; RANAUDO, M. A.; KHAZEN, J.; BORGES, B.; PEREIRA, J. C.; MÉNDEZ, B. Isolation and characterization of low and high molecular weight acidic compounds from Cerro Negro extraheavy crude oil. Role of these acids in the interfacial properties of the crude oil emulsions. Energy Fuels. 1999, 13, 333-335.

ALEXANDRIDIS, P.; OLSSON, U.; LINDMAN, B. A record nine different phases (four cubic, two hexagonal, and one lamellar lyotropic liquid crystalline and two micellar solutions) in a ternary isothermal system of an amphiphilic block copolymer and selective solvents (water and oil). Langmuir. 1998, 14, 2627-2638.

ALVES, D. R.; CARNEIRO, J. S. A.; OLIVEIRA, I. F.; FAÇANHA JR., F.; SANTOS, A. F.; DARIVA, C.; FRANCESCHI, E.; FORTUNY, M. Influence of the salinity on the interfacial properties of a Brazilian crude oil-brine systems. Fuel. 2014, 118, 21-26.

ANDERSEN, S. I.; MAHAVADI, S. C.; ABDALLAH, W.; BUITING, J. J. Infrared spectroscopic analysis of the composition of an oil/water interfacial film. Energy Fuels, 2017, 31 (9), 8959-8966.

ANGLO-PERSIAN OIL COMPANY, 2011, Heavy Oil vs. Light Oil: Legislative Brown bag, accessed 12 feb 2019, <http://www.aoga.org/wp-content/uploads/2011/03/HRES-3.10.11-Lunch-Learn-BP-Heavy-Oil1.pdf>.

ANP, 2019, Boletim da Produção de Petróleo e Gás Natural, Dezembro de 2018, n. 100, acessed 07 feb 2019, <http://www.anp.gov.br/images/publicacoes/boletins-anp/Boletim_Mensal-Producao_Petroleo_Gas_Natural/boletim-dezembro-2018.pdf>

BAGHERI, S. R.; BAZYLEVA, A.; GRAY, M. R.; MCCAFFREY, W. C.; SHAW, J. M. Observation of liquid crystals in heavy petroleum fractions. Energy Fuels. 2010, 24, 4327-4332.

BAGHERI, S. R.; MASIK, B.; ARBOLEDA, P.; WEN, Q.; MICHAELIAN, K. H.; SHAW, J. M. Physical properties of liquid crystals in Athabasca bitumen fractions, Energy Fuels. 2012, 26, 4978-4987.

BECHTOLD, I. H. Cristais líquidos: um sistema complexo de simples aplicação. Rev. Bras. Ensino Fis. 2005, 27 (3), 333-342.

BINKS, B. P.; HOROZOV, T. S. Colloidal particles at liquid interfaces, 1st ed. Cambridge, Cambridge University Press, 2008, 520 p.

BRANDAL, Ø.; SJÖBLOM, J.; ØYE, G. Interfacial behavior of naphthenic acids and multivalent cations in systems with oil and water. I. A pendant drop study of interactions between n-dodecyl benzoic acid and divalent cations. J. Dispersion Sci. Technol. 2004, 25 (3), 367-374.

BRANDAL, Ø.; HANNESETH, A.-M. D.; SJÖBLOM, J. Interactions between synthetic and indigenous naphthenic acids and divalent cations across oil-water interfaces: effects of addition of oil-soluble non-ionic surfactants, Colloid. Polym. Sci. 2005, 284, 124-133.

BRASIL, N. I. Introdução a Engenharia Química, 3rd ed. Interciência, Rio de Janeiro, 2017, 448 p.

BRIENT, J. A.; WESSNER, P. J.; DOYLE, M. N. Naphthenic acids, in: Kirk-Othmer Encyclopedia of Chemical Technology, John Wiley & Sons, Inc., 4 dez. 2000.

BROWN, L. D.; ULRICH, A. C. Oil sands naphthenic acids: A review of properties, measurement, and treatment. Chemosphere. 2015, 127, 276-290.

BRUICE, P. Y. Química Orgânica, 4th ed. vol 1. Pearson Prentice Hall, São Paulo, 2006, 590 p.

CAMPOS, D. D. P.; CASSU, S. N.; GARCIA, R. B. R.; QUEIROZ, H. A. A. S.; GONÇALVES, R. F. B.; KAWACHI, E. Y. Avaliação por SAXS e DSC das interações entre H_2O e RENEX-100. Quim. Nova. 2012, 35 (2), 355-359.

CANTOR, R. S. Lipid composition and the lateral pressure profile in bilayers. Biophys. J. 1999, 76, 2625-2639.

CARLTON, R. A, Polarized light microscopy, In: CARLTON, R. A. Pharmaceutical Microscopy, Springer Science & Business Media. 2011, 335 p.

CHEN, J.; ZHANG, J.; LI, H. Determining the wax content of crude oils by using differential scanning calorimetry. Thermochim. Acta. 2004, 410, 23-26.

CHIARI, B. G.; ALMEIDA, M. G. J.; CORRÊA, M. A.; ISAAC, V. L. B. Cosmetics' Quality Control. In: AKYAR, I. (Ed). Latest Research into Quality Control. InTech. 2012, 337-364.

CLEMENTE, J. S.; YEN, T.-W.; FEDORAK, P. M. Development of a high performance liquid chromatography method to monitor the biodegradation of naphthenic acids, J. Environ. Eng. Sci. 2003, 2, 177-186.

CLINGENPEEL, A. C.; ROWLAND, S. M.; CORILO, Y. E.; ZITO, P.; RODGERS, R. P. Fractionation of interfacial material reveals a continuum of acidic species that contribute to stable emulsion formation. Energy Fuels, 2017, 31 (6), 5933-5939.

CORNELIUS, C. D. Classification of natural bitumen: A physical and chemical approach. In RICHARD F. MEYER (Ed.), Exploration for heavy crude oil and natural bitumen: AAPG Studies in Geology; 25, 165-174, 1987.

CRABTREE, R. H.; MINGOS, D. M. P. Comprehensive Organometallic Chemistry III, Elsevier Science, New York, vol. 1−13, 2007, 958 p.

CRAIEVICH, A. F. Synchrotron SAXS studies of nanostructured materials and colloidal solutions. Mater. Res. 2002, 5 (1), 1-11.

CZARNECKI, J.; MORAN, K.; YANG, X. On the “rag layer” and diluted bitumen froth dewatering. Can. J. Chem. Eng. 2007, 85, 748-755.

CZARNECKI, J. Stabilization of water in crude oil emulsions. Part 2. Energy Fuels. 2009, 23,1253-1257.

CZARNECKI, J.; TCHOUKOV, P.; DABROS, T. Possible role of asphaltenes in the stabilization of water-in-crude oil emulsions. Energy Fuels. 2012, 26 (9), 5782-5786.

DANIELSSON, I. Lyotropic mesomorphism: phase equilibria and relation to micellar systems, In: FRIBERG, S. (Ed.) Lyotropic Liquid Crystals and the Structure of Biomembranes. ACS, 1976, p. 13-27, 152 p.

DIAS, H. P., PEREIRA, T. M. C., VANINI, G., DIXINI, P. V., CELANTE, V. G., CASTRO, E. V. R., VAZ, B. G., FLEMING, F. P., GOMES, A. O., AQUIJE, G. M. F. V., ROMÃO, W. Monitoring the degradation and the corrosion of naphthenic acids by electrospray ionization Fourier transform ion cyclotron resonance mass spectrometry and atomic force microscopy. Fuel, 2014, 126, 85-95.

DONG, Y-D.; BOYD, B. J. Applications of X-ray scattering in pharmaceutical science, Int. J. Pharm. 2011, 417, 101-111.

DUNCKE, A. C. P.; MARINHO, T. O.; BARBATO, C. N. FREITAS, G. B.; OLIVEIRA, M. C. K.; NELE, M. Liquid crystal observations in emulsion fractions from Brazilian crude oils by polarized light microscopy. Energy Fuels. 2016, 30 (5), 3815-3820.

ENGELS, T.; FÖRSTER, T.; VON RYBINSKI, W. The influence of coemulsifier type on the stability of oil-in-water emulsions. Colloids Surf., A. 1995, 99, 141-149.

ESE, M. H.; KILPATRICK, P. K. Stabilization of water-in-oil emulsions by naphthenic acids and their salts: model compounds, role of pH, and soap: acid ratio. J. Dispersion Sci. Technol. 2004, 25 (3), 253-261.

EZRAHI, S. ASERIN, A. GARTI, N. Aggregation behavior in one-phase (Winsor IV) microemulsion systems, In: KUMAR, P. AND MITTAL, K. L. (Ed) Hanbook of Microemulsion Science and Technology, Marcel Dekker, Inc., New York, 1999, 842 p.

FORMARIZ, T. P.; URBAN, M. C. C.; SILVA JÚNIOR, A. A.; GREMIÃO, M. P. D.; OLIVEIRA, A. G. Microemulsões e fases liquídas cristalinas como sistemas de liberação de fármacos. Rev. Bras. Ciênc. Farm. 2005, 41 (3), 301-313.

FORTUNY, M.; RAMOS, A. L. D.; DARIVA, C.; EGUES, S. M. S.; SANTOS, A. F.; NELE, M.; COUTINHO, R. C. C. Principais aplicações das micro-ondas na produção e refino de petróleo. Quim. Nova. 2008, 31 (6), 1553-1561.

FRANK, C.; SOTTMANN, T.; STUBENRAUCH, C.; ALLGAIER, J.; STREY, R. Influence of amphiphilic block copolymers on lyotropic liquid crystals in water-oil-surfactant systems. Langmuir. 2005, 21, 9058-9067.

FRIBERG, S. E.; SOLANS, C. Surfactant association structures and the stability of emulsions and foams. Langmuir. 1986, 2 (2), 121-126.

FULLER, G. G. VERMANT, J. Complex fluid-fluid interfaces: rheology and structure. Ann. Rev. Chem. Biomol. Eng. 2012, 3, 519-43.

GAO, S.; MORAN, K.; XU, Z.; MASLIYAH, J. Role of naphthenic acids in stabilizing water-in-diluted model oil emulsions, J. Phys. Chem. B. 2010, 114, 7710-7718.

GENNES, P. G.; PROST, J. Physics of Liquid Crystals, Oxford University Press Inc., 2nd ed, New York, 1993, 616 p.

GLATTER, O.; KRATKY, O. Small-Angle X-ray scattering, Academic Press Inc. Ltd, New York, 1982. 515 p.

HAMLEY, I. W. Introduction to Soft Matter: Synthetic and Biological Self-Assembling Materials. John Wiley & Sons Ltd. Revised Edition, England, 2007, 332 p.

HIEMENZ, P. C.; RAJAGOPALAN, R. Principles of Colloid and Surface Chemistry. Marcel Dekker Inc., 3rd ed, New York, 1997, 671 p.

HIROMI, P. I; SCHEER, A.P; WEINSCHUTZ, R.; SANTOS, B. M. Estudo do efeito da água em emulsões de petróleo. 4° PDPetro, Campinas, SP. 2007.

HODGE, S. M.; ROUSSEAU, D. Flocculation and coalescence in water-in-oil emulsions stabilized by paraffin wax crystals. Food Res. Int. 2003, 36, 695–702.

HORVÁTH-SZABO, G.; CZARNECKI, J.; MASLIYAH, J. Liquid crystals in aqueous solutions of sodium naphthenates, J. Colloid Interface Sci. 2001a, 236, 233-241.

HORVÁTH-SZABÓ, G.; MASLIYAH, J. H.; CZARNECKI, J. Phase behavior of sodium naphthenates, toluene, and water. J. Colloid Interface Sci. 2001b, 242 (1), 247-254.

HORVÁTH-SZABO, G.; CZARNECKI, J.; MASLIYAH, J. H. Sandwich structures at oil-water interface under alkaline conditions, J. Colloid Interface Sci. 2002, 253, 427-434.

HORVÁTH-SZABÓ, G.; MASLIYAH, J. H.; CZARNECKI, J. Emulsion stability based on phase behavior in sodium naphthenates containing systems: Gels with a high organic solvent content. J. Colloid Interface Sci. 2003, 257, 299-309.

HORVÁTH-SZABÓ, G.; MASLIYAH, J. H.; CZARNECKI, J. Friberg correlations in oil recovery. J. Dispersion Sci. Technol. 2006, 27 (5), 625-633.

HU, G.; YANG, H.; HOU, Q.; GUO, D.; CHEN, G.; LIU, F.; CHEN, T.; SHI, X.; SU, Y.; WANG, J. A pH and salt dually responsive emulsion in the presence of amphiphilic macromolecules. Soft Matter. 2018, 14, 405-410.

ISHIZUKA, C.; ARIMA, S.; ARAMAKI, K. Head group effects on molecular packing in lamellar liquid crystals. J. Colloid Interface Sci. 2011, 361, 148-153.

JARVIS, J. M.; ROBBINS, W. K.; CORILO, Y. E.; RODGERS, R. P. Novel method to isolate interfacial material. Energy Fuels. 2015, 29 (11), 7058-7064.

KARIMI, S.; FEIZY, J. MEHRJO, F.; FARROKHNIA, M. Detection and quantification of food colorant adulteration in saffron sample using chemometric analysis of FT-IR spectra. RSC Adv. 2016, 6, 23085-23093.

KASUMU, A. S.; ARUMUGAM, S.; MEHROTRA, A. K. Effect of cooling rate on the wax precipitation temperature of ‘‘waxy’’ mixtures. Fuel. 2013, 103, 1144-1147.

KLEIN, K. Liquid crystals and emulsions: a wonderful marriage. In: WIECHERS J. W. (Ed.) Skin Barrier: Chemistry of Delivery Systems. Allured, 2008, p. 265-269, 657 p.

KOKAL, S. Crude oil emulsions: a state of the art review. SPE Prod. Facil. 2005, 5-13.

KUMAR, S. Liquid crystals: experimental study of physical properties and phase transitions. Cambridge University Press, United Kingdom, 2001, 33 p.

LASHKARBOLOOKI, M.; AYATOLLAHI, S.; RIAZI, M. Effect of salinity, resin, and asphaltene on the surface properties of acidic crude oil/smart water/rock system. Energy Fuel. 2014, 28, 6820-6829.

LÉTOFFÉ, J. M.; CLAUDY, P.; KOK, M. V.; GARCIN, M.; VOLLE. J. L. Crude oils: characterization of waxes precipitated on cooling by DSC and thermomicroscopy. Fuel. 1995, 74 (6), 810-817.

LI, H.; ZHANG, J. A generalized model for predicting non-Newtonian viscosity of waxy crude as a function of temperature and precipitated wax. Fuel. 2003, 82, 1387-1397.

LIGIERO, L. M.; DICHARRY, C.; PASSADE-BOUPAT, N.; BOUYSSIERE, B.; LALLI, P. M.; RODGERS, R. P.; BARRÈRE-MANGOTE, C.; GIUSTI, P; BOURIAT, P. Characterization of crude oil interfacial material isolated by the wet silica method. Part 2: dilatational and shear interfacial properties. Energy Fuels, 2017, 31 (2), 1072-1081.

LIU, F.; DARJANI, S.; AKHMETKHANOVA, N.; MALDARELLI, C.; BANERJEE, S.; PAUCHARD, V. Mixture effect on the dilatation rheology of asphaltenes-laden interfaces. Langmuir, 2017, 33 (8), 1927-1942.

MAKAI, M.; CSÁNYI, E.; NÉMETH, Z.; PÁLINKÁS, J.; ERŐS, I. Structure and drug release of lamellar liquid crystals containing glycerol, Int. J. Pharm. 2003, 256, 95-107.

MANOVA, A.; VIKTOROVA, J.; KÖHLER, J.; THEILER, S.; KEUL, H.; PIRYAZEV, A. A.; IVANOV, D. A.; TSARKOVA, L.; MÖLLER, M. Multilamellar thermoresponsive emulsions stabilized with biocompatible semicrystalline block copolymers. ACS Macro Lett. 2016, 5, 163-167.

MARSH, H. Carbonization and liquid-crystal (mesophase) development: part 1. the significance of the mesophase during carbonization of coking coals. Fuel. 1973, 52, 205-212.

MARTINS, R. G.; TORRES, R. B.; SANTOS, R. G. Interfacial behavior of systems containing asphaltenes and polar compounds In: PetroPhase, 17th, 2016, Elsinore-DK, Conference Book, DTU Chemical Engineering, 2016, p. 59.

MARTINS, L. L.; DA SILVA, P. F.; DA CRUZ, G. F.; PUDENZI, M. A.; EBERLIN, M. N.; RIEHL, C. A. S.; SOUZA, D. Estudo da acidez naftênica e potencial corrosivo de petróleos brasileiros por ESI(-) FT-ICR MS, Rev. Virtual Quím. 2018, 10 (3), 625-640.

McCLEMENTS, D. J. Context and background. In: Food Emulsions: Principles, practices, and techniques. Boca Raton: CRC Press. 2004.

McMURRY, J. Química Orgânica. Cengage Learning, São Paulo, 2009.

MELE, S.; MURGIA, S.; MONDUZZI, M. Monoolein based liquid crystals to form long-term stable emulsions. Colloids Surf. A. 2003, 228, 57-63.

MILLER, R.; KRÄGEL, J.; FAINERMAN, V. B.; MAKIEVSKI, A. V.; GRIGORIEV, D. O.; RAVERA, F.; LIGGIERI, L.; KWOK, D. Y.; NEUMANN, A. W. Characterization of water/oil interfaces, In: SJOBLOM, J. (ed). Encyclopedic handbook of emulsion technology, Marcel Dekker Inc., New York, mar. 2001, 760 p.

MÜLLER-GOYMANN, C. C. Physicochemical characterization of colloidal drug delivery systems such as reverse micelles, vesicles, liquid crystals and nanoparticles for topical administration. Eur. J. Pharm. Biopharm. 2004, 58, 343-356.

MYERS, D. Surfaces, Interfaces, and Colloids: Principles and Applications. John Wiley & Sons, Inc. 2nd Edition, New York, 1999, 519 p.

NAGEL, M. TERVOORT, T. A. VERMANT, J. From drop-shape analysis to stress-fitting elastometry, Adv. Colloid Interface Sci. 2017, 247, 33-51.

NETO, A. M. F.; SALINAS, S. R. A. The physics of lyotropic liquid crystals: phase transitions and structural properties, In: Monographs on the Physics and Chemistry of Materials. Oxford University Press Inc., New York, 2005, 316 p.

OKA, T.; MIYAHARA, R.; TESHIGAWARA, T.; WATANABE, K. Development of novel cosmetic base using sterol surfactant. I. preparation of novel emulsified particles with sterol surfactant. J. Oleo Sci. 2008, 57 (10), 567-575.

OLIVEIRA, M. C. K.; ROSÁRIO, F. F.; BERTELLI, J. N.; PEREIRA, R. C. L.; ALBUQUERQUE, F. C.; MARQUES, L. C. C., Flow assurance solutions to mitigate naphthenates problems in crude oil production, In: SPE Annual Technical Conference and Exhibition, 2013, New Orleans-USA, 2013.

ONDRIS-CRAWFORD, R.; BOYKO, E. P.; WAGNER, B. G.; ERDMANN, J. H.; ZUMER, S.; DOANE, J. W. Microscope textures of nematic droplets in polymer dispersed liquid crystals, J. Appl. Phys. 1991, 69, 6380-6386.

OYAFUSO, M. H.; CARVALHO, F. C.; TAKESHITA, T. M.; SOUZA, A. L. R.; ARAÚJO, D. R.; MERINO, V.; GREMIÃO, M. P. D.; CHORILLI, M. Development and in vitro evaluation of lyotropic liquid crystals for the controlled release of dexamethasone. Polym. 2017, 9, 330-345.

PAVIA, D. L.; LAMPMAN, G. M.; KRIZ, G. S. Introduction to Spectroscopy, 3rd ed. Thomson Learning, Inc. Washington, 2001, 680 p.

PEDERSEN, K. S.; RØNNINGSEN, H. P. Effect of precipitated wax on viscosity: a model for predicting non-Newtonian viscosity of crude oils. Energy Fuels. 2000, 14. 43-51.

PRADILLA, D.; SIMON, S.; SJÖBLOM, J. Desorption of asphaltenes and asphaltene model compounds from the oil/water interface. In: PetroPhase, 17th, 2016, Elsinore-DK, Conference Book, DTU Chemical Engineering, 2016, p. 82.

PRODUCED WATER SOCIETY, 2017, Produced Water 101, accessed 14 jul 2018, <http://www.producedwatersociety.com/produced-water-101/>.

QIAN, K.; ROBBINS, W. K.; HUGHEY, C. A.; COOPER, H. J.; RODGERS, R. P.; MARSHALL, A. G. Resolution and identification of elemental compositions for more than 3000 crude acids in heavy petroleum by negative-ion microelectrospray high-field Fourier transform ion cyclotron resonance mass spectrometry, Energy Fuel, 2001, 15, 1505-1511.

QIN, C.; On organic liquid crystal transfer from bitumen-rich to water-rich phases: a combined laboratory and SAGD field study; Chemical Engineering Master Thesis, 2014, Edmonton, Alberta.

RODRIGUEZ-ABREU, C.; ACHARYA, D. P.; ARAMAKI, K.; KUNIEDA, H. Structure and rheology of direct and reverse liquid-crystal phases in a block copolymer/water/oil system. Colloids Surf., A. 2005, 269, 59-66.

ROSEN, M. J.; KUNJAPPU, J. T. Dispersion and aggregation of solids in liquid media by surfactants. In: Surfactants and Interfacial Phenomena, 4th ed. John Wiley & Sons, Inc. 2012. 368-391.

ROSEVEAR, F. B. Liquid crystals: the mesomorphic phases of surfactant composition. J. Soc. Cosmet. Chem. 1968, 19, 581-594.

RÖTGER, H. Relaxation times and viscosity. J. Non-Cryst. Solids, 1974, 14, 201-217.

RUSSEL, W. B. Mechanics of drying colloidal dispersions: Fluid/solid transitions, skinning, crystallization, cracking, and peeling. AIChE J. 2011, 57(6), 1378-1385.

SALAGER, J-L. ANTÓN, R. E. Ionic microemulsions, In: KUMAR, P. AND MITTAL, K. L. (Ed) Hanbook of Microemulsion Science and Technology, Marcel Dekker, Inc., New York, 1999, 842 p.

SAULNIER, P.; ANTON, N.; HEURTAULT, B.; BENOIT, J.-P. Liquid crystals and emulsions in the formulation of drug carriers, C.R. Chim. 2008, 11, 221-228.

SHENG, J. J. Modern chemical enhanced oil recovery: theory and practice, 1st ed, Gulf Professional Publishing, 2011, 648 p.

SIMMONS, M. J. H.; WILSON, J. A.; AZZOPARDI, B. J. Interpretation of the flow characteristics of a primary oil–water separator from the residence time distribution, Trans IChem E. 2002, 80 (part A), 471-481.

SIMON, S.; SJÖBLOM, J. Application of interfacial shear rheology to petroleum systems, In: PetroPhase, 17th, 2016, Elsinore-DK, Conference Book, DTU Chemical Engineering, 2016, p. 193.

SJÖBLOM, J. Encyclopedic handbook of emulsion technology, Marcel Dekker Inc., New York, 2001, 760 p.

SJÖBLOM, J.; NARVE A.; AUFLEM, I. H.; BRANDAL, Ø.; HAVRE, T. E.; SÆTHER, Ø.; WESTVIK, A.; JOHNSEN, E. E.; KALLEVIK, H. Our current understanding of water-in-crude oil emulsions: Recent characterization techniques and high-pressure performance. Adv. Colloid Interface Sci. 2003, 100-102, 399-473.

SPEIGHT, J G. Enhanced recovery methods for heavy oil and tar sands, 1st ed, Gulf Publishing Company, 2009, 354 p.

STEWART, M.; ARNOLD, K. Produced Water Treating Systems. In: Produced Water Treatment Field Manual, Gulf Professional Publishing, 2011, 1-134.

SZLEIFER, I.; KRAMER, D.; BENSHAUL, A.; GELBART, W. M.; SAFRAN, S. A. Molecular theory of curvature elasticity in surfactant films. J. Chem. Phys. 1990, 92, 6800-6817.

SZTUKOWSKI, D. M.; YARRANTON, H. W. Oilfield solids and water-in-oil emulsion stability, J. Colloid Interface Sci. 2005a, 285, 821-833.

SZTUKOWSKI, D. M.; YARRANTON, H. W. Rheology of asphaltene-toluene/water interfaces. Langmuir. 2005b, 21, 11651-11658.

TAYLOR, S. D.; CZARNECKI, J.; MASLIYAH, J. Stepwise thickening in aqueous foam films stabilized by sodium naphthenates, J. Colloid Interface Sci. 2005, 282 (2), 499-502.

TEIXEIRA, A. M. R. F.; LOPES, D. C. N.; TEIXEIRA, M. A. G. Aplicação de troca iônica em resinas comerciais para isolamento e fracionamento de ácidos naftênicos de petróleos nacionais, In: 2° PDPetro, 2003.

THOMPSON, D. G.; TAYLOR, A. S.; GRAHAM, D. E. Emulsification and demulsification related to crude oil production, Colloids Surf., A. 1985, 15, 175-189.

TONG, H.; WAN, P.; WENTAO, M.; ZHONG, G.; CAO, L.; HU, J. Yolk spherocrystal: The structure, composition and liquid crystal template, J. Struct. Biol. 2008, 163, 1-9.

URDAHL, O.; SJOBLOM, J. Water-in-crude oil emulsions from the Norwegian continental shelf: a stabilization and destabilization study. J. Dispersion Sci. Technol. 1995, 16, 557-574.

VALENCIA-DÁVILA, J. A.; ORREGO, J. A.; COMBARIZA, M. Y.; BLANCO-TIRADO, C. Influence of naphthenic acids on the water in oil emulsion stability of two heavy crude oils with low and high total acid numbers. In: PetroPhase, 17th, 2016, Elsinore-DK, Conference Book, DTU Chemical Engineering, 2016, p. 199.

VARADARAJ, R.; BRONS, C. Molecular origins of heavy oil interfacial activity, part 1: fundamental interfacial properties of asphaltenes derived from heavy crude oils and their correlation to chemical composition. Energy Fuels. 2007a, 21, 195-198.

VARADARAJ, R.; BRONS, C. Molecular origins of heavy crude oil interfacial activity part 2: fundamental interfacial properties of model naphthenic acids and naphthenic acids separated from heavy crude oils, Energy Fuels. 2007b, 21, 199-204.

VERRUTO, V. J. LE, R. K. KILPATRICK, P. K. Adsorption and molecular rearrangement of amphoteric species at oil water interface. J. Phys. Chem. B. 2009, 113 (42), 12.

VISINTIN, R. F. G.; LAPASIN, R.; VIGNATI, E.; D'ANTONA, P.; LOCKHART, T. P. Rheological behavior and structural interpretation of waxy crude oil gels. Langmuir. 2005, 21, 6240-6249.

VISINTIN, R. F. G.; LOCKHART, T. P.; LAPASIN, R.; D'ANTONA, P. Structure of waxy crude oil emulsion gels. J. Non-Newtonian Fluid Mech. 2008, 149, 34-39.

WEI, D.; SIMON, S.; SJÖBLOM, J. Interfacial and emulsion stabilizing properties of indigenous acidic and esterified asphaltenes, In: PetroPhase, 17th, 2016, Elsinore-DK, Conference Book, DTU Chemical Engineering, 2016, p. 194.

XU, Z.; SJÖBLOM, J.; MASLIYAH, J.; LIU, Q.; HARBOTTLE, D. Molecular mechanisms of petroleum emulsion stabilization and demulsification, In: PetroPhase, 17th, 2016, Elsinore-DK, Conference Book, DTU Chemical Engineering, 2016, p. 182.

YI, S.; ZHANG, J. Relationship between waxy crude oil composition and change in the morphology and structure of wax crystals induced by pour-point-depressant beneficiation. Energy Fuels, 2011, 25, 1686-1696.

YUNKER, P. J.; STILL, T.; LOHR, M. A.; YODH, A. G. Suppression of the coffee-ring effect by shape-dependent capillary interactions. Nature, 2011, 476 (7360), 308-311.

ZHENG, M.; WANG, Z.; LIU, F.; MI, Q.; WU, J. Study on the microstructure and rheological property of fish oil lyotropic liquid crystals. Colloids Surf., A. 2011, 385 (1-3), 47-54.

Internet images from sites:

Photographs of optical microscopes <https://www.zeiss.com> Acess in: 14 jun. 2017.

Bragg Law figure <https://pt.wikipedia.org/wiki/Lei_de_Bragg> Acess in: 21 jun. 2017.